| No. | Tank ID | PGA (g) | Diameter, D (m) | Height, H (m) | H / D | H Liq (m) | Pct Full | DS | Damage Observed | Remarks | Tank Anchors | Source |
|---|---|---|---|---|---|---|---|---|---|---|---|---|
| 17 | Holanda Chem Plant | 0.35 | | | | | | 1 | No damage | | UA | Spectra, Vol 7, B, 1991 |
| 18 | Holanda Chem Plant | 0.35 | | | | | | 1 | No damage | | UA | Spectra, Vol 7, B, 1991 |
| 19 | Holanda Chem Plant | 0.35 | | | | | | 1 | No damage | | UA | Spectra, Vol 7, B, 1991 |
| 20 | Holanda Chem Plant | 0.35 | | | | | | 1 | No damage | | UA | Spectra, Vol 7, B, 1991 |
| 21 | Holanda Chem Plant | 0.35 | | | | | | 1 | No damage | | UA | Spectra, Vol 7, B, 1991 |
| 22 | Holanda Chem Plant | 0.35 | | | | | | 1 | No damage | | UA | Spectra, Vol 7, B, 1991 |
| 23 | Holanda Chem Plant | 0.35 | | | | | | 1 | No damage | | UA | Spectra, Vol 7, B, 1991 |
| 24 | Holanda Chem Plant | 0.35 | | | | | | 1 | No damage | | UA | Spectra, Vol 7, B, 1991 |
| 25 | Holanda Chem Plant | 0.35 | | | | | | 1 | No damage | | UA | Spectra, Vol 7, B, 1991 |
| 26 | Holanda Chem Plant | 0.35 | | | | | | 1 | No damage | | UA | Spectra, Vol 7, B, 1991 |
| 27 | Transmerquim | 0.35 | 8.66 | 8.66 | | | | 3 | EFB - severe, no leak | Built 1989 | UA | Spectra, Vol 7, B, 1991 |
| 28 | Transmerquim | 0.35 | 8.66 | 8.66 | | | | 3 | EFB - severe, no leak | Built 1989 | UA | Spectra, Vol 7, B, 1991 |
| 29 | Transmerquim | 0.35 | | | | | | 2 | Rocking, broken inlent/outlet pipe, loss of some contents | | UA | Spectra, Vol 7, B, 1991 |
| 30 | Transmerquim | 0.35 | | | | | | 1 | No damage | | UA | Spectra, Vol 7, B, 1991 |
| 31 | Transmerquim | 0.35 | | | | | | 1 | No damage | | UA | Spectra, Vol 7, B, 1991 |
| 32 | Transmerquim | 0.35 | | | | | | 1 | No damage | | UA | Spectra, Vol 7, B, 1991 |
| 33 | Transmerquim | 0.35 | | | | | | 1 | No damage | | UA | Spectra, Vol 7, B, 1991 |
| 34 | Transmerquim | 0.35 | | | | | | 1 | No damage | | UA | Spectra, Vol 7, B, 1991 |

| No. | Tank ID | PGA (g) | Diameter, D (m) | Height, H (m) | H / D | H Liq (m) | Pct Full | DS | Damage Observed | Remarks | Tank Anchors | Source |
|---|---|---|---|---|---|---|---|---|---|---|---|---|
| 35 | Transmerquim | 0.35 | | | | | | 1 | No damage | | UA | Spectra, Vol 7, B, 1991 |
| 36 | Transmerquim | 0.35 | | | | | | 1 | No damage | | UA | Spectra, Vol 7, B, 1991 |
| 37 | Transmerquim | 0.35 | | | | | | 1 | No damage | | UA | Spectra, Vol 7, B, 1991 |
| 38 | Transmerquim | 0.35 | | | | | | 1 | No damage | | UA | Spectra, Vol 7, B, 1991 |

Comments

Tanks 1 - 14 at Recope Refinery, Port of Moin, Costa Rica

Spillage of oil from at least one tank was confined in a dike. This is arbitrarily assigned to tank 738 (DS=4)

Holanda Chemical Plant. 2 of 12 tanks were damaged

Transmerquim plant located next to Holanda. 2 of 12 tanks suffered EFB

The level of ground shaking at these three sites was considered "moderate" but not instrumental recordings available

Ground motion for Port of Moin, near Limon, was estimated based on mapped intensity MMI VIII = PGA 0.35g.

*Table B-16. Costa Rica 1992 M7.5*

| No. | Tank ID | PGA (g) | Diameter, D (m) | Height, H (m) | H / D | H Liq (m) | Pct Full | DS | Damage Observed | Remarks | Tank Anchors | Source |
|---|---|---|---|---|---|---|---|---|---|---|---|---|
| 1 | BDVWA A | 0.56 | 16.90 | 7.30 | 0.43 | 6.68 | 0.92 | 4 | EFP around entire tank, failed at shell / bottom plate at 2 locations. 6" overflow pipe failed, lifted 2 feet out of ground. Tank shifted 3" laterally. Failure of side pipe | Welded steel, AWWA D100 1974, 0.25: shell, 0.25" bottom, 3/16" roof | UA | Cooper 1997, Ballantyne and Crouse 1997 |
| 2 | BDVWA B | 0.55 | 8.10 | 7.30 | 0.90 | 6.95 | 0.95 | 2 | Minor damage | | UA | Cooper 1997, Ballantyne and Crouse 1997 |
| 3 | BDVWA C | 0.55 | 18.10 | 7.30 | 0.40 | 6.89 | 0.94 | 2 | Minor damage | | UA | Cooper 1997, Ballantyne and Crouse 1997 |
| 4 | BDVWA 10 | 0.55 | 9.90 | 4.90 | 0.49 | 4.45 | 0.91 | 2 | Minor damage | | UA | Cooper 1997, Ballantyne and Crouse 1997 |
| 5 | BDVWA 22-A | 0.54 | 9.90 | 4.90 | 0.49 | 4.45 | 0.91 | 2 | Minor damage | | UA | Cooper 1997, Ballantyne and Crouse 1997 |
| 6 | BDVWA 22-B | 0.54 | 9.90 | 4.90 | 0.49 | 4.45 | 0.91 | 2 | Minor damage | | UA | Cooper 1997, Ballantyne and Crouse 1997 |
| 7 | BDVWA 22-C | 0.54 | 14.00 | 4.90 | 0.35 | 4.45 | 0.91 | 2 | Minor damage | | UA | Cooper 1997, Ballantyne and Crouse 1997 |
| 8 | BDVWA 22-D | 0.54 | 22.30 | 4.90 | 0.22 | 4.42 | 0.90 | 2 | Minor damage | | UA | Cooper 1997, Ballantyne and Crouse 1997 |
| 9 | BDVWA 34 | 0.55 | 6.40 | 4.90 | 0.77 | 4.48 | 0.91 | 2 | Minor damage | | UA | Cooper 1997, Ballantyne and Crouse 1997 |
| 10 | HDWD 2 M.G. | 0.15 | 36.60 | 7.30 | 0.20 | U | | 1 | No significant damage | | UA | Cooper 1997, Wald 1998 |
| 11 | HDWD R-7 | 0.15 | 25.90 | 7.30 | 0.28 | U | | 1 | No significant damage | | UA | Cooper 1997, Wald 1998 |
| 12 | HDWD R-8 | 0.15 | 10.00 | 7.30 | 0.73 | U | | 1 | No significant damage | | UA | Cooper 1997, Wald 1998 |
| 13 | HDWD R-14 | 0.20 | 21.30 | 5.50 | 0.26 | U | | 1 | No significant damage | | UA | Cooper 1997, Wald 1998 |
| 14 | HDWD R-15 | 0.19 | 22.90 | 7.30 | 0.32 | U | | 1 | No significant damage | | UA | Cooper 1997, Wald 1998 |
| 15 | HDWD R-2 | 0.15 | 25.90 | 7.30 | 0.28 | U | | 1 | No significant damage | | UA | Cooper 1997, Wald 1998 |
| 16 | HDWD R-3 | 0.20 | 25.90 | 7.30 | 0.28 | U | | 1 | No significant damage | | UA | Cooper 1997, Wald 1998 |
| 17 | HDWD R-4 | 0.20 | 9.10 | 7.30 | 0.80 | U | | 1 | No significant damage | | UA | Cooper 1997, Wald 1998 |
| 18 | HDWD R-5 | 0.20 | 7.90 | 7.30 | 0.92 | U | | 1 | No significant damage | | UA | Cooper 1997, Wald 1998 |

| No. | Tank ID | PGA (g) | Diameter, D (m) | Height, H (m) | H / D | H Liq (m) | Pct Full | DS | Damage Observed | Remarks | Tank Anchors | Source |
|---|---|---|---|---|---|---|---|---|---|---|---|---|
| 19 | HDWD Upper Ridge | 0.10 | 13.10 | 7.30 | 0.56 | U | | 1 | No significant damage | | UA | Cooper 1997, Wald 1998 |
| 20 | HDWD Lower Ridge | 0.10 | 5.50 | 4.9 | 0.89 | U | | 1 | No significant damage | | UA | Cooper 1997, Wald 1998 |
| 21 | HDWD Upper Fox | 0.15 | 24.40 | 12.2 | 0.50 | U | | 1 | No significant damage | | UA | Cooper 1997, Wald 1998 |
| 22 | HDWD Lower Fox | 0.15 | 10.90 | 4.9 | 0.45 | U | | 1 | No significant damage | | UA | Cooper 1997, Wald 1998 |
| 23 | HDWD Golden Bee | 0.15 | 14.40 | 9.8 | 0.68 | U | | 1 | No significant damage | | UA | Cooper 1997, Wald 1998 |
| 24 | HDWD Homestead | 0.10 | 11.80 | 7.3 | 0.62 | U | | 1 | No significant damage | | UA | Cooper 1997, Wald 1998 |
| 25 | HDWD Hospital Desert Gold | 0.15 | 11.8 | 7.3 | 0.62 | U | | 1 | No significant damage | | UA | Cooper 1997, Wald 1998 |
| 26 | CSA 70-1 | 0.47 | 11.8 | 7.3 | 0.62 | 6.71 | 0.92 | 4 | EFB all around, shell tearing, pullout of dresser couplings for 2 side attached pipes | Designed per API 12B, 1979, Bolted steel, 10 ga shell 10ga bottom plate | UA | Cooper 1997, Wald 1998 |
| 27 | Beryl - SCWC | 0.14 | 9.14 | 7.32 | 0.80 | 6.4 | 0.87 | 2 | Small Leakage of bottom flange | Bolted | U | Ballantune and Crouse 1997 |
| 28 | Basalt - SCWC | 0.14 | 9.14 | 7.32 | 0.80 | 6.4 | 0.87 | 2 | Failure of pipe through bottom penetration | Bolted | U | Ballantune and Crouse 1997 |
| 29 | Arville-N - SCWC | 0.14 | 8.93 | 12.65 | 1.42 | 11.28 | 0.89 | 2 | Failure of pipe through bottom penetration | Welded (fillet) | U | Ballantune and Crouse 1997 |
| 30 | Arville-S - SCWC | 0.14 | 8.93 | 13.56 | 1.52 | 12.19 | 0.90 | 1 | tank lateral movement | Welded | U | Ballantune and Crouse 1997 |
| 31 | SCE Coolwater 1 of 3 | 0.53 | 83.2 | 15.2 | 0.18 | 15.2 | 1.00 | 1 | No damage | API 650 | U | Cooper 1997 |
| 32 | SCE Coolwater 2 of 3 | 0.53 | 83.2 | 15.2 | 0.18 | 13.68 | 0.90 | 1 | No damage | API 650 | U | Cooper 1997 |

| No. | Tank ID | PGA (g) | Diameter, D (m) | Height, H (m) | H / D | H Liq (m) | Pct Full | DS | Damage Observed | Remarks | Tank Anchors | Source |
|---|---|---|---|---|---|---|---|---|---|---|---|---|
| 33 | SCE Coolwater 3 of 3 | 0.53 | 67.2 | 14.5 | 0.22 | 1.45 | 0.10 | 1 | No damage | API 650 | U | Cooper 1997 |

Comments
Landers Mw 7.3 followed by Big Bear M 6.5 3 hours later
All damage in this table due to Landers event
BDVWA = Bighorn Desert View Water Agency. HDWD = Hi Desert Water District. CSA = San Bernardino County Service Area 70
SCWC - 4 tanks in Barstow, CA

*Table B-17. Landers 1992 M7.3*

| No. | Tank ID | PGA (g) | Diameter, D (m) | Height, H (m) | H / D | H Liq (m) | Pct Full | DS | Damage Observed | Remarks | Tank Anchors | Source |
|---|---|---|---|---|---|---|---|---|---|---|---|---|
| 1 | Van Nuys 1 | 0.55 | 8.80 | 14.60 | 1.66 | 7.90 | 0.54 | 1 | Bolt shearing on tank walkway | Assumed between 1/3 and 2/3 full. API 650 1963 | UA | Cooper 1997, Wald 1998 |
| 2 | Van Nuys 2 | 0.55 | 11.00 | 13.70 | 1.25 | 6.85 | 0.50 | 1 | Bolt shearing on tank walkway | Assumed between 1/3 and 2/3 full. API 650 1963 | UA | Cooper 1997, Wald 1998 |
| 3 | Van Nuys 3 | 0.55 | 20.40 | 14.60 | 0.72 | 7.30 | 0.50 | 1 | Bolt shearing on tank walkway | Assumed between 1/3 and 2/3 full. API 650 1963 | UA | Cooper 1997, Wald 1998 |
| 4 | Van Nuys 4 | 0.55 | 21.90 | 14.60 | 0.67 | 7.30 | 0.50 | 1 | Bolt shearing on tank walkway | Assumed between 1/3 and 2/3 full. API 650 1963 | UA | Cooper 1997, Wald 1998 |
| 5 | Van Nuys 5 | 0.55 | 4.60 | 9.10 | 1.98 | 4.55 | 0.50 | 1 | Bolt shearing on tank walkway | Assumed between 1/3 and 2/3 full. API 650 1963 | UA | Cooper 1997, Wald 1998 |
| 6 | 1 of 5 | 0.55 | 3.20 | 10.00 | 3.13 | 9.50 | 0.95 | 1 | Minor damage to walkway | Assumed nearly full | UA | Cooper 1997, Wald 1998 |
| 7 | 2 of 5 | 0.55 | 3.20 | 10.00 | 3.13 | 9.50 | 0.95 | 1 | Minor damage to walkway | Assumed nearly full | UA | Cooper 1997, Wald 1998 |
| 8 | 3 of 5 | 0.55 | 3.20 | 10.00 | 3.13 | 0.00 | 0.00 | 1 | Minor damage to walkway | Assumed nearly full | UA | Cooper 1997, Wald 1998 |
| 9 | 4 of 5 | 0.55 | 3.20 | 10.00 | 3.13 | 0.00 | 0.00 | 1 | Minor damage to walkway | Assumed nearly full | UA | Cooper 1997, Wald 1998 |
| 10 | 5 of 5 | 0.55 | 3.20 | 10.00 | 3.13 | 0.00 | 0.00 | 1 | No significant damage | Assumed other 3 tanks out of service had no liquid | UA | Cooper 1997, Wald 1998 |
| 11 | A Sepulveda Terminal | 0.90 | 19.80 | 11.00 | 0.56 | 7.32 | 0.67 | 1 | Slight sloshing | API 650, mid-60s | UA | Cooper 1997, Wald 1998, EERI 1995 |
| 12 | B | 0.90 | 21.90 | 11.00 | 0.50 | 3.66 | 0.33 | 1 | Slight sloshing | API 650, mid-60s | UA | Cooper 1997, Wald 1998, EERI 1995 |
| 13 | C | 0.90 | 18.30 | 11.00 | 0.60 | 3.66 | 0.33 | 1 | Slight sloshing | API 650, mid-60s | UA | Cooper 1997, Wald 1998, EERI 1995 |
| 14 | AG 1 | 0.90 | 3.70 | 7.30 | 1.97 | 7.30 | 1.00 | 1 | Minor paint cracks | UL 142, mid-60s | A | Cooper 1997, Wald 1998 |
| 15 | AG 2 | 0.90 | 3.70 | 7.30 | 1.97 | 0.00 | 0.00 | 1 | No significant damage | UL 142, mid-60s | A | Cooper 1997, Wald 1998 |
| 16 | Aliso 1 | 0.70 | 12.20 | 7.30 | 0.60 | U | 0.75 | 5 | Collapse | Bolted, mostly full based on amount of leakage | U | Cooper 1997, Wald 1998 |

| No. | Tank ID | PGA (g) | Diameter, D (m) | Height, H (m) | H / D | H Liq (m) | Pct Full | DS | Damage Observed | Remarks | Tank Anchors | Source |
|---|---|---|---|---|---|---|---|---|---|---|---|---|
| 17 | Aliso 2 | 0.70 | 12.20 | 7.30 | 0.60 | U | | 3 | Photo shows some shell damage | Bolted, may be damaged | U | Cooper 1997, Wald 1998 |
| 18 | Aliso 3 | 0.70 | 12.20 | 7.30 | 0.60 | U | | 1 | No significant damage | Bolted | U | Cooper 1997, Wald 1998 |
| 19 | Aliso 4 | 0.70 | 12.20 | 7.30 | 0.60 | U | | 1 | No significant damage | Bolted | U | Cooper 1997, Wald 1998 |
| 20 | Amir | 0.90 | 12.80 | 9.09 | 0.71 | U | | 3 | EFB | | U | Ballantyne and Crouse 1997, Wald 1998 |
| 21 | Lautenschlager 1 | 0.90 | 19.00 | 6.7 | 0.35 | 5.94 | 0.89 | 1 | No significant damage | Welded, 1965 | U | Cooper 1997, Ballantyne and Crouse 1997 Wald 1998 |
| 22 | Lautenschlager 2 | 0.90 | 19.00 | 7.3 | 0.38 | 5.94 | 0.81 | 1 | No significant damage | Welded 1988 | U | Cooper 1997, Ballantyne and Crouse 1997 Wald 1998 |
| 23 | Tapo | 0.90 | 40.00 | 9.8 | 0.25 | 8.69 | 0.89 | 1 | No significant damage | Welded 1963 | U | Cooper 1997, Ballantyne and Crouse 1997 Wald 1998 |
| 24 | Crater East | 0.75 | 9.10 | 7.3 | 0.80 | 6.13 | 0.84 | 1 | No significant damage | Survived, pct full from text in Cooper | U | Cooper 1997, Ballantyne and Crouse 1997 Wald 1998 |
| 25 | Crater West | 0.75 | 11.90 | 7.3 | 0.61 | 6.13 | 0.84 | 1 | No significant damage | Survived, pct full from text in Cooper | U | Cooper 1997, Ballantyne and Crouse 1997 Wald 1998 |
| 26 | Alamo | 0.70 | 30.50 | 6.3 | 0.21 | 6.25 | 0.99 | 1 | No significant damage | Welded 1964 | U | Cooper 1997, Ballantyne and Crouse 1997 Wald 1998 |
| 27 | Katerine | 0.90 | 12.00 | 7.3 | 0.61 | 6.25 | 0.86 | 4 | Failed by EFB with loss of contents | Bolted, built 1964 | U | Cooper 1997, Ballantyne and Crouse 1997 Wald 1998 |
| 28 | Rebecca North | 0.85 | 12.00 | 7.3 | 0.61 | 6.86 | 0.94 | 4 | Failed by EFB with loss of contents | Bolted, built 1964 | U | Cooper 1997, Ballantyne and Crouse 1997 Wald 1998 |
| 29 | Rebecca South | 0.85 | 12.00 | 7.3 | 0.61 | 6.86 | 0.94 | 4 | Failed by EFB with loss of contents | Bolted, built 1964 | U | Cooper 1997, Ballantyne and Crouse 1997 Wald 1998 |

| No. | Tank ID | PGA (g) | Diameter, D (m) | Height, H (m) | H / D | H Liq (m) | Pct Full | DS | Damage Observed | Remarks | Tank Anchors | Source |
|---|---|---|---|---|---|---|---|---|---|---|---|---|
| 30 | Sycamore North | 0.70 | 9.10 | 7.3 | 0.80 | 5.03 | 0.69 | 4 | Failed by EFB with loss of contents | Bolted, built 1964 | U | Cooper 1997, Ballantyne and Crouse 1997 Wald 1998 |
| 31 | Sycamore South | 0.70 | 9.10 | 7.3 | 0.80 | 5.03 | 0.69 | 4 | Failed by EFB with loss of contents | Bolted, built 1964 | U | Cooper 1997, Ballantyne and Crouse 1997 Wald 1998 |
| 32 | SCWC 1 of 4 | 0.70 | 15.80 | 9.8 | 0.62 | U | 0.99 | 1 | Survived | Welded | U | Cooper 1997, Wald 1998 |
| 33 | SCWC 2 of 4 | 0.70 | 15.80 | 9.8 | 0.62 | U | | 1 | Survived | Welded | U | Cooper 1997, Wald 1998 |
| 34 | SCWC 3 of 4 | 0.70 | 27.40 | 9.8 | 0.36 | U | | 1 | Survived | Welded | U | Cooper 1997, Wald 1998 |
| 35 | SCWC 4 of 4 | 0.70 | 39.00 | 9.8 | 0.25 | U | | 1 | Survived | Welded | U | Cooper 1997, Wald 1998 |
| 36 | LADWP Topanga | 0.40 | 11.00 | 9 | 0.82 | 8.08 | 0.90 | 2 | Replaced broken inlet / outlet valve. Loss of contents | Pct full from B&C. Welded steel, built 1936 | UA | Cooper 1997, Ballantyne and Crouse 1997, Brown et al 1995 |
| 37 | LADWP Zelzah | 0.50 | 21.30 | 12.2 | 0.57 | 9.85 | 0.81 | 2 | Roof collapsed, local buckling at top, broken valve. Loss of contents | Pct full from B&C. Welded steel built 1948 | UA | Cooper 1997, Ballantyne and Crouse 1997, Brown et al 1995 |
| 38 | LADWP Mulholland | 0.40 | 15.80 | 10.2 | 0.65 | 0 | 0.00 | 2 | overflow pipe pulled away. Loss of contents | Pct full from B&C. Welded steel built 1931 | UA | Cooper 1997, Ballantyne and Crouse 1997, Brown et al 1995 |
| 39 | LADWP Beverly Glen | 0.50 | 30.50 | 12.3 | 0.40 | U | | 2 | Roof collapsed, local buckling, dresser coupling pulled out. Loss of contents | Riveted, built 1932. Wood roof replaced with hypalon bladder | UA | Cooper 1997, Brown et al 1995 |
| 40 | MWD Jensen Clearwell | 0.70 | 42.67 | 12.19 | 0.29 | 11.67 | 0.96 | 1 | No tank damage | | UA | Cooper 1997, Ballantyne and Crouse 1997, Brown et al 1995 |
| 41 | LADWP Coldwater | 0.30 | 30.48 | 12.19 | 0.40 | U | | 2 | Roof shifted and collapsed, inlet / outlet pipe failure. Loss of contents | Riveted built 1925. Wood roof shifted and collapsed. | UA | Ballantyne and Crouse 1997, Brown et al 1995 |
| 42 | LADWP Granada High | 1.00 | 16.80 | 10.7 | 0.64 | 9.66 | 0.90 | 5 | Tank collapsed and tank removed | Riveted built 1929. Same tank was damaged in the 1971 San Fernando EQ | UA | Cooper 1997, Ballantyne and Crouse 1997, Brown et al 1995 |

| No. | Tank ID | PGA (g) | Diameter, D (m) | Height, H (m) | H / D | H Liq (m) | Pct Full | DS | Damage Observed | Remarks | Tank Anchors | Source |
|---|---|---|---|---|---|---|---|---|---|---|---|---|
| 43 | LADWP Alta Vista 1 | 0.60 | 16.46 | 8.78 | 0.53 | 8.84 | 1.01 | 1 | No tank damage | Riveted built 1929 | UA | Cooper 1997, Ballantyne and Crouse 1997, Brown et al 1995 |
| 44 | LADWP Alta Vista 2 | 0.60 | 28.96 | 11.13 | 0.38 | 9.3 | 0.84 | 1 | No tank damage | Welded steel, built 1954. Assumed same pga as Alta Vista 1 | UA | Cooper 1997, Ballantyne and Crouse 1997, Brown et al 1995 |
| 45 | LADWP Alta View | 0.30 | 19.81 | 12.95 | 0.65 | 12.5 | 0.97 | 1 | Settlement | | UA | Ballantyne and Crouse 1997, Brown et al 1995 |
| 46 | LADWP Kittridge 3 | 0.30 | 57.90 | 15.54 | 0.27 | U | | 1 | No tank damage | Welded built 1973 | UA | Ballantyne and Crouse 1997, Brown et al 1995 |
| 47 | LADWP Kittridge 4 | 0.30 | 57.90 | 15.54 | 0.27 | U | | 1 | No tank damage | Welded built 1987 | UA | Ballantyne and Crouse 1997, Brown et al 1995 |
| 48 | LADWP Corbin | 0.43 | 47.50 | 9.1 | 0.19 | 7.62 | 0.84 | 2 | Minor drain line damage, partially buried | Welded built 1987 | UA | Cooper 1997, Ballantyne and Crouse 1997, Brown et al 1995 |
| 49 | Donick | 0.30 | 37.43 | 7.32 | 0.20 | 6.86 | 0.94 | 1 | No tank damage | | UA | Ballantyne and Crouse 1997, Brown et al 1995 |
| 50 | Santa Clarita | 0.56 | 24.38 | 12.19 | 0.50 | 11.89 | 0.98 | 4 | EFB, roof damage | Assumed same PGA as Magic Mountain tanks (also located at Valencia) | U | Cooper 1997, Ballantyne and Crouse 1997, Wald 1998 |
| 51 | Valencia Round Moutain | 0.56 | 40.30 | 9.8 | 0.24 | 9.07 | 0.93 | 1 | No tank damage | AWWA D100 | U | Cooper 1997, Ballantyne and Crouse 1997, Wald 1998 |
| 52 | Hasley | 0.50 | 36.60 | 12.2 | 0.33 | 11.29 | 0.93 | 1 | No tank damage | AWWA D100 | U | Cooper 1997, Wald 1998 |
| 53 | Magic Mountain 2 | 0.56 | 22.30 | 7.3 | 0.33 | 6.1 | 0.84 | U | Damaged by outflow of MM 1 | Bolted, 1975 | U | Cooper 1997, Ballantyne and Crouse 1997, Wald 1998 |
| 54 | Magic Mountain 1 | 0.56 | 18.30 | 7.3 | 0.40 | 6.1 | 0.84 | 5 | Complete failure, bottom shell torn at base, collapse | Bolted, 1971 | U | Cooper 1997, Ballantyne and Crouse 1997, Wald 1998 |
| 55 | Magic Mountain 3 | 0.56 | 24.40 | 9.8 | 0.40 | 9.07 | 0.93 | 1 | No damage, tank partially buried 2.5 feet | AWWA D100. Welded with external roof rafters | U | Cooper 1997, Ballantyne and Crouse 1997, Wald 1998 |

| No. | Tank ID | PGA (g) | Diameter, D (m) | Height, H (m) | H / D | H Liq (m) | Pct Full | DS | Damage Observed | Remarks | Tank Anchors | Source |
|---|---|---|---|---|---|---|---|---|---|---|---|---|
| 56 | Presley | 0.50 | 21.30 | 9.8 | 0.46 | 9.07 | 0.93 | 1 | No damage | AWWA D100 | U | Cooper 1997, Wald 1998 |
| 57 | 4 Million | 0.55 | 45.70 | 9.1 | 0.20 | 8.42 | 0.93 | 1 | No damage | AWWA D100 | U | Cooper 1997, Wald 1998 |
| 58 | Seco | 0.43 | 22.30 | 7.3 | 0.33 | 6.75 | 0.92 | 1 | No damage | AWWA D100 | U | Cooper 1997, Wald 1998 |
| 59 | Larwin | 0.55 | 18.30 | 12.2 | 0.67 | 9.75 | 0.80 | 5 | Complete failure, EFB, tie down straps pulled, lifted foundation, nozzle tear outs | AWWA D100 1986. Straps 3/8"x3" at 4" On Center. | A | Cooper 1997, Wald 1998, EERI 1995 |
| 60 | Poe | 0.55 | 27.40 | 9 | 0.33 | 8.33 | 0.93 | 2 | Roof rafter damage, sagging roof, no EFB | AWWA D100 | U | Cooper 1997, Wald 1998 |
| 61 | Paragon | 0.43 | 22.30 | 9.8 | 0.44 | 9.07 | 0.93 | 1 | No damage | AWWA D100 | U | Cooper 1997, Wald 1998 |
| 62 | Newhall 1 | 0.63 | 18.29 | 9.14 | 0.50 | 8.23 | 0.90 | 5 | EFB, collapse, piping damage. Tasnk failed | Welded | UA | Cooper 1997, Wald 1998, EERI 1995 |
| 63 | Newhall 2 | 0.63 | 12.20 | 9.8 | 0.80 | 8.82 | 0.90 | 3 | Broken piping. EFB, Foundation settling | Built 1954, welded | UA | Cooper 1997, Wald 1998, EERI 1995 |
| 64 | Newhall 3 | 0.63 | 12.20 | 9.8 | 0.80 | 8.82 | 0.90 | 3 | Broken piping, EFB, Foundation settling | Built 1954, welded | UA | Cooper 1997, Wald 1998, EERI 1995 |
| 65 | Newhall 4 | 0.63 | 12.20 | 9.8 | 0.80 | 8.82 | 0.90 | 3 | Broken piping, EFB, Foundation settling, Roof rafters pulled out | Built 1962, AWWA | UA | Cooper 1997, Wald 1998, EERI 1995 |
| 66 | Newhall 5 | 0.63 | 19.50 | 9.8 | 0.50 | 8.82 | 0.90 | 4 | Roof rafter damage, EFB, inlet/outlet piping sheared | Built 1962. DS changed from 3 to 4 | UA | Cooper 1997, Wald 1998, EERI 1995 |
| 67 | Newhall 6 | 0.63 | 6.10 | 6.1 | 1.00 | 5.49 | 0.90 | 5 | EFB, piping failure, plate failure, Tank replaced | Built 1960s | UA | Cooper 1997, Wald 1998, EERI 1995 |
| 68 | Newhall 7 | 0.63 | 27.40 | 9.8 | 0.36 | 8.82 | 0.90 | 2 | Roof shell seam opened, rafters fell, no EFB | Built 1975. Bottom course t=0.5" | UA | Cooper 1997, Wald 1998, EERI 1995 |
| 69 | Newhall 8 | 0.63 | 18.30 | 7.3 | 0.40 | 6.57 | 0.90 | 2 | Roof rafters pulled away from the shell, roof damage | | UA | Cooper 1997, Wald 1998 |
| 70 | Newhall 10 | 0.63 | 24.40 | 12.2 | 0.50 | 10.98 | 0.90 | 1 | No apparent damage | Built 1989, AWWA | UA | Cooper 1997, Wald 1998 |

| Comments |
| --- |
| City of Simi Water District. 34 tanks in District, about 10 had damage. All damaged tanks were at east end of District (closer to fault). None of these tanks are in the table above |
| Simi: one tank had a failed underdrain pipe. Visual inspection of 2 tanks showed them unanchored, likely all were unanchored. This data not in above table |
| SCWC = Southern California Water Company |
| LADWP = Los Angeles Department of Water and Power |
| Tanks 51 - 61 are part of the Valencia Water Company |
| Tanks 62-70 are all welded, built to AWWA D100 or similar criteria |
| 8 Prestressed concrete circular tanks in region with strong shaking (>0.2g) (6 buried or partially buried) performed well, built 1958-1992 |
| There were other steel tanks at industrial sites which had EFB, which are not reported in this table |
| Tanks A, B, C, AG1, AG2 are at the Sepulveda terminal |

*Table B-18. Northridge 1994 M6.7*

| No. | Tank ID | PGA (g) | Diameter, D (m) | Height, H (m) | H / D | H Liq (m) | Pct Full | DS | Damage Observed | Remarks | Tank Anchors | Source |
|---|---|---|---|---|---|---|---|---|---|---|---|---|
| 1 | Fuel Pier Yard. Small craft refuel tank | 0.20 | 10.04 | 15.06 | 1.50 | 7.53 | 0.50 | 1 | | | A | Hashimoto 1989 |
| 2 | Power Plant #3, Tank 4 | 0.20 | 5.44 | 8.15 | 1.50 | 6.12 | 0.75 | 1 | | | A | Hashimoto 1989 |
| 3 | Power Plant #3, Tank 5 | 0.20 | 5.44 | 8.15 | 1.50 | 6.12 | 0.75 | 1 | | | A | Hashimoto 1989 |
| 4 | Las Ventanas Power Plant | 0.25 | 6.08 | 9.12 | 1.50 | 6.84 | 0.75 | 1 | | Capacity estimated | A | Hashimoto 1989 |
| 5 | Las Ventanas Power Plant | 0.25 | 6.08 | 9.12 | 1.50 | 6.84 | 0.75 | 1 | | Capacity estimated | A | Hashimoto 1989 |
| 6 | Las Ventanas Power Plant | 0.25 | 6.08 | 9.12 | 1.50 | 6.84 | 0.75 | 1 | | Capacity estimated | A | Hashimoto 1989 |
| 7 | LVPP Oil storage day tank | 0.25 | 9.30 | 13.94 | 1.50 | 10.46 | 0.75 | 1 | | Capacity estimated | A | Hashimoto 1989 |
| 8 | LVPP Oil storage day tank | 0.25 | 9.30 | 13.94 | 1.50 | 10.46 | 0.75 | 1 | | Capacity estimated | A | Hashimoto 1989 |
| 9 | Kettleman Gas Compressor Stn Lube Oil Fuel Tank 2 | 0.20 | 2.85 | 4.27 | 1.50 | 3.21 | 0.75 | 1 | | | A | Hashimoto 1989 |
| 10 | Kettleman Gas Compressor Stn Lube Oil Fuel Tank 3 | 0.20 | 2.85 | 4.27 | 1.50 | 3.21 | 0.75 | 1 | | | A | Hashimoto 1989 |
| 11 | Kettleman Gas Compressor Stn Lube Oil Fuel Tank 6 | 0.20 | 2.85 | 4.27 | 1.50 | 3.21 | 0.75 | 1 | | | A | Hashimoto 1989 |
| 12 | Pleasant Valley Pump Station Surge Tower | 0.56 | 6.31 | 48.37 | 7.66 | 36.27 | 0.75 | 2 | All anchor bolts stretched 1.5". No leaks | Anchored with 1.5" diameter J bolts. PGA from nearby recording | A | Hashimoto 1989 |
| 13 | San Lucas Canal Pump Station 17-R Surge Tank | 0.35 | 2.85 | 5.93 | 2.08 | 4.45 | 0.75 | 4 | Tank rocked, stretched or broken most anchors. 24" pipeline failed, likely loss of contents | Average tank dimensions. PGA = 0.35g is average for all pump stations, this one had more damage and may have had more PGA | A | Hashimoto 1989 |
| 14 | Union Oil Butane Plant Diesel Fuel Oil Tank | 0.60 | 2.42 | 3.63 | 1.50 | 2.72 | 0.75 | 1 | | | A | Hashimoto 1989 |
| 15 | Union Oil Butane Plant Diesel Fuel Oil Tank | 0.60 | 2.42 | 3.63 | 1.50 | 2.72 | 0.75 | 1 | | | A | Hashimoto 1989 |
| 16 | Humboldt Bay 3 Condensate Storage Tank | 0.30 | 4.56 | 7.99 | 1.75 | 5.99 | 0.75 | 1 | | Aluminum tank | A | Hashimoto 1989 |
| 17 | Humboldt Bay 3 Condensate Storage Tank | 0.25 | 4.56 | 7.99 | 1.75 | 5.99 | 0.75 | 1 | | Aluminum tank | A | Hashimoto 1989 |
| 18 | Sandia Fuel Oil Tank | 0.25 | 7.43 | 14.85 | 2.00 | 11.14 | 0.75 | 3 | All 20 Wejit anchors failed. Elephant foot buckling without leak | | A | Hashimoto 1989 |
| 19 | Asososca Lake Surge Tank | 0.50 | 4.86 | 21.40 | 4.40 | 14.70 | 0.67 | 2 | Stretched 16 anchor bolts, no | Capacity estimated | A | Hashimoto 1989 |

| No. | Tank ID | PGA (g) | Diameter, D (m) | Height, H (m) | H / D | H Liq (m) | Pct Full | DS | Damage Observed | Remarks | Tank Anchors | Source |
|---|---|---|---|---|---|---|---|---|---|---|---|---|
| | | | | | | | | | loss of contents | | | |
| 20 | Sendai Refinery Fire Water Storage Tank | 0.28 | 11.71 | 17.57 | 1.50 | 15.24 | | 2 | Anchor bolts stretched or pulled 1 to 6 inches, some leaking at a vlave, no buckling or rapid loss of water | Capacity estimated. Shell t = 3/8" est., btoom plate = .25" est. 14 1.25" diam anchor bolts A307, attached by chairs | A | Hashimoto 1989 |
| 21 | Caxton Paper Mill Chip storage silo | 0.40 | 11.31 | 16.96 | 1.50 | 12.72 | 0.75 | 1 | | Capacity estimated | A | Hashimoto 1989 |
| 22 | Caxton Paper Mill Hydrogen Peroxide Tank | 0.40 | 2.64 | 3.95 | 1.50 | 2.97 | 0.75 | 1 | | Capacity estimated | A | Hashimoto 1989 |
| 23 | Caxton Paper Mill Secondary Bleach Tower | 0.40 | 5.44 | 8.15 | 1.50 | 6.85 | 0.84 | 1 | | Capacity estimated | A | Hashimoto 1989 |
| 24 | New Zealand Distillery Bulk Storage Tank #2 | 0.50 | 7.48 | 5.61 | 0.75 | 4.71 | 0.84 | 1 | | Capacity estimated | A | Hashimoto 1989 |
| 25 | New Zealand Distillery Bulk Storage Tank #5 | 0.50 | 4.59 | 3.44 | 0.75 | 2.58 | 0.75 | 1 | | Capacity estimated | A | Hashimoto 1989 |
| 26 | New Zealand Distillery Bulk Storage Tank #6 | 0.50 | 4.59 | 3.44 | 0.75 | 2.58 | 0.75 | 1 | | Capacity estimated | A | Hashimoto 1989 |
| 27 | New Zealand Distillery Bulk Storage Tank #7 | 0.50 | 8.77 | 6.58 | 0.75 | 4.93 | 0.75 | 1 | | Capacity estimated | A | Hashimoto 1989 |
| 28 | New Zealand Distillery Receiver Tank #9 | 0.50 | 3.32 | 2.49 | 0.75 | 1.87 | 0.75 | 1 | | Capacity estimated | A | Hashimoto 1989 |
| 29 | Whakatane Board Mills Pulp Tank | 0.30 | 7.84 | 11.76 | 1.50 | 8.82 | 0.75 | 1 | | Capacity estimated | A | Hashimoto 1989 |
| 30 | Whakatane Board Mills Pulp Tank | 0.30 | 7.84 | 11.76 | 1.50 | 8.82 | 0.75 | 1 | | Capacity estimated | A | Hashimoto 1989 |
| 31 | Whakatane Board Mills Pulp Tank | 0.30 | 7.84 | 11.76 | 1.50 | 8.82 | 0.75 | 1 | | Capacity estimated | A | Hashimoto 1989 |
| 32 | Glendale power plant Distilled Water tank 1A | 0.28 | 3.62 | 5.42 | 1.50 | 4.07 | 0.75 | 1 | | | A | Hashimoto 1989 |
| 33 | Glendale power plant Distilled Water tank 1B | 0.28 | 3.62 | 5.42 | 1.50 | 4.07 | 0.75 | 1 | | | A | Hashimoto 1989 |
| 34 | Glendale power plant Distilled Water tank 2 | 0.28 | 4.01 | 6.01 | 1.50 | 4.51 | 0.75 | 1 | | Capacity estimated | A | Hashimoto 1989 |
| 35 | Glendale power plant Fuel oil day tank #1 | 0.28 | 3.62 | 5.42 | 1.50 | 4.07 | 0.75 | 1 | | | A | Hashimoto 1989 |
| 36 | Pasadena Power plant Unit B1 distilled water tank | 0.20 | 7.28 | 10.92 | 1.50 | 8.19 | 0.75 | 1 | | Capacity estimated | A | Hashimoto 1989 |

| No. | Tank ID | PGA (g) | Diameter, D (m) | Height, H (m) | H / D | H Liq (m) | Pct Full | DS | Damage Observed | Remarks | Tank Anchors | Source |
|---|---|---|---|---|---|---|---|---|---|---|---|---|
| 37 | Pasadena Power plant Unit B2 distilled water tank | 0.20 | 7.78 | 9.56 | 1.23 | 8.54 | 0.89 | 1 | | A36. t= 5/16" lower course, 1/4" upper course, 1/4" bottom plate. 10 1.25" diam anchor bolts A307 using chairs | A | Hashimoto 1989 |
| 38 | Pasadena Power plant Unit B3 distilled water tank | 0.20 | 5.46 | 13.92 | 2.55 | 12.19 | 0.88 | 1 | | A283 Gr B. t= 5/16" lower course, 1/4" upper course, .375" bottom plate. 24 1.5" diam. Anchor bolts A307 using chairs | A | Hashimoto 1989 |
| 39 | Pasadena Power plant Unit B1 distilled water tank | 0.17 | 7.28 | 10.92 | 1.50 | 8.19 | 0.75 | 1 | | Capacity estimated | A | Hashimoto 1989 |
| 40 | Pasadena Power plant Unit B2 distilled water tank | 0.17 | 7.78 | 9.56 | 1.23 | 8.54 | 0.89 | 1 | No damage | A36. t= 5/16" lower course, 1/4" upper course, 1/4" bottom plate. 10 1.25" diam anchor bolts A307 using chairs | A | Hashimoto 1989 |
| 41 | Pasadena Power plant Unit B3 distilled water tank | 0.17 | 5.48 | 13.92 | 2.55 | 12.19 | 0.88 | 1 | No damage | A283 Gr B. t= 5/16" lower course, 1/4" upper course, .375" bottom plate. 24 1.5" diam. Anchor bolts A307 using chairs | A | Hashimoto 1989 |

Comments

Tanks 1 - 3. Adak 1986. Tanks 4 - 8. Chile 1985. Tanks 9 - 15. Coalinga 1983. Tank 16. Ferndale 1975. Tank 16. Ferndale 1975.

Tank 18. Greenville 1980. Tank 19. Managua 1972. Tank 20. Miyagi-ken-ogi 1978. Tanks 21 - 31. New Zealand 1987. Tanks 32 - 38 San Fernando 1971. Tanks 39 - 41 Whittier 1987.

Most tanks at least 50% full at time of earthquake. Unless otherwise specified in Hashimoto, set at 75% full

*Table B-19. Anchored Tanks, Various Earthquakes*

| Abbreviation | Description |
|---|---|
| A | Anchored |
| API | American Petroleum Institute (API 650 code) |
| AWWA | American Water Waorks Association (AWWA D100 code) |
| D | Diameter. For most tanks, the diameter dimension is the inside diameter of the tank |
| DS | Damage State. See text for descriptions. May be from 1 to 5 |
| EERI | Earthquake Engineering Research Institute |
| EFB | Elephant Foot Buckling |
| g | acceleration of gravity (=32.2 ft / sec / sec) |
| ga | gage thickness |
| H | Height. Generally the height from the top of the floor to the overflow level. The actual tank may be higher (above the overflow level) |
| I/O | Inlet / outlet pipe |
| Liq | Height of Liquid. The estimated (sometimes known) height of fluid contents at the time of the earthquake |
| m | meter. Note: most tanks in these tables are actually sized to the nearest foot. The metric conversion here does not infer accuracy to the exact dimension in feet. |
| MMI | Modified Mercalli Intensity |
| Pct Full | The percent full of the tank (= H Liq / H) |
| PGA | Peak Ground Acceleration in g |
| U | Unknown |
| UA | Unanchored |
| Z | Design level peak ground acceleration |

*Table B-20. Legend for Tables B-8 through B-19*

## B.6 Fragility Curve Fitting Procedure

The empirical data in Tables B-8 through B-18 are assembled into one database. Fragility curves are then fitted into this dataset.

Fragilities were developed using the complete tank database as follows:

- A subset of the complete database was developed for only those tanks with the attributes desired. If a particular tank did not have the attribute, then it was excluded from the analysis.
- The tanks were “binned” into nine PGA bins. Each bin was for a range of 0.1g, with the exception of 0.71 to 0.90g and 0.91g to 1.20g. The higher g bins were wider as there were fewer tanks in these PGA ranges. The PGA for each bin was set at the average of the PGA values for each tank in that bin. The percent of tanks reaching or exceeding a particular damage state was calculated for each bin.
- A lognormal fragility curve was calculated for each of the four damage state ranges. For example, a fragility curve was calculated for all tanks that reached damage state 2 (DS2) or above, DS3 or above, DS4 or above and DS5. The fragility curve uses the median acceleration to reach that damage state or above and a lognormal dispersion parameter, $\beta$. The “best fit” fragility curve was selected by performing a least square regression for all possible fragility curves in the range of A=0.01g to 5.00g (in 0.01g steps) and $\beta$=0.01 to 0.80 (in 0.01 steps).

- Since an unequal number of tanks are in each bin, the analysis was performed using just an unweighted regression analysis with nine data points for the nine bins, and also a weighted regression analysis in which the number of data points in each bin reflect the actual number of tanks in each bin. The weighted analysis is considered a better representation. Using the data in Table 5-9, 263 tanks are in the 0.16g bin and just 10 tanks are in the 1.18g bin. In the weighted analysis, the 0.16g bin is given about 26 times more weight in the regression analysis.

## B.7 Analytical Formulation for Steel Tank Fragility Curves

Section 5.7 of Part 1 presents representative fragility curves for various classes of water tanks: steel, concrete, wood, elevated. The procedures used to develop analytical or stress-based fragility curves is described in some detail by Bandpadhyay et al [1993] and Kennedy et al [1989]. See Section 5.8 of Part 1 for references.

Section B.7 provides some examples to show how analytically based fragility curves can be developed for specific tank geometries.

Steel tank with a wood-framed roof (see Figure B-1). The tank is 75 feet in diameter and 32 feet high. Maximum water depth is 31 feet above the base plate, with a maximum capacity of 1 million gallons. The tank wall thickness is sized to achieve a 15,000 psi hoop tensile stress under normal static conditions. The tank is supported in a reinforced concrete ring beam with embedded hold-down anchors spaced at 6.5 feet intervals around the circumference of the tank.

The wood framed roof consists of 3/4 inch plywood sheathing supported by 3-by-12 radial joists at 4-feet on-center and by 4 x 12 radial beams. The beams are supported by the perimeter of the tank and by interior pipe columns.

The following calculations are based on developing the overturning moment for the tank. Minor adjustments to the calculations to account for inner and outer radius, etc. are left for detailed design. See AWWA D100 [AWWA] for the nomenclature used in this example.

R = 37.5 feet (tank radius)

L = 32 feet (tank height)

H = 31 feet (water height)

t = 0.375 inches (weighted average over height)

E = 29,000 ksi (modulus of elasticity, steel)

rho = 0.490 kcf (density of steel, kip per cubic foot)

H/R = 0.827

t/R = 0.000833

From Figure C.1 of ASCE [1984), ef = 0.05, es = 0.15, ea = 0.465.

For the tank filled with water, the impulsive first mode frequency is 7.1 Hz, following ASCE 1984 procedures. Note that a slightly different frequency would be computed using AWWA D100 simplified rules.

The convective first mode frequency is 0.19 Hz using equation (7-8) of ASCE [1984].

The shell has four 8-foot high courses. The bottom course has t = 0.5 inches, the second course has t = 0.375 inches, and the top two courses have t = 0.25 inches. Note that the t to be used in calculating the fundamental impulsive frequency is weighted over the height with a parabolic weighting function. More detailed analysis can be performed to refine the first mode frequency if the situation warrants.

Note that the top course t need only be 0.104 inches thick if the shell is designed using hoop stress as the only criteria. Some tank owners specify that t = 0.25 inches is the minimum.

The average dead weight of the wooden roof is assumed to be 10 pounds per square foot.
Wr = 10 psf. Wr = 44.2 kips. Xr = 33 feet.

The dead weight of the tank shell is 0.449 kips per linear foot of circumference.
Ws = 0.449 klf. Ws = 105.8 kips. Xs = 13.45 feet.

The weight of water when the tank is full (31 foot depth) is Ww = 1.934 ksf. Ws = 8,546 kips.

The total weight of roof, water and shell is Wt = 8,546 kips.

Following AWWA D100:

W1/Wt = 0.47. X1/H = 0.38 (impulsive component)

W1 = 4,017 kips, X1 = 11.78 feet

W2/Wt = 0.51. X2/H = 0.58 (convective component)

W2 = 4,358 kips. X2 = 17.98 feet.

To establish the overturning moment for purposes of assessing elephant foot buckling, the following assumptions are made:

- A ‘SRSS’ combination of the impulsive and convective components is assumed the be the best fit. Current codes use an absolute sum method, which will generally overpredict the true maximum overturning moment by a slight amount.
- The spectral acceleration of the convective mode is assumed to be 10% of the impulsive mode. This is a simplified generalization, and will depend upon the actual shape of the response spectra for the tank-specific site. However, this simplification is reasonable for many situations, and allows the estimation of the overturning moment to be a function of only one spectral ordinate.
- For purposes of developing a fragility curve, the input demand will be the 5% damped spectral ordinate at the impulsive mode frequency.

$$OTM = \sqrt{\left[\frac{S_{ai}}{g}\left(W_s X_s + W_r X_r + W_1 X_1\right)\right]^2 + \left[\frac{S_{ac}}{g}\left(W_2 X_2\right)\right]^2}$$

Using the above values, OTM = 50,810 foot-pounds times (Sai)/(g) where Sai = 5% damped spectral acceleration at the impulsive mode frequency, and g is in the same units as Sai.

Using the allowable compressive stresses for the lowest course shell (t = 0.5 inch) based on AWWA D100 Section 13.3.3.4.1(1991 edition):

fa = 2.14 ksi - ignoring internal water pressure

delta fc = 5.16 ksi - increase in compressive allowable to reflect internal hoop pressure

fc = 6.29 ksi - includes the effect of internal hoop pressure, plus 1.33 seismic increase factor

The overturning moment to reach fc = 6.29 ksi is M = 164,385 kip-feet. As the actual OTM is 50,810 kip-feet for a 1g spectral acceleration at 7.1 Hz, the required spectral acceleration needed to reach the code-limit fc is 3.24g (=164,385/50,810).

Table B-21 summarizes the various overstrength factors and uncertainties that are implied in the above calculations.

| **Factor** | **F** | βu | βr |
|---|---|---|---|
| F_strength | 1.5 | 0.05 | 0.05 |
| F_ductility | 1.0 | 0.0 | 0.0 |
| F_workmanship | 1.0 | 0.15 | 0.0 |
| F_damping | 1.0 | 0.1 | 0.1 |
| F_period | 1.0 | 0.2 | 0.1 |
| F_model | 0.75 | 0.25 | 0.2 |
| F_total | 1.13 | 0.37 | 0.25 |

*Table B-21. Probabilistic Factors for Sample Steel Tank – Elephant Foot Buckling*

F_total is the multiplicative sum of the various items under column F. Note that the strength value of 1.5 factors in that the true dynamic buckling capacity is estimated at 50% higher than the code-specified value. The value of 0.75 recognizes that the modeling approach taken here may have underestimated the true seismic forces by 25%. Tcantilever beam model is only a crude representation of the complex state of response of a tank shell that is subject to uplift, and may not predict the true highest compressive stress; vertical earthquake issues were ignored, etc. Also note that in this calculation for elephant foot buckling, there is no obvious analytical justification for the code-specified Rw values from 3.5 to 4.5. The above calculation is to predict the onset of buckling, and there is some margin before a buckle extends far enough to rupture the steel. This depends on the ductility of the steel, the lack of stress discontinuities that would be impacted by the buckle and the dynamic behavior of the tank, which would tend to limit the formation of the buckle if the overturning moment is due to high-frequency loading. Note that in the manhole location in Figure B-1, a tear could be expected at only moderate buckled deformation.

βu total is the square root of the sum of the squares of the βu column, = 0.37. βr total is the square root of the sum of the squares of the βr column, = 0.25. See Section B.2 for a further

description. The beta values represent uncertainty and randomness in the calculation above, but assume perfect knowledge of the ground motion response spectra. Beta total for the tank only is 0.45, which is the square root of the sum of the squares of βu and βr.

If the ground motion beta is 0.40, and if the user wishes to compute a single overall beta, then βu would increase to 0.55 and the total beta would be βt = 0.60.

The overall fragility curve for this damage state would be: A (median) = 3.65g (5% spectral acceleration) and βt = 0.60.

In a similar manner, this tank should be checked for other damage states such as roof damage due to water sloshing, in which the tank remains functional but sustains large repair costs; anchor bolt damage due to uplift forces, in which the tank remains functional but sustains small repair costs; bottom plate-to-bottom course weld damage caused by uplift once anchor bolts are stretched or fail, in which the tank is non-functional and sustains moderate repair costs; damage to the top courses of the shell from excessive roof damage, in which the tank remains partially functional and sustains moderately high repair costs; sliding of the tank, leading to damage of the attached pipes, in which the tank is non-functional and sustains moderate repair costs.

## B.8 References

American Water Works Association, *Welded Steel Tanks for Water Storage*, AWWA Standard D100, Denver, Colorado.

ATC, *Earthquake Damage Evaluation Data for California*, ATC 13, Applied Technology Council, 1985.

Ballantyne, D., Crouse, C., *Reliability and Restoration of Water Supply Systems for Fire Suppression and Drinking Following Earthquakes*, prepared for National Institute of Standards and Technology, NIST GCR 97-730, 1997.

Bandyopadhyay, K., Cornell, A., Costantino, C., Kennedy, R.P., Miller, C. and Veletsos, A., *Seismic Design and Evaluation Guidelines for The Department of Energy high-Level Waste Storage Tanks and Appurtenances*, Brookhaven National Laboratory, BNL 52361, Jan. 1993.

Brown, K., Rugar, P., Davis, C., Rulla, T., "Seismic Performance of Los Angeles Water Tanks, Lifeline Earthquake Engineering," in *Proceedings, 4th US Conference,* ASCE, TCLEE Monograph No. 6, San Francisco, 1995.

Cooper, T. W., *A Study of the Performance of Petroleum Storage Tanks During Earthquakes, 1933-1995*, prepared for the National Institute of Standards and Technology, Gaithersburg, MD, June 1997.

EERI, "Loma Prieta Reconnaissance Report," *Earthquake Spectra*, Earthquake Engineering Research Institute, Supplement to Vol. 6, May 1990.

Haroun, M., "Behavior of Unanchored Oil Storage Tanks: Imperial Valley Earthquake," *Journal of Technical Topics in Civil Engineering*, ASCE, Vol. 109, No. 1, April 1983.

Hashimoto, P.S., and Tiong, L.W., *Earthquake Experience Data on Anchored Ground Mounted Vertical Storage Tanks*, EPRI Report NP-6276, March 1989.

HAZUS, *Earthquake Loss Estimation Methodology*, National Institute of Building Sciences, prepared by Risk Management Solutions, Menlo Park, California, 1997.

Kennedy, R. P. and Kassawara, R. P., "Seismic Evaluation of Large Flat-Bottomed Tanks," *Second Symposium on Current Issues Related to Nuclear Power Plant Structures, Equipment, and Piping with Emphasis on Resolution of Seismic Issues in Low-Seismicity Regions*, EPRI NP-6437-D, May 1989.

McCann, M., Sauter, F., and Shah, H.C., "A Technical Note on PGA-Intensity Relationship with Applications to Damage Estimation," *BSSA*, Vol. 7, No. 2, pp 631-637, 1980.

O'Rourke, M. and So, P., "Seismic Behavior of On-Grade Steel Tanks; Fragility Curves," in *Optimizing Post-Earthquake Lifeline System Reliability*, ed. W. Elliott and P. McDonough, Technical Council on Lifeline Earthquake Engineering, Monograph No. 16, ASCE, Aug. 1999.

Scawthorne, C., and Khater, M., *A Model Methodology for Assessment of Seismic Vulnerability and Impact of Disruption of Water Supply Systems*, C. Rojahn, Principal Investigator, Applied Technology Council, ATC-25-1, 1992.

So, Pak, *Seismic Behavior of On-Grade Steel Tanks; Fragility Curves*, thesis submitted to the Graduate Faculty of Rensselaer Polytechnic Institute, RPI, Troy, NY, April 1999.

Wald, J., Quitoriano, V., Heaton, T., Kanamori, H., and Scrivner, C., TRINET Shakemaps: Rapid Generation of Peak Ground Motion and Intensity Maps for Earthquakes in Southern California, *Earthquake Spectra*, Oct. 1998.

## B.9 Figures

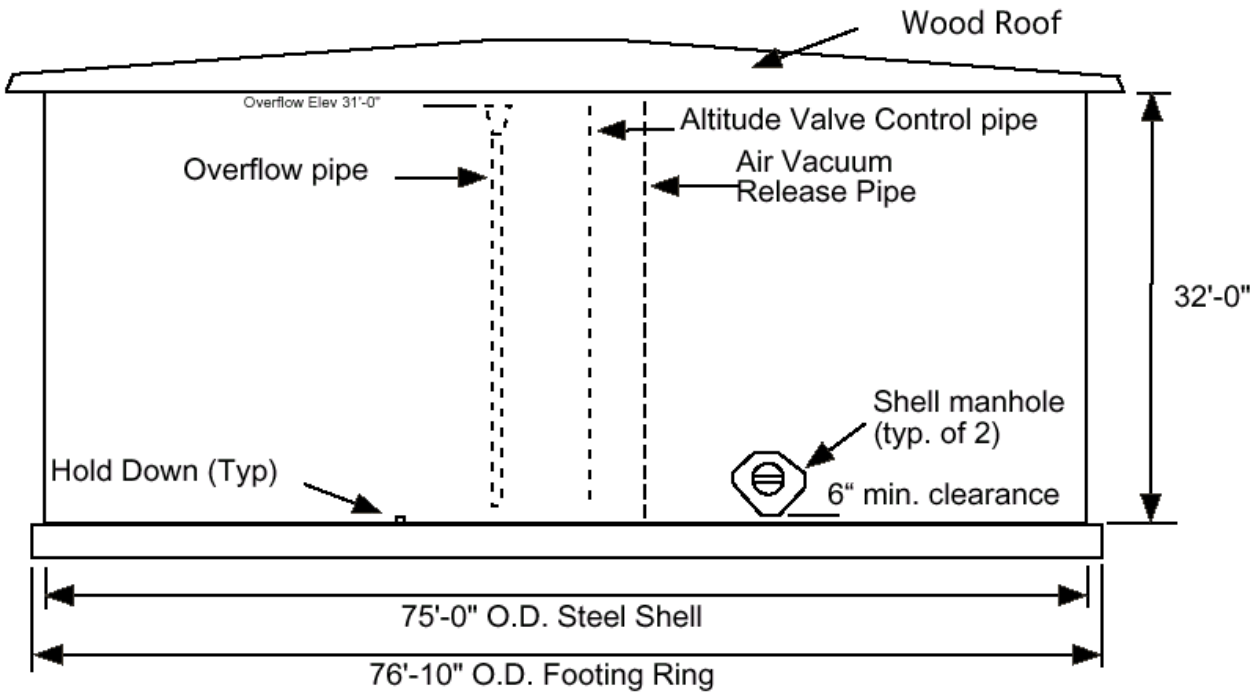


*Figure B-1. Elevation of Example Tank*

# C. Commentary – Tunnels

Section C.1 describes two sets of fragility curves: those in HAZUS and those in ATC-13.

Sections C.2 through C.5 provide information on the performance of tunnels in past earthquakes.

Section C.6 provides the complete tunnel database, including analyses of tunnels by liner attribute.

## C.1 Tunnel Fragility Curves – Prior Studies

### C.1.1 HAZUS Fragility Curves

The HAZUS computer program [HAZUS, 1997] includes a number of fragility curves for tunnels. These are provided for ground shaking and ground failure hazards in the form of landslides or fault offset.

For ground shaking hazards, data from post earthquake reconnaissance of 68 tunnels [Dowding and Rozen, 1978] were reduced to establish fragility parameters. Figure C-1 shows the empirical dataset; Table C-1 provides the specific values; Table C-1 was prepared as follows:

- The tunnel locations in the Dowding and Rozen study were identified. For each earthquake, the distance from the tunnel to the causative fault was determined. A suitable attenuation model was used—at the median level of shaking, such as using equation 3.3— to estimate the peak horizontal ground motion at the tunnel location.
- Three damage states could be assessed: none, slight and moderate. Descriptions of the damage states are as follows: Slight Damage—minor cracking of tunnel liner, minor rock falls, spalling of shotcrete or other supporting materials; Moderate Damage—moderate cracking of tunnel liner and rock falls.
- The empirical data was binned into three groups – tunnels with no observed damage, tunnels with minor damage and tunnels with moderate damage.
- The mean and standard deviation were computed for each bin. These are reported directly beneath the empirical data.
- The lognormal median and beta values were computed directly from the mean and standard deviation values as shown in the bottom of Table C-1.

Approximately 17% of the tunnels were reportedly in competent rock; the remaining were in sheared or broken rock, soil or unknown ground conditions. Tunnels were constructed between 1800 and 1960. For the most part, older tunnels represent poor-to-average construction quality, although the data does not specifically segregate tunnels with respect to quality of construction. For each tunnel, the peak horizontal ground acceleration was established using empirical attenuation relationships based on the distance from the earthquake epicenter to the site.

| Tunnel Number | PGA - with No Damage |
|---|---|
| 1 | 0.075 |
| 2 | 0.075 |
| 3 | 0.08 |
| 4 | 0.08 |
| 5 | 0.08 |
| 6 | 0.079 |
| 7 | 0.99 |
| 8 | 0.1 |
| 9 | 0.12 |
| 10 | 0.12 |
| 11 | 0.13 |
| 12 | 0.13 |
| 13 | 0.14 |
| 14 | 0.14 |
| 15 | 0.145 |
| 16 | 0.15 |
| 17 | 0.16 |
| 18 | 0.16 |
| 19 | 0.16 |
| 20 | 0.16 |
| 21 | 0.165 |
| 22 | 0.165 |
| 23 | 0.17 |
| 24 | 0.18 |
| 25 | 0.185 |
| 26 | 0.185 |
| 27 | 0.19 |
| 28 | 0.19 |
| 29 | 0.19 |
| 30 | 0.19 |
| 31 | 0.2 |
| 32 | 0.21 |
| 33 | 0.21 |
| 34 | 0.22 |
| 35 | 0.22 |
| 36 | 0.22 |
| 37 | 0.24 |
| 38 | 0.24 |
| 39 | 0.31 |
| Mean | 0.1834 |
| Std Dev | 0.1429 |

| Tunnel Number | PGA - With Slight Damage |
|---|---|
| 1 | 0.185 |
| 2 | 0.195 |
| 3 | 0.225 |
| 4 | 0.230 |
| 5 | 0.250 |
| 6 | 0.260 |
| 7 | 0.300 |
| 8 | 0.305 |
| 9 | 0.420 |
| 10 | 0.460 |
| 11 | 0.550 |
| 12 | 0.550 |
| 13 | 0.580 |
| 14 | 0.580 |
| 15 | 0.720 |
| Mean | 0.3873 |
| Std Dev | 0.1738 |

| Tunnel Number | PGA - With Moderate Damage |
|---|---|
| 1 | 0.255 |
| 2 | 0.340 |
| 3 | 0.420 |
| 4 | 0.480 |
| 5 | 0.482 |
| 6 | 0.510 |
| 7 | 0.520 |
| 8 | 0.525 |
| 9 | 0.550 |
| 10 | 0.560 |
| 11 | 0.590 |
| 12 | 0.620 |
| 13 | 0.640 |
| 14 | 0.690 |
| Mean | 0.5130 |
| Std Dev | 0.1163 |

| Tunnel Number | PGA - Portal Damage Only |
|---|---|
| 1 | 0.515 |

Source Data
Dowding, C.H. and Rozen, A.,
"Damage to Rock Tunnels from Earthquake Shaking"
Journal o fthe Geotechnical Engineering Division, ASCE, Feb. 1978

| Damage State | Mean | Stnd Dev | CoVariance | Beta**2 | Beta | A=-0.5 * BETA**2 | Median = Mean * exp(A) |
|---|---|---|---|---|---|---|---|
| None | 0.1834 | 0.1429 | 0.779 | 0.474 | 0.689 | -0.2370 | 0.145 |
| Minor | 0.3873 | 0.1738 | 0.449 | 0.183 | 0.428 | -0.0917 | 0.353 |
| Moderate | 0.5130 | 0.1163 | 0.227 | 0.050 | 0.224 | -0.0251 | 0.500 |

*Table C-1. Raw Data – Tunnel Fragility Curves*

| EQID | CASE | EQNAME | DATE | Mw | TNAME | OWNER | FUN | LINER SYSTEM | ROCK SOIL | COVER (M) | PGA (G) | DS | REFERENCE, NOTES |
|---|---|---|---|---|---|---|---|---|---|---|---|---|---|
| 1 | 1-1 | San Francisco, CA | 18/4/06 | 7.8 | SF #1 | SPRR | RR | 4 | R | 24 | 0.41 | 1 | Sharma & Judd, 1991 |
| 2 | 1-2 | San Francisco, CA | 18/4/06 | 7.8 | SF #3 | SPRR | RR | 4 | R | 46 | 0.41 | 1 | Sharma & Judd, 1991 |
| 3 | 1-3 | San Francisco, CA | 18/4/06 | 7.8 | SF #4 | SPRR | RR | 4 | R | 24 | 0.43 | 1 | Sharma & Judd, 1991 |
| 4 | 1-4 | San Francisco, CA | 18/4/06 | 7.8 | SF #5 | SPRR | RR | 4 | R | 24 | 0.45 | 2 | Sharma & Judd, 1991 |
| 5 | 1-5 | San Francisco, CA | 18/4/06 | 7.8 | Corte M. T, | NPC | RR | 1 | R | 60 | 0.38 | 1 | Sharma & Judd, 1991 |
| 6 | 1-6 | San Francisco, CA | 18/4/06 | 7.8 | Pilarcitos Res #1 | SFWD | WT | 4 | R | 68 | 0.65 | 1-3 | Schussler, H., 1906 |
| 7 | 1-7 | San Francisco, CA | 18/4/06 | 7.8 | Pilarcitos Res #2 | SFWD | WT | 4 | R | 152 | 0.65 | 1-3 | Schussler, H., 1906 |
| 8 | 1-8 | San Francisco, CA | 18/4/06 | 7.8 | Pilarcitos Res #3 | SFWD | WT | 4 | R | 137 | 0.69 | 1-3 | Schussler, H., 1906 |
| 9 | 2-1 | Kanto, Japan | 1/10/27 | 7.9 | Nagoye | Nat. RW | RR | 1 | | 30 | 0.40 | 2 | Sharma & Judd, 1991 |
| 10 | 2-2 | Kanto, Japan | 1/10/27 | 7.9 | Meno-Kamiana | Nat. RW | RR | 4 | R | 17 | 0.60 | 3 | Sharma & Judd, 1991 |
| 11 | 2-3 | Kanto, Japan | 1/10/27 | 7.9 | Yonegami Yama | Nat. RW | RR | 4 | | 50 | 0.66 | 2 | Sharma & Judd, 1991 |
| 12 | 2-4 | Kanto, Japan | 1/10/27 | 7.9 | Shimomaki Matsu | Nat. RW | RR | 4 | | 29 | 0.69 | 3 | Sharma & Judd, 1991 |
| 13 | 2-5 | Kanto, Japan | 1/10/27 | 7.9 | Happon-Matzu | Nat. RW | RR | 1 | S | 20 | 0.73 | 3 | Sharma & Judd, 1991 |
| 14 | 2-6 | Kanto, Japan | 1/10/27 | 7.9 | Nagasha-Yama | Nat. RW | RR | 4-5 | | 90 | 0.73 | 3 | Sharma & Judd, 1991 |
| 15 | 2-7 | Kanto, Japan | 1/10/27 | 7.9 | Hakone #1 | Nat. RW | RR | 1 | | 61 | 0.44 | 2 | Sharma & Judd, 1991 |
| 16 | 2-8 | Kanto, Japan | 1/10/27 | 7.9 | Hakone #3 | Nat. RW | RR | 1 | | 46 | 0.56 | 3 | Sharma & Judd, 1991 |
| 17 | 2-9 | Kanto, Japan | 1/10/27 | 7.9 | Hakone #4 | Nat. RW | RR | 1 | | 46 | 0.54 | 2 | Sharma & Judd, 1991 |
| 18 | 2-10 | Kanto, Japan | 1/10/27 | 7.9 | Hakone #7 | Nat. RW | RR | 1 | R | 31 | 0.63 | 3 | Sharma & Judd, 1991 |
| 19 | 2-11 | Kanto, Japan | 1/10/27 | 7.9 | Yose | Nat. RW | RR | 1 | R | 20 | 0.33 | 4 | Sharma & Judd, 1991 |
| 20 | 2-12 | Kanto, Japan | 1/10/27 | 7.9 | Doki | Nat. RW | RR | 4 | | | 0.25 | 4 | Sharma & Judd, 1991 |
| 21 | 2-13 | Kanto, Japan | 1/10/27 | 7.9 | Namuya | Nat. RW | RR | 5 | | 75 | 0.52 | 4 | Sharma & Judd, 1991 |
| 22 | 3-1 | Kern County, CA | 21/7/52 | 7.4 | Saugus | SPRR | RR | 1 | R | 40 | 0.06 | 1 | Sharma & Judd, 1991 |
| 23 | 3-2 | Kern County, CA | 21/7/52 | 7.4 | San Francisquito | SPRR | RR | 1 | R | 160 | 0.08 | 1 | Sharma & Judd, 1991 |
| 24 | 3-3 | Kern County, CA | 21/7/52 | 7.4 | Elizabeth | SPRR | RR | 1 | R | 250 | 0.10 | 1 | Sharma & Judd, 1991 |
| 25 | 3-4 | Kern County, CA | 21/7/52 | 7.4 | Antelope | SPRR | RR | 1 | R | 30 | 0.16 | 1 | Sharma & Judd, 1991 |
| 26 | 4-1 | Alaska | 27/3/64 | 8.4 | Whittier #1 | | RR | 1 | R | 400 | 0.22 | 2 | Sharma & Judd, 1991 |
| 27 | 4-2 | Alaska | 27/3/64 | 8.4 | Whittier #2 | | RR | 1 | R | 350 | 0.21 | 1 | Sharma & Judd, 1991 |
| 28 | 4-3 | Alaska | 27/3/64 | 8.4 | Seward #1 | | RR | 1 | R | 20 | 0.25 | 1 | Sharma & Judd, 1991 |
| 29 | 4-4 | Alaska | 27/3/64 | 8.4 | Seward #2 | | RR | 1 | R | 20 | 0.25 | 1 | Sharma & Judd, 1991 |
| 30 | 4-5 | Alaska | 27/3/64 | 8.4 | Seward #3 | | RR | 1 | R | 20 | 0.25 | 1 | Sharma & Judd, 1991 |
| 31 | 4-6 | Alaska | 27/3/64 | 8.4 | Seward #4 | | RR | 1 | R | 20 | 0.25 | 1 | Sharma & Judd, 1991 |
| 32 | 4-7 | Alaska | 27/3/64 | 8.4 | Seward #5 | | RR | 1 | R | 20 | 0.25 | 1 | Sharma & Judd, 1991 |
| 33 | 4-8 | Alaska | 27/3/64 | 8.4 | Seward #6 | | RR | 1 | R | 20 | 0.25 | 1 | Sharma & Judd, 1991 |
| 34 | 5-1 | San Fernando, CA | 9/3/75 | 6.6 | San Fernando | MWD | WT | 5-6-7 | S | 45 | 0.69 | 2 | Sharma & Judd, 1991 |

| EQID | CASE | EQNAME | DATE | Mw | TNAME | OWNER | FUN | LINER SYSTEM | ROCK SOIL | COVER (M) | PGA (G) | DS | REFERENCE, NOTES |
|---|---|---|---|---|---|---|---|---|---|---|---|---|---|
| 35 | 5-2 | San Fernando, CA | 9/3/75 | 6.6 | Tehachapi #1 | SPRR | RR | 1 | R | 30 | 0.04 | 1 | Sharma & Judd, 1991 |
| 36 | 5-3 | San Fernando, CA | 9/3/75 | 6.6 | Tehachapi #2 | SPRR | RR | 1 | R | 30 | 0.04 | 1 | Sharma & Judd, 1991 |
| 37 | 5-4 | San Fernando, CA | 9/3/75 | 6.6 | Tehachapi #3 | SPRR | RR | 1 | R | 30 | 0.04 | 1 | Sharma & Judd, 1991 |
| 38 | 5-5 | San Fernando, CA | 9/3/75 | 6.6 | Saugus | SPRR | RR | 1 | R | 40 | 0.30 | 1 | Sharma & Judd, 1991 |
| 39 | 5-6 | San Fernando, CA | 9/3/75 | 6.6 | San Francisquito | SPRR | RR | 1 | R | 160 | 0.24 | 1 | Sharma & Judd, 1991 |
| 40 | 5-7 | San Fernando, CA | 9/3/75 | 6.6 | Elizabeth | SPRR | RR | 1 | R | 250 | 0.15 | 1 | Sharma & Judd, 1991 |
| 41 | 5-8 | San Fernando, CA | 9/3/75 | 6.6 | Antelope | SPRR | RR | 1 | R | 30 | 0.10 | 1 | Sharma & Judd, 1991 |
| 42 | 5-9 | San Fernando, CA | 9/3/75 | 6.6 | Pacoima Dam SpillwayTunnels, CA | | WT | 1 | R | 43 | 0.69 | 2 | Sharma & Judd, 1991 |
| 43 | 6-1 | Loma Prieta, CA | 17/10/89 | 7.1 | Fort Baker-Berry | NPS | HW | 5 | R | 61 | 0.04 | 1 | COE, NPS |
| 44 | 6-2 | Loma Prieta, CA | 17/10/89 | 7.1 | Presidio Park | Caltrans | HW | 6 | R | 22 | 0.04 | 1 | Yashinsky, 1998 |
| 45 | 6-3 | Loma Prieta, CA | 17/10/89 | 7.1 | Alameda Creek Div | SFWD | WT | | | 300 | 0.12 | 1 | SFWD |
| 46 | 6-4 | Loma Prieta, CA | 17/10/89 | 7.1 | Coast Range | SFWD | WT | 5 | R | 240 | 0.09 | 1 | SFWD |
| 47 | 6-5 | Loma Prieta, CA | 17/10/89 | 7.1 | Pulgas | SFWD | WT | 5 | R | 92 | 0.09 | 1 | SFWD |
| 48 | 6-6 | Loma Prieta, CA | 17/10/89 | 7.1 | Irvington | SFWD | WT | 5 | R | 122 | 0.10 | 1 | SFWD |
| 49 | 6-7 | Loma Prieta, CA | 17/10/89 | 7.1 | Crystal Spr Baypass | SFWD | WT | 5-6-7 | R | 76 | 0.09 | 1 | SFWD |
| 50 | 6-8 | Loma Prieta, CA | 17/10/89 | 7.1 | Downtown S.F. | Caltrain | RR | | R | | 0.05 | 1 | |
| 51 | 6-9 | Loma Prieta, CA | 17/10/89 | 7.1 | Stanford Linear Collider | SU | AC | 5 | R | | 0.25 | 1 | Rose, 1990; Fisher, 1989 |
| 52 | 6-10 | Loma Prieta, CA | 17/10/89 | 7.1 | Lomita Mall | | | 5 | S | | 0.14 | 1 | Kaneshiro, 1989 |
| 53 | 6-11 | Loma Prieta, CA | 17/10/89 | 7.1 | Santa Teresa | SCVWD | WT | 7 | R | | 0.26 | 1 | SCVWD |
| 54 | 6-12 | Loma Prieta, CA | 17/10/89 | 7.1 | Tunnel #5 | SC,BT.PRR | RR | 3 | R | | 0.40 | 1 | SC,BT,PR |
| 55 | 6-13 | Loma Prieta, CA | 17/10/89 | 7.1 | Tunnel #6 | SC,BT.PRR | RR | 3 | R | | 0.28 | 1 | SC,BT,PR |
| 56 | 6-14 | Loma Prieta, CA | 17/10/89 | 7.1 | Caldecott | Caltrans | HW | 6 | R | 243 | 0.04 | 1 | Yashinsky, 1998 |
| 57 | 6-15 | Loma Prieta, CA | 17/10/89 | 7.1 | MacArthur | Caltrans | HW | | R | 46 | 0.04 | 1 | Yashinsky, 1998 |
| 58 | 6-16 | Loma Prieta, CA | 17/10/89 | 7.1 | Stanford | SFWD | WT | 5-7 | R | 23 | 0.14 | 1 | SFWD |
| 59 | 6-17 | Loma Prieta, CA | 17/10/89 | 7.1 | Hillsborough | SFWD | WT | 5-7 | R | 62 | 0.08 | 1 | SFWD |
| 60 | 6-18 | Loma Prieta, CA | 17/10/89 | 7.1 | Sunol Aqud. #1 | SFWD | WT | 5 | R | | 0.09 | 1 | SFWD |
| 61 | 6-19 | Loma Prieta, CA | 17/10/89 | 7.1 | Sunol Aqud. #2 | SFWD | WT | 5 | R | | 0.09 | 1 | SFWD |
| 62 | 6-20 | Loma Prieta, CA | 17/10/89 | 7.1 | Sunol Aqud. #3 | SFWD | WT | 5 | R | | 0.09 | 1 | SFWD |
| 63 | 6-21 | Loma Prieta, CA | 17/10/89 | 7.1 | Sunol Aqud. #4 | SFWD | WT | 5 | R | | 0.09 | 1 | SFWD |
| 64 | 6-22 | Loma Prieta, CA | 17/10/89 | 7.1 | Sunol Aqud. #5 | SFWD | WT | 5 | R | | 0.09 | 1 | SFWD |
| 65 | 7-1 | Petrolia, CA | 25/4/92 | 6.9 | Tunnel #40 | NCRR | RR | 5 | S | | 0.13 | 1 | NCRR |
| 66 | 7-2 | Petrolia, CA | 25/4/92 | 6.9 | Tunnel #39 | NCRR | RR | 5-3 | R | | 0.25 | 1 | NCRR |
| 67 | 7-3 | Petrolia, CA | 25/4/92 | 6.9 | Tunnel #38 | NCRR | RR | 5-3 | R | | 0.21 | 2 | NCRR |

| EQID | CASE | EQNAME | DATE | Mw | TNAME | OWNER | FUN | LINER SYSTEM | ROCK SOIL | COVER (M) | PGA (G) | DS | REFERENCE, NOTES |
|---|---|---|---|---|---|---|---|---|---|---|---|---|---|
| 68 | 7-4 | Petrolia, CA | 25/4/92 | 6.9 | Tunnel #37 | NCRR | RR | 5 | R | | 0.15 | 1 | NCRR |
| 69 | 7-5 | Petrolia, CA | 25/4/92 | 6.9 | Tunnel #36 | NCRR | RR | 5-3 | R | | 0.13 | 1 | NCRR |
| 70 | 7-6 | Petrolia, CA | 25/4/92 | 6.9 | Tunnel #35 | NCRR | RR | 5-3 | R | | 0.12 | 1 | NCRR |
| 71 | 7-7 | Petrolia, CA | 25/4/92 | 6.9 | Tunnel #34 | NCRR | RR | 5-3 | R | | 0.12 | 2 | NCRR |
| 72 | 7-8 | Petrolia, CA | 25/4/92 | 6.9 | Tunnel #31 | NCRR | RR | 5-3 | R | | 0.08 | 1 | NCRR |
| 73 | 7-9 | Petrolia, CA | 25/4/92 | 6.9 | Tunnel #30 | NCRR | RR | 5 | R | | 0.08 | 1 | NCRR |
| 74 | 7-10 | Petrolia, CA | 25/4/92 | 6.9 | Tunnel #29 | NCRR | RR | 5 | R | | 0.06 | 1 | NCRR |
| 75 | 7-11 | Petrolia, CA | 25/4/92 | 6.9 | Tunnel #28 | NCRR | RR | 5-3 | R | | 0.06 | 1 | NCRR |
| 76 | 8-1 | Hokkaido, Japan | 0/0/93 | 7.8 | Seikan | | HW | 6 | | | 0.32 | 1 | JTA, 1994 |
| 77 | 9-1 | Northridge, CA | 17/1/94 | 6.7 | Pershing Sq St. | LAMT | RR | 6 | R | | 0.27 | 1 | Tunnels & Tunneling, 1994 |
| 78 | 9-2 | Northridge, CA | 17/1/94 | 6.7 | McArthur St. | LAMT | RR | 6 | R | | 0.27 | 1 | Tunnels & Tunneling, 1994 |
| 79 | 9-3 | Northridge, CA | 17/1/94 | 6.7 | Civic Center St. | LAMT | RR | 6 | R | | 0.27 | 1 | Tunnels & Tunneling, 1994 |
| 80 | 9-4 | Northridge, CA | 17/1/94 | 6.7 | Tun# 25 @ I-5/14 | SPRR | RR | 5 | R | 92 | 0.67 | 2 | METROLINK |
| 81 | 9-5 | Northridge, CA | 17/1/94 | 6.7 | Santa Susana | SPRR | RR | 5 | R | | 0.47 | 1 | SPRR |
| 82 | 9-6 | Northridge, CA | 17/1/94 | 6.7 | Chatworth | SPRR | RR | 5 | R | | 0.50 | 1 | SPRR |
| 83 | 9-7 | Northridge, CA | 17/1/94 | 6.7 | Chatworth | SPRR | RR | 5 | R | | 0.50 | 1 | SPRR |
| 84 | 9-8 | Northridge, CA | 17/1/94 | 6.7 | Near I15 at Cajon Junc | ATSF | RR | | R | | 0.10 | 1 | ATSF |
| 85 | 9-9 | Northridge, CA | 17/1/94 | 6.7 | Balboa inlet | MWD | WT | 2-5-6-7 | R | | 0.67 | 1 | MWD |
| 86 | 9-10 | Northridge, CA | 17/1/94 | 6.7 | Balboa outlet | MWD | WT | | R | | 0.58 | 1 | MWD |
| 87 | 9-11 | Northridge, CA | 17/1/94 | 6.7 | Castaic #1 | MWD | WT | 6-7 | R | | 0.29 | 1 | MWD |
| 88 | 9-12 | Northridge, CA | 17/1/94 | 6.7 | Castaic #2 | MWD | WT | 6-7 | R | | 0.36 | 1 | MWD |
| 89 | 9-13 | Northridge, CA | 17/1/94 | 6.7 | Saugus | MWD | WT | 6-7 | S | | 0.54 | 1 | MWD |
| 90 | 9-14 | Northridge, CA | 17/1/94 | 6.7 | Placerita | MWD | WT | 6-7 | R | | 0.62 | 1 | MWD |
| 91 | 9-15 | Northridge, CA | 17/1/94 | 6.7 | Newhall | MWD | WT | 2-5-6-7 | R | | 0.68 | 3-4 | MWD. Damage attributed to fluid pressure buildup behind tunnel and not to earthquake shaking |
| 92 | 9-16 | Northridge, CA | 17/1/94 | 6.7 | San Fernando | MWD | WT | 5-6-7 | R/S | | 0.50 | 1 | MWD |
| 93 | 9-17 | Northridge, CA | 17/1/94 | 6.7 | Sepulveda | MWD | WT | 5-7 | R | | 0.27 | 1 | MWD |
| 94 | 9-18 | Northridge, CA | 17/1/94 | 6.7 | Hollywood | MWD | WT | | R | | 0.22 | 1 | MWD |
| 95 | 9-19 | Northridge, CA | 17/1/94 | 6.7 | San Rafael #1 | MWD | WT | 6 | R | | 0.16 | 1 | MWD |
| 96 | 9-20 | Northridge, CA | 17/1/94 | 6.7 | San Rafael #2 | MWD | WT | 6 | R | | 0.18 | 1 | MWD |
| 97 | 9-21 | Northridge, CA | 17/1/94 | 6.7 | Pasadena | MWD | WT | 6 | S | | 0.15 | 1 | MWD |
| 98 | 9-22 | Northridge, CA | 17/1/94 | 6.7 | Siera Madre | MWD | WT | | S | | 0.13 | 1 | MWD |
| 99 | 9-23 | Northridge, CA | 17/1/94 | 6.7 | Monrovia #1, #2 | MWD | WT | 5-6 | R | | 0.09 | 1 | MWD |

| EQID | CASE | EQNAME | DATE | Mw | TNAME | OWNER | FUN | LINER SYSTEM | ROCK SOIL | COVER (M) | PGA (G) | DS | REFERENCE, NOTES |
|---|---|---|---|---|---|---|---|---|---|---|---|---|---|
| 100 | 9-24 | Northridge, CA | 17/1/94 | 6.7 | Monrovia #3 | MWD | WT | 5-6 | R | | 0.10 | 1 | MWD |
| 101 | 9-25 | Northridge, CA | 17/1/94 | 6.7 | Monrovia #4 | MWD | WT | 5-6 | R | | 0.10 | 1 | MWD |
| 102 | 9-26 | Northridge, CA | 17/1/94 | 6.7 | Glendora | MWD | WT | 2-5-6-7 | R/S | | 0.07 | 1 | MWD |
| 103 | 9-27 | Northridge, CA | 17/1/94 | 6.7 | Oakhill | MWD | WT | | R | | 0.15 | 1 | MWD |
| 104 | 9-28 | Northridge, CA | 17/1/94 | 6.7 | Ascat | MWD | WT | | R | | 0.14 | 1 | MWD |
| 105 | 9-29 | Northridge, CA | 17/1/94 | 6.7 | Tonner #1 | MWD | WT | 5-7 | R | | 0.06 | 1 | MWD |
| 106 | 9-30 | Northridge, CA | 17/1/94 | 6.7 | Tonner #2 | MWD | WT | 5-7 | R | | 0.06 | 1 | MWD |
| 107 | 9-31 | Northridge, CA | 17/1/94 | 6.7 | LA Aqueduct | LADWP | WT | 5 | | 46 | 0.67 | 2 | LADWP |
| 108 | 10-1 | Kobe, Japan | 17/1/95 | 6.9 | Rokkou (#1) | JRN | RR | 5 | | 460 | 0.60 | 3 | Geo. Eng. Assn., 1996 |
| 109 | 10-2 | Kobe, Japan | 17/1/95 | 6.9 | Kobe (#2) | JRN | RR | 5 | | 272 | 0.57 | 2 | Geo. Eng. Assn., 1996 |
| 110 | 10-3 | Kobe, Japan | 17/1/95 | 6.9 | Suma (#3) | JRN | RR | 5 | | 45 | 0.53 | 1 | Geo. Eng. Assn., 1996 |
| 111 | 10-4 | Kobe, Japan | 17/1/95 | 6.9 | Okuhata (#4) | JRN | RR | 5 | | 90 | 0.50 | 1 | Geo. Eng. Assn., 1996 |
| 112 | 10-5 | Kobe, Japan | 17/1/95 | 6.9 | Takatsukay(#5) | JRN | RR | 5 | | 85 | 0.49 | 1 | Geo. Eng. Assn., 1996 |
| 113 | 10-6 | Kobe, Japan | 17/1/95 | 6.9 | Nagasaka (#6) | JRN | RR | 5 | | 20 | 0.48 | 2 | Geo. Eng. Assn., 1996 |
| 114 | 10-7 | Kobe, Japan | 17/1/95 | 6.9 | Daiichinas (#7) | JRN | RR | 5 | | 150 | 0.55 | 1 | Geo. Eng. Assn., 1996 |
| 115 | 10-8 | Kobe, Japan | 17/1/95 | 6.9 | Ikuse (#8) | JRN | RR | 5 | | 250 | 0.57 | 1 | Geo. Eng. Assn., 1996 |
| 116 | 10-9 | Kobe, Japan | 17/1/95 | 6.9 | Daiichitaked(#9) | JRN | RR | 5 | | 95 | 0.43 | 1 | Geo. Eng. Assn., 1996 |
| 117 | 10-10 | Kobe, Japan | 17/1/95 | 6.9 | Arima (#12) | KBD | RR | 5 | | 25 | 0.46 | 3 | Geo. Eng. Assn., 1996 |
| 118 | 10-11 | Kobe, Japan | 17/1/95 | 6.9 | Gosha (#13) | KBD | RR | 5 | | 40 | 0.41 | 1 | Geo. Eng. Assn., 1996 |
| 119 | 10-12 | Kobe, Japan | 17/1/95 | 6.9 | Kitakami (#14) | HOE | RR | 6 | | 350 | 0.51 | 3 | Geo. Eng. Assn., 1996 |
| 120 | 10-13 | Kobe, Japan | 17/1/95 | 6.9 | Iwataki (#15) | HRP | HW | 5 | | 135 | 0.58 | 3 | Geo. Eng. Assn., 1996 |
| 121 | 10-14 | Kobe, Japan | 17/1/95 | 6.9 | Nunohiki(#18) | MRP | HW | 5 | | 260 | 0.58 | 3 | Geo. Eng. Assn., 1996 |
| 122 | 10-15 | Kobe, Japan | 17/1/95 | 6.9 | Daini Nun (#19) | MRP | HW | 5 | | 240 | 0.58 | 2 | Geo. Eng. Assn., 1996 |
| 123 | 10-16 | Kobe, Japan | 17/1/95 | 6.9 | Hirano (#20) | MRP | HW | 5 | | 85 | 0.58 | 1 | Geo. Eng. Assn., 1996 |
| 124 | 10-17 | Kobe, Japan | 17/1/95 | 6.9 | K. Daiichi (#21) | MRP | HW | 5 | | 32 | 0.58 | 1 | Geo. Eng. Assn., 1996 |
| 125 | 10-18 | Kobe, Japan | 17/1/95 | 6.9 | K. Daini (#22) | MRP | HW | 5 | | 25 | 0.58 | 1 | Geo. Eng. Assn., 1996 |
| 126 | 10-19 | Kobe, Japan | 17/1/95 | 6.9 | Kamoetsu 1(#23) | MRP | HW | 5 | | 29 | 0.55 | 1 | Geo. Eng. Assn., 1996 |
| 127 | 10-20 | Kobe, Japan | 17/1/95 | 6.9 | Kamoetsu 2(#24) | MRP | HW | 5 | | 40 | 0.55 | 2 | Geo. Eng. Assn., 1996 |
| 128 | 10-21 | Kobe, Japan | 17/1/95 | 6.9 | Kamoetsu 3(#25) | MRP | HW | 5 | | 47 | 0.55 | 2 | Geo. Eng. Assn., 1996 |
| 129 | 10-22 | Kobe, Japan | 17/1/95 | 6.9 | Hiyodori (#26) | MRP | HW | 5 | | 40 | 0.54 | 1 | Geo. Eng. Assn., 1996 |
| 130 | 10-23 | Kobe, Japan | 17/1/95 | 6.9 | Shin-kobe 1(#27) | MRP | HW | 5 | | 330 | 0.49 | 2 | Geo. Eng. Assn., 1996 |
| 131 | 10-24 | Kobe, Japan | 17/1/95 | 6.9 | Shin-kobe 2(#28) | MRP | HW | 5 | | 330 | 0.49 | 2 | Geo. Eng. Assn., 1996 |
| 132 | 10-25 | Kobe, Japan | 17/1/95 | 6.9 | Karaki (#29) | MRP | HW | 5 | | 145 | 0.42 | 3 | Geo. Eng. Assn., 1996 |
| 133 | 10-26 | Kobe, Japan | 17/1/95 | 6.9 | Arino 1 (#30) | MRP | HW | 5 | | 25 | 0.39 | 1 | Geo. Eng. Assn., 1996 |

| EQID | CASE | EQNAME | DATE | Mw | TNAME | OWNER | FUN | LINER SYSTEM | ROCK SOIL | COVER (M) | PGA (G) | DS | REFERENCE, NOTES |
|---|---|---|---|---|---|---|---|---|---|---|---|---|---|
| 134 | 10-27 | Kobe, Japan | 17/1/95 | 6.9 | Arino 2 (#31) | MRP | HW | 5 | | 35 | 0.38 | 1 | Geo. Eng. Assn., 1996 |
| 135 | 10-28 | Kobe, Japan | 17/1/95 | 6.9 | Rokkousan (#32) | MRP | HW | 5 | | 280 | 0.51 | 2 | Geo. Eng. Assn., 1996 |
| 136 | 10-29 | Kobe, Japan | 17/1/95 | 6.9 | Shinohara (#33) | MRP | HW | 5 | | 15 | 0.55 | 1 | Geo. Eng. Assn., 1996 |
| 137 | 10-30 | Kobe, Japan | 17/1/95 | 6.9 | Hiyodori (#34) | MRP | HW | 5 | | 67 | 0.59 | 2 | Geo. Eng. Assn., 1996 |
| 138 | 10-31 | Kobe, Japan | 17/1/95 | 6.9 | Suma (#36) | CDO | | 5 | | 140 | 0.44 | 1 | Geo. Eng. Assn., 1996 |
| 139 | 10-32 | Kobe, Japan | 17/1/95 | 6.9 | Suma ext (#37) | CDO | | 5 | | | 0.58 | 1 | Geo. Eng. Assn., 1996 |
| 140 | 10-33 | Kobe, Japan | 17/1/95 | 6.9 | Ibuki (#38) | HHP | HW | 5 | | 20 | 0.43 | 1 | Geo. Eng. Assn., 1996 |
| 141 | 10-34 | Kobe, Japan | 17/1/95 | 6.9 | Taizanji,1E(#39) | HHP | HW | 5 | | 53 | 0.44 | 1 | Geo. Eng. Assn., 1996 |
| 142 | 10-35 | Kobe, Japan | 17/1/95 | 6.9 | Taizanji,1W(#40) | HHP | HW | 5 | | 37 | 0.44 | 1 | Geo. Eng. Assn., 1996 |
| 143 | 10-36 | Kobe, Japan | 17/1/95 | 6.9 | Taizanji,2E(#41) | HHP | HW | 5 | | 25 | 0.45 | 1 | Geo. Eng. Assn., 1996 |
| 144 | 10-37 | Kobe, Japan | 17/1/95 | 6.9 | Taizanji,2W(#42) | HHP | HW | 5 | | 17 | 0.45 | 1 | Geo. Eng. Assn., 1996 |
| 145 | 10-38 | Kobe, Japan | 17/1/95 | 6.9 | Aina, E(#43) | HHP | HW | 5 | | 68 | 0.46 | 1 | Geo. Eng. Assn., 1996 |
| 146 | 10-39 | Kobe, Japan | 17/1/95 | 6.9 | Aina, W(#44) | HHP | HW | 5 | | 65 | 0.46 | 1 | Geo. Eng. Assn., 1996 |
| 147 | 10-40 | Kobe, Japan | 17/1/95 | 6.9 | Nagasaka.,E(#45) | HHP | HW | 5 | | 68 | 0.42 | 1 | Geo. Eng. Assn., 1996 |
| 148 | 10-41 | Kobe, Japan | 17/1/95 | 6.9 | Nagasaka.,W(#46) | HHP | HW | 5 | | 68 | 0.42 | 1 | Geo. Eng. Assn., 1996 |
| 149 | 10-42 | Kobe, Japan | 17/1/95 | 6.9 | T.Higa.,TOK(#47) | JHP | HW | 5 | | 62 | 0.58 | 1 | Geo. Eng. Assn., 1996 |
| 150 | 10-43 | Kobe, Japan | 17/1/95 | 6.9 | T.Higa.,KYU(#48) | JHP | HW | 5 | | 59 | 0.58 | 1 | Geo. Eng. Assn., 1996 |
| 151 | 10-44 | Kobe, Japan | 17/1/95 | 6.9 | T.Nishi,TOK(#49) | JHP | HW | 5 | | 42 | 0.57 | 1 | Geo. Eng. Assn., 1996 |
| 152 | 10-45 | Kobe, Japan | 17/1/95 | 6.9 | T.Nishi,KYU(#50) | JHP | HW | 5 | | 42 | 0.57 | 1 | Geo. Eng. Assn., 1996 |
| 153 | 10-46 | Kobe, Japan | 17/1/95 | 6.9 | Takak.,1TOK(#51) | JHP | HW | 5 | | 97 | 0.59 | 1 | Geo. Eng. Assn., 1996 |
| 154 | 10-47 | Kobe, Japan | 17/1/95 | 6.9 | Takak.,2TOK(#52) | JHP | HW | 5 | | 86 | 0.59 | 1 | Geo. Eng. Assn., 1996 |
| 155 | 10-48 | Kobe, Japan | 17/1/95 | 6.9 | Takak.,KYU(#53) | JHP | HW | 5 | | 87 | 0.59 | 1 | Geo. Eng. Assn., 1996 |
| 156 | 10-49 | Kobe, Japan | 17/1/95 | 6.9 | Tsuki.,TOK(#54) | JHP | HW | 5 | | 43 | 0.60 | 1 | Geo. Eng. Assn., 1996 |
| 157 | 10-50 | Kobe, Japan | 17/1/95 | 6.9 | Takak.,KYU(#55) | JHP | HW | 5 | | 34 | 0.60 | 1 | Geo. Eng. Assn., 1996 |
| 158 | 10-51 | Kobe, Japan | 17/1/95 | 6.9 | Omoteyama 1(#61) | KTB | RR | 5 | | 41 | 0.41 | 1 | Geo. Eng. Assn., 1996 |
| 159 | 10-52 | Kobe, Japan | 17/1/95 | 6.9 | Ochiai (#63) | KTB | RR | 5 | | | 0.56 | 1 | Geo. Eng. Assn., 1996 |
| 160 | 10-53 | Kobe, Japan | 17/1/95 | 6.9 | Yokoo, 1 (#64) | KTB | RR | 5 | | | 0.59 | 1 | Geo. Eng. Assn., 1996 |
| 161 | 10-54 | Kobe, Japan | 17/1/95 | 6.9 | Yokoo, 2 (#65) | KTB | RR | 5 | | | 0.60 | 1 | Geo. Eng. Assn., 1996 |
| 162 | 10-55 | Kobe, Japan | 17/1/95 | 6.9 | Shiroyama (#66) | JRN | RR | 5 | | | 0.58 | 1 | Geo. Eng. Assn., 1996 |
| 163 | 10-56 | Kobe, Japan | 17/1/95 | 6.9 | Nashio 2 (#67) | JRN | RR | 5 | | | 0.48 | 1 | Geo. Eng. Assn., 1996 |
| 164 | 10-57 | Kobe, Japan | 17/1/95 | 6.9 | Takedo 2 (#68) | JRN | RR | 5 | | | 0.40 | 1 | Geo. Eng. Assn., 1996 |
| 165 | 10-58 | Kobe, Japan | 17/1/95 | 6.9 | Douba 1 (#69) | JRN | RR | 5 | | | 0.40 | 1 | Geo. Eng. Assn., 1996 |
| 166 | 10-59 | Kobe, Japan | 17/1/95 | 6.9 | Douba 2 (#70) | JRN | RR | 5 | | | 0.37 | 1 | Geo. Eng. Assn., 1996 |
| 167 | 10-60 | Kobe, Japan | 17/1/95 | 6.9 | Douba 3 (#71) | JRN | RR | 5 | | | 0.36 | 1 | Geo. Eng. Assn., 1996 |

| EQID | CASE | EQNAME | DATE | Mw | TNAME | OWNER | FUN | LINER SYSTEM | ROCK SOIL | COVER (M) | PGA (G) | DS | REFERENCE, NOTES |
|---|---|---|---|---|---|---|---|---|---|---|---|---|---|
| 168 | 10-61 | Kobe, Japan | 17/1/95 | 6.9 | Keietu (#76) | KBD | RR | 5 | | | 0.58 | 1 | Geo. Eng. Assn., 1996 |
| 169 | 10-62 | Kobe, Japan | 17/1/95 | 6.9 | Nakayama(#77) | KBD | RR | 5 | | | 0.58 | 1 | Geo. Eng. Assn., 1996 |
| 170 | 10-63 | Kobe, Japan | 17/1/95 | 6.9 | Kadoyama (#78) | KBD | RR | 5 | | | 0.58 | 1 | Geo. Eng. Assn., 1996 |
| 171 | 10-64 | Kobe, Japan | 17/1/95 | 6.9 | Kudari (#79) | KBD | RR | 5 | | | 0.54 | 1 | Geo. Eng. Assn., 1996 |
| 172 | 10-65 | Kobe, Japan | 17/1/95 | 6.9 | Kik, Nobori(#81) | KBD | RR | 5 | | | 0.54 | 1 | Geo. Eng. Assn., 1996 |
| 173 | 10-66 | Kobe, Japan | 17/1/95 | 6.9 | Tanigami (#82) | KBD | RR | 6 | | | 0.41 | 1 | Geo. Eng. Assn., 1996 |
| 174 | 10-67 | Kobe, Japan | 17/1/95 | 6.9 | Kobe (#84) | KBD | RR | | | | 0.56 | 1 | Geo. Eng. Assn., 1996 |
| 175 | 10-68 | Kobe, Japan | 17/1/95 | 6.9 | Aina (#85) | KBD | RR | | | | 0.48 | 1 | Geo. Eng. Assn., 1996 |
| 176 | 10-69 | Kobe, Japan | 17/1/95 | 6.9 | Tetsukaiy (#87) | MRP | HW | 5 | | 20 | 0.60 | 1 | Geo. Eng. Assn., 1996 |
| 177 | 10-70 | Kobe, Japan | 17/1/95 | 6.9 | Taisanji (#88) | MRP | HW | 5 | | 50 | 0.44 | 1 | Geo. Eng. Assn., 1996 |
| 178 | 10-71 | Kobe, Japan | 17/1/95 | 6.9 | Kaibara (#89) | MRP | HW | 5 | | 20 | 0.36 | 1 | Geo. Eng. Assn., 1996 |
| 179 | 10-72 | Kobe, Japan | 17/1/95 | 6.9 | Shimohata (#91) | MRP | HW | 5 | | 20 | 0.60 | 1 | Geo. Eng. Assn., 1996 |
| 180 | 10-73 | Kobe, Japan | 17/1/95 | 6.9 | Fukuchi (#92) | MRP | HW | 5 | | 20 | 0.36 | 1 | Geo. Eng. Assn., 1996 |
| 181 | 10-74 | Kobe, Japan | 17/1/95 | 6.9 | Sumadera (#93) | MRP | HW | 5 | | 15 | 0.60 | 1 | Geo. Eng. Assn., 1996 |
| 182 | 10-75 | Kobe, Japan | 17/1/95 | 6.9 | Shin Arima (#95) | MRP | HW | 5 | | 20 | 0.48 | 1 | Geo. Eng. Assn., 1996 |
| 183 | 10-76 | Kobe, Japan | 17/1/95 | 6.9 | HigashiAina(#96) | MRP | HW | 5 | | 10 | 0.43 | 1 | Geo. Eng. Assn., 1996 |
| 184 | 10-77 | Kobe, Japan | 17/1/95 | 6.9 | Fukuyama (#97) | MRP | HW | 5 | | 15 | 0.59 | 1 | Geo. Eng. Assn., 1996 |
| 185 | 10-78 | Kobe, Japan | 17/1/95 | 6.9 | Minoya (#98) | MRP | HW | 5 | | 20 | 0.40 | 1 | Geo. Eng. Assn., 1996 |
| 186 | 10-79 | Kobe, Japan | 17/1/95 | 6.9 | Iwayama (#99) | MRP | HW | 5 | | 30 | 0.56 | 1 | Geo. Eng. Assn., 1996 |
| 187 | 10-80 | Kobe, Japan | 17/1/95 | 6.9 | Tamasaka (#100) | MRP | HW | 5 | | 10 | 0.58 | 1 | Geo. Eng. Assn., 1996 |
| 188 | 10-81 | Kobe, Japan | 17/1/95 | 6.9 | Fukiage (#101) | MWB | HW | 5 | | 30 | 0.44 | 1 | Geo. Eng. Assn., 1996 |
| 189 | 10-82 | Kobe, Japan | 17/1/95 | 6.9 | Maesaki (#102) | MWB | HW | 5 | | 10 | 0.43 | 1 | Geo. Eng. Assn., 1996 |
| 190 | 10-83 | Kobe, Japan | 17/1/95 | 6.9 | Nishikou 2 (103) | MWB | HW | 5 | | 20 | 0.39 | 1 | Geo. Eng. Assn., 1996 |
| 191 | 10-84 | Kobe, Japan | 17/1/95 | 6.9 | Fusehatagami (104) | MWB | HW | 5 | | 30 | 0.47 | 1 | Geo. Eng. Assn., 1996 |
| 192 | 10-85 | Kobe, Japan | 17/1/95 | 6.9 | Fusehatashita (105) | MWB | HW | 5 | | 30 | 0.47 | 1 | Geo. Eng. Assn., 1996 |
| 193 | 10-86 | Kobe, Japan | 17/1/95 | 6.9 | Enoshitayama (109) | | WT | 4 | | 37 | 0.60 | 3 | Geo. Eng. Assn., 1996 |
| 194 | 10-87 | Kobe, Japan | 17/1/95 | 6.9 | Motoyama (110) | | WT | | | 96 | 0.59 | 3 | Geo. Eng. Assn., 1996 |
| 195 | 10-88 | Kobe, Japan | 17/1/95 | 6.9 | N. of Itayada St. | KMS | RR | 6 | | | 0.60 | 1 | Japan Society of Civil Eng, 1995 |
| 196 | 10-89 | Kobe, Japan | 17/1/95 | 6.9 | Near Natani | KMS | RR | 5 | | | 0.60 | 1 | Japan Society of Civil Eng, 1995 |
| 197 | 10-90 | Kobe, Japan | 17/1/95 | 6.9 | Koigawa river | | WT | 6 | | | 0.60 | 1 | Geo. Eng. Ass., 1996 |
| 198 | 10-91 | Kobe, Japan | 17/1/95 | 6.9 | Hosoyadani | | WT | 5 | | 6 | 0.59 | 1 | Geo. Eng. Ass., 1996 |
| 199 | 10-92 | Kobe, Japan | 17/1/95 | 6.9 | Sennomori | | WT | 5 | | 30 | 0.59 | 2 | Geo. Eng. Ass., 1996 |
| 200 | 10-93 | Kobe, Japan | 17/1/95 | 6.9 | Shioyadani | | WT | 5 | | 25 | 0.59 | 2 | Geo. Eng. Ass., 1996 |

| EQID | CASE | EQNAME | DATE | Mw | TNAME | OWNER | FUN | LINER SYSTEM | ROCK SOIL | COVER (M) | PGA (G) | DS | REFERENCE, NOTES |
|---|---|---|---|---|---|---|---|---|---|---|---|---|---|
| 201 | 10-94 | Kobe, Japan | 17/1/95 | 6.9 | Kabutoyama-Ashiya | HWC | WT | 5 | | 25 | 0.58 | 1 | Geo. Eng. Ass., 1996 |
| 202 | 10-95 | Kobe, Japan | 17/1/95 | 6.9 | Sannomiya St. 3 | | UT | 6 | | 25 | 0.59 | 2 | Geo. Eng. Ass., 1996 |
| 203 | 10-96 | Kobe, Japan | 17/1/95 | 6.9 | NTT @ Chuo-ku | NTT | UT | 6 | S | | 0.60 | 2 | Japan Society of Civil Eng, 1995 |
| 204 | 10-97 | Kobe, Japan | 17/1/95 | 6.9 | Kansai Electric | KEP | UT | 5 | S | | 0.60 | 2 | Japan Society of Civil Eng, 1995 |
| 205 | | Kobe, Japan | 17/1/95 | 6.9 | HIGASHIYAMA (#10) | KER | RR | 4, 5 | | 4-8 | 0.70 | 3 | Asakura and Sato, 1998 |
| 206 | | Kobe, Japan | 17/1/95 | 6.9 | EGEYAMA (#11) | KER | RR | 4, 5 | | 2-13 | 0.68 | 3 | Asakura and Sato, 1998 |
| 207 | | Kobe, Japan | 17/1/95 | 6.9 | MAIKO (UP) (#16) | HSB | HW | 5 | | 4-50 | 0.62 | 2 | Asakura and Sato, 1998 |
| 208 | | Kobe, Japan | 17/1/95 | 6.9 | MAIKO (DOWN) (#17) | HSB | HW | 5 | | 4-50 | 0.62 | 2 | Asakura and Sato, 1998 |
| 209 | | Kobe, Japan | 17/1/95 | 6.9 | SHIOYA-DAN (#35) | KPW | HW | 5 | | 4-80 | 0.70 | 3 | Asakura and Sato, 1998 |
| 210 | | Kobe, Japan | 17/1/95 | 6.9 | SEISHIN (2) (#58) | KTB | RR | 6 | | 7 | 0.36 | 1 | Asakura and Sato, 1998 |
| 211 | | Kobe, Japan | 17/1/95 | 6.9 | SEISHIN (1) (#59) | KTB | RR | 6 | | 3 | 0.37 | 1 | Asakura and Sato, 1998 |
| 212 | | Kobe, Japan | 17/1/95 | 6.9 | OMOTEYAMA (2) (#60) | KTB | RR | 6 | | | 0.41 | 1 | Asakura and Sato, 1998 |
| 213 | | Kobe, Japan | 17/1/95 | 6.9 | KODERA (#62) | KTB | RR | 6 | | 7 | 0.47 | 1 | Asakura and Sato, 1998 |
| 214 | | Kobe, Japan | 17/1/95 | 6.9 | OBU (#86) | KPW | HW | 5 | | 50 | 0.55 | 1 | Asakura and Sato, 1998 |
| 215 | | Kobe, Japan | 17/1/95 | 6.9 | AINA (#90) | KPW | HW | 5 | | 2 | 0.43 | 1 | Asakura and Sato, 1998 |
| 216 | | Kobe, Japan | 17/1/95 | 6.9 | FUTATABI (#94) | KPW | | 5 | | 20 | 0.70 | 1 | Asakura and Sato, 1998 |
| 217 | | Kobe, Japan | 17/1/95 | 6.9 | SENGARI (#111) | KWS | WT | 5 | | 2-25 | 0.60 | 3 | Asakura and Sato, 1998 |

*Table C-2. Bored Tunnel Seismic Performance Database*

| Earthquake | Date and Time | Location of Epicenter | Magnitude, JMA Intensity | Area Most Severely Affected | Tunnel Performance | Selected References |
|---|---|---|---|---|---|---|
| 1923 Kanto | Sep. 1<br>11:58 AM | Sagami Bay<br>139.3 E, 35.2 N (unknown) | 7.90<br>VI | Kanagawa and Tokyo | Extensive, severest damage to more than 100 tunnels in southern Kanto area | JSCE [1984]<br>Yoshikawa [1979] |
| 1927 Kits-Tango | Mar. 7<br>6:27 PM | 7 km WNW of Miyazu, Kyoto<br>135.15 E, 35.53 N (0) | 7.30<br>VI | Joint section of Tango Peninsula | Very slight damage to 2 railroad tunnels in the epicentral region | Yoshikawa [1979]<br>Yoshikawa [1984] |
| 1930 Kita-Isu | Nov. 26<br>4:02 AM | 7 km west of Atami, Shizuoka<br>139.0 E, 35.1 N (0) | 7.30<br>VI | Northerm part of Izu Peninsula | Very severe damage to one railroad tunnel due to earthquake fault crossing | Yoshikawa [1979]<br>Yoshikawa [1982] |
| 1948 Fukui | June 28<br>4:13 PM | 12 km north of Fukui City<br>136.20 E, 36.17 N (0) | 7.10<br>VI | Fukui Plain | Severe damage to 2 railroad tunnels within 8 km from the earthquake fault | Yoshikawa [1979] |
| 1952 Tokachi-oki | Mar. 4<br>10:23 AM | Pacific Ocean 90 km ESE of f the Cape Erimo<br>144.13 E, 41.80 N (0) | 8.20<br>VI – V | Southern part of Hokkaido | Slight damage to 10 rail-road tunnels in Hokkaido | Committee Report [1954]<br>Yoshikawa [1979] |
| 1961 Kita-Mino | Aug. 19<br>2:33 PM | Border of Fukui and Gifu Prefectures<br>136 46'E, 36 0l'N (0) | 7.00<br>IV | Vicinity along the border of Fuikui and Gifu Prefs. | Cracking damage to a couple of aqueduct tunnels | Okamoto, et al. [1963]<br>Okamoto [1973] |
| 1964 Niigata | June 16<br>1:01 PM | Japan Sea 50 km NNE of Nugata City<br>139 ll'E, 38 21'N (40) | 7.50<br>V – VI | Nugata City | Extensive damage to about 20 railroad tunnels and one road tunnel | JSCE [1966]<br>Kawasumi [1968]<br>Yoshikawa [1979] |
| 1968 Tokachi-oki | May 16<br>9:49 AM | Pacific Ocean 140 km south off the Cape Erimo<br>143 35~E, 40 44~N (0) | 7.90<br>V | Aomori Prefecture | Slight damage to 23 rail-road tunnels in Hokkaido | Committee Report [1969] |
| 1978 Izu-Oshima-kinkai | Jan. 14<br>12:24 PM | In the sea between Oshima Isl. and Inatori, Shizuoka<br>139 15'E, 34 46N (0) | 7.00<br>V VI | South-eastern region of Izu Peninsula | Very severe damage to 9 railroad and 4 road tunnels in a limited area | Onoda, et al. [1978]<br>Konda [1978]<br>Yoshikawa [1979][(1982] |
| 1978 Miyagiken-oki | June 12<br>5:14 PM | Pacific Ocean 115 km east of Sendai City, Miyagi<br>142 l0'E, 38 09~N (40) | 7.40<br>V | Sendai City and vicinity | Slight damage to 6 railroad tunnels mainly existing in Miyagi Prefecture | Committee Report [1980] |
| 1982 Urakawa-oki | Mar. 21<br>11:32 AM | Pcific Ocean 18 km SW of Urakawa, Hokkaido | 7.10<br>IV – V | Urakawa-Cho and Shizunsi-Cho, | Slight damage to 6 railroad tunnels near Urakawa | Yoshikawa [1984] |

| Earthquake | Date and Time | Location of Epicenter | Magnitude, JMA Intensity | Area Most Severely Affected | Tunnel Performance | Selected References |
|---|---|---|---|---|---|---|
| | | 142 36'E, 42 04'N (40) | | southern Hokkaido | | |
| 1983 Nihonkai-chubu | May 26 11:59 AM | Japan Sea 90 km west of Noshiro City, Akita 139 04.6'E, 40 21.4'N (14) | 7.70 V | Noshiro City and Oga City, Akita | Slight damage to 8 railroad tunnels in Akita, etc. | Yoshikawa [1984] JSCE [1986] |
| 1984 Naganoken-seibu | Sep. 14 8:48 AM | 9 km SE of Mt. Ontake, Nagano 137 33.6'E, 35 49.3'N (2) | 6.80 VI - V | Otaki Village, Nagano | Cracking damage to one headrace tunnel | Matauda, et al. [1985] |
| 1993 Notohanto-oki | Feb. 7 10:27 PM | Japan Sea 24 km north of Suzu City, Ishikawa 137 18'E, 37 39'N (25) | 6.60 V | Suzu City | Severe damage to one road tunnel | Kitaura, et al. [1993] Kunita, et al. [1993] |
| 1993 Hokkaido-nansei-oki | July 12 10:17 PM | Japan Sea 86 km west of Suttsu, Hokkaido 139 12'E, 42 47'N (34) | 8 VI - V | Okushiri Isi. and south-western part of Hokkaido | Severe damage to one road tunnel due to a direct hit of falling rock | Miyajima, et al. [1993] Nishikawa, et al. [1993] JSEEP News [1993] |

*Table C-3. Tunnel Performance in Japanese Earthquake*

| JMA | Intensity Scale | Definition | Acceleration (in gals) |
|---|---|---|---|
| 0 | No feeling | Shocks too weak to be felt by humans and registered only by seismographs. | < 0.8 |
| I | Slight | Extremely feeble shocks felt only by persons at rest, or by those who are observant of earthquakes. | 0.8 to 2.5 |
| II | Weak | Shocks felt by most persons; slight shaking of doors and Japanese latticed sliding doors (shoji). | 2.5 to 8 |
| III | Rather Strong | Slight shaking of houses and buildings, rattling of doors and shoji, swinging of hanging objects like electric lamps, and moving of liquids in vessels. | 8 to 25 |
| IV | Strong | Strong shaking of houses and buildings, overturning of unstable objects, and spilling of liquids out of vessels. | 25 to 80 |
| V | Very Strong | Cracks in sidewalks, overturning of gravestone and stone lanterns, etc.; damage to chimneys and mud and plaster warehouses. | 80 to 250 |
| VI | Disastrous | Demolition of houses, but of less than 30% of the total, landslides, fissures in the ground. | 250 to 400 |
| VII | Very Disastrous | Demolition of more than 30% of the total number of houses, intense landslides, large fissures in the ground and faults. | > 400 |

*Table C-4. Japan Meteorological Agency Intensity Scale*

| ID | Earthquake | Name of Tunnel | Location | Use | Length (m) | Cross Section Width x Height (m) | Liner System | Liner Thickness (cm) | Geological Feature | Cover (m) |
|---|---|---|---|---|---|---|---|---|---|---|
| 1 | 1923 Kanto | Hakone No. 1 (up) | Yamakita-Yaga | RR | 284.7 | 4.3 x 4.7 | 4 | 34 - 57 | marlstone, soil | |
| | | (down) | (on Tokaido [Gotemba) Line) | | 285.2 | 4.6 x 5.0 | 4 | 23 - 46 | | |
| 2 | 1923 Kanto | Hakone No. 3 (up) | Yamakita-Yaga | RR | 312.0 | 4.3 x 4.7 | 4 | 23 - 57 | | 4 - 47 |
| | | (down) | (on Tokaido [Gotemba) Line) | | 318.1 | 4.6 x 5.0 | 4 | 23 - 46 | | |
| 3 | 1923 Kanto | Hakone No. 4 (up) | Yamakita-Yaga | RR | 269.9 | 4.3 x 4.7 | 4 | 23 - 57 | | 4 - 53 |
| | | (down) | (on Tokaido [Gotemba] Line) | | 306.8 | 4.6 x 5.0 | 4 | 23 - 57 | | |
| 4 | 1923 Kanto | Hakone No. 7 (up) | Yaga – Surugaoyama | RR | 211.2 | 4.6 x 5.0 | 4 | 34 - 46 | | |
| | | (down) | (on Tokaido [Gotemba] Line) | | 232.9 | 4.3 x 4.7 | 4 | 34 - 57 | | |
| 5 | 1923 Kanto | Nagoe (up) | Kamakura – Zushi | RR | 442.6 | 4.9 x 6.0 | 4-5 | 34 - 46 | mudstone | |
| | | (down) | (on Yokosuka Line) | | 344.3 | 4.3 x 5.6 | 4-5 | 23 - 57 | | |
| 6 | 1923 Kanto | Komine | Odawara – Hayakawa | RR | 260.5 | 9.1 x 6.0 (box) | 4-5 | 126 - 137 | soil | 1 - 17 |
| | | | (on Atami Tokaido] Line) | | | 8.5 x 6.9 (tube) | | | | |
| 7 | 1923 Kanto | Fudoyama | Hayakawa – Nebukawa | RR | 100.6 | 8.7 x 6.9 | 4-5 | 69 - 114 | red agglomerate | 4 - 20 |
| | | | (on Atami Tokaido Line) | | | | | | | |
| 8 | 1923 Kanto | Nenoueyama | Hayakawa – Nebukawa | RR | 105.6 | 8.7 x 6.9 | 4-5 | 91 | black agglomerate, | 12 - 17 |
| | | | (on Atami Tokaido Line) | | | | | | pyroxene andesite | |
| 9 | 1923 Kanto | Komekamiyama | Hayakawa – Nebukawa | RR | 278.6 | 8.7 x 6.9 | 4-5 | 57 - 103 | pyroxene andesite, | 2 - 51 |
| | | | (on Atami Tokaido Line) | | | | | | agglomerate, volcanic ash | |
| 10 | 1923 Kanto | Shimomakiyayama | Hayakawa – Nebukawa | RR | 160.9 | 8.7 x 6.9 | 4-5 | 69 - 103 | pyroxene andesite, | 14 - 31 |
| | | | (on Ataini [Tokaido] Line) | | | | | | volcanic ash | |
| 11 | 1923 Kanto | Happonmatan | Nebukawa – Manazurn | RR | 76.4 | 8.7 x 6.9 | 4-5 | 69 - 91 | loose agglomerate | < 17 |
| | | | (on Atami [Tokaido] Line) | | | | | | | |
| 12 | 1923 Kanto | Nagasakayama | Nebukawa – Manazurn | RR | 673.9 | 8.5 x 6.9 | 4-5 | 57 - 91 | agglomerate | 11 - 94 |
| | | | (on Atami Tokaido] Line) | | | | | | | |
| 13 | 1923 Kanto | Yose | Sagainiko – Fujino | RR | 292.6 | 4.6 x 5.0 | 4 | 46 - 69 | soil | 4 - 21 |
| | | | (on Chuo Line) | | | | | | | |

| ID | Earthquake | Name of Tunnel | Location | Use | Length (m) | Cross Section Width x Height (m) | Liner System | Liner Thickness (cm) | Geological Feature | Cover (m) |
|---|---|---|---|---|---|---|---|---|---|---|
| 14 | 1923 Kanto | Toke | Toke – Ohami (on Boso [Sotobo] Line) | RR | 353.3 | 4.3 x 4.5 | 4 | 34 - 46 | mudstone | 12 - 20 |
| 15 | 1923 Kanto | Namuya | Iwal – Tomiura (on Hojo [Uchibo] Line) | RR | 740.3 | 4.9 x 6.0 | 4-5 | 30 - 57 | shale, tuffite | 9 - 70 |
| 16 | 1923 Kanto | Mineokayama | Futorni - Awakamogawa (on Awa [Uchibo] Line) | RR | 772.5 | 4.9 x 6.0 | 4 | 30 - 47 | sandstone, shale, gabbro | |
| 17 | 1930 Kita-Izu | Tanna | Atami – Kannami (on Atami [Tokaido] Line) | RR | 7804.0 | 8.5 x 6.4 | 4-5 | 32 - 136 | amdesite, agglomerate | |
| 18 | 1961 Kita-Mino | I Power Plant | upperstream of Tedori River | WT | 2538.0 | 2.1 x 2.2<br>2.4 x 2.45 | 5<br>5 | 20 - 40<br>20 - 40 | sandstone, soil | |
| 19 | 1964 Niigata | Budo | Murakami – Buya (on Route 7) | HW | 320.0 | 8.6 x 5.8 | 5 | 50 - 60 | rhyolite, talus, perlite clay | |
| 20 | 1964 Niigata | Terasaka | Nezugaseki - Koiwagawa (on Uetsu Line) | RR | 79.4 | | 4-5 | 47 - 107 | soft mudstone | |
| 21 | 1964 Niigata | Nezugaseki | Nezugaseki - Koiwagawa (on Uetsu Line) | RR | 104.0 | | | | soft mudstone | |
| 22 | 1968 Tokachi-oki | Otofuke | Nukabira – Horoka (on Shihoro Line) | RR | 165.0 | 4.8 x 5.2 | 4-5 | 25 - 60 | tuff | < 50 |
| 23 | 1978 Izu-Oshima-kinkai | Inatori | Inatori – haihatna (on Izu-kyuko Une) | RR | 906.0 | 4.4 x 5.1 | 5 | 40 - 70 | metamorphic andesite<br>solfataric clay | < 90 |
| 24 | 1978 Izu-Oshima-kinkai | Okawa | Okawa – Hokkawa (on lzu-kyuko Une) | RR | 1219.5 | | | | andesite, fault clay | |
| 25 | 1978 Izu-Oshima-kinkai | Atagawa | Atagawa - Kataseshirata (on Izu-kyuko Une) | RR | 1277.0 | | | | andesite, solfararic clay | |
| 26 | 1978 Izu-Oshima-kinkai | Shiroyama | Imaihama – Kawazu (on Izu-kyuko Line) | RR | | | | | | |
| 27 | 1978 Izu-Oshima-kinkai | Tomoro | Shirata – Inatori (on Higashi-Izu Toll Road) | HW | 425.5 | | 5 | | andesite | |

| ID | Earthquake | Name of Tunnel | Location | Use | Length (m) | Cross Section Width x Height (m) | Liner System | Liner Thickness (cm) | Geological Feature | Cover (m) |
|---|---|---|---|---|---|---|---|---|---|---|
| 28 | 1978 Izu-Oshima-kinkai | Shirata | Shirata – Inatori (on Route 135) | HW | 88.7 | | | | audesite | |
| 29 | 1978 Izu-Oshima-kinkai | Joto | Shirata - Inatori (on Route 135) | HW | 127.3 | | 4-6 | | audesite | |
| 30 | 1978 Izu-Oshima-kinkai | Kurone | Shirata - Inatori (on Route 135) | HW | 400.0 | | | | andesite, scoria | |
| 31 | 1978 Miyagiken-oki | Nakayama No.2 | Naruko - Nakayamadaira (on Rikuu-east Line) | RR | 262.1 | 4.9 x 6.1 | 4-5 | 59 - 69 | | |
| 32 | 1984 Naganoken-seibu | Otakigawa Dam | Otaki, Nagano | UT | | 2.7 x 3.0 | 5 | | sandstone, shale | |
| 33 | 1993 Notohanto-oki | Kinoura | Orido, Suzu, Ishikawa Shimamaki Village | HW | 76.0 | 6.8 x 5.1 | 5 | | mudstone, tuff | < 26 |
| 34 | 1993 Hokkaido-nansei-oki | Shiraito No. 2 | (on Route 229) | HW | 1463.0 | | 6 | 60 | talus | |

*Table C-5a. Tunnels with Moderate to Heavy Damage (Japanese) (1 of 2)*

| ID | Earthquake | Name of Tunnel | Damage at Portals | Damge within 30 m of portals | Damage to Liner > 30 m from portal | Notes |
|---|---|---|---|---|---|---|
| 1 | 1923 Kanto | Hakone No. 1 (up) (down) | 2 | 2 | 1 | |
| 2 | 1923 Kanto | Hakone No. 3 (up) (down) | 4 - slide | 3 | 1 | |
| 3 | 1923 Kanto | Hakone No. 4 (up) (down) | 4 - slide | 3 | 1 | Damage varies from Table C-2. |
| 4 | 1923 Kanto | Hakone No. 7 (up) (down) | 2 | 4 | 1 | lesser damage to down (mountain side) Damage varies from Table C-2. |
| 5 | 1923 Kanto | Nagoe (up) (down) | 1 | 2 | 3 | Damage varies from Table C-2. |
| 6 | 1923 Kanto | Komine | 4 (Box section) | 4 (box section) | 3 (tube section) | liner type depends on location |
| 7 | 1923 Kanto | Fudoyama | 2 | 2 | 1 | |
| 8 | 1923 Kanto | Nenoueyama | 4 - slide | 3 | 4 | steep slope |
| 9 | 1923 Kanto | Komekamiyama | 4 | 3 | 1 | liner with invert arch |
| 10 | 1923 Kanto | Shimomakiyayama | 4 - slide | 4 | 1 | steep slope Damage varies from Table C-2. |
| 11 | 1923 Kanto | Happonmatan | 4 - slide | 3 | 1 | steep slope |
| 12 | 1923 Kanto | Nagasakayama | 2 | 3 | 4 | Damage varies from Table C-2. |
| 13 | 1923 Kanto | Yose | 1 | 2 | 4 | collapse accident reported during construction |
| 14 | 1923 Kanto | Toke | 1 | 1 | 4 | |
| 15 | 1923 Kanto | Namuya | 2 | 3 | 4 | steep slope, landslide suspected, |

| ID | Earthquake | Name of Tunnel | Damage at Portals | Damge within 30 m of portals | Damage to Liner > 30 m from portal | Notes |
|---|---|---|---|---|---|---|
| | | | | | | water acceident reported during construction |
| 16 | 1923 Kanto | Mineokayama | 2 | 3 | 4 of drift | under construction at time of earthquake, progressive failure after the main shock |
| 17 | 1930 Kita-Izu | Tanna | 1 | 1 | 4 | under construction at time of earthquake, earthquake fault crossing the tunnel |
| 18 | 1961 Kita-Mino | I Power Plant | 1 | 1 | 3 | cracking 32% of whole length longitudinal crck dominant |
| 19 | 1964 Niigata | Budo | 1 | 2 | 2 | under construction at time of earthquake cracking on the ground surface |
| 20 | 1964 Niigata | Terasaka | 1 | 3 | 3 | landslide area cracking on the ground |
| 21 | 1964 Niigata | Nezugaseki | 2 | 2 | 2 | landslide area |
| 22 | 1968 Tokachi-oki | Otofuke | 1 | 1 | 3 | landslide area, slope |
| 23 | 1978 Izu-Oshima-kinkai | Inatori | 3 | 2 | 3 | earthquake fault crossing the tunnel trouble with geology during construction |
| 24 | 1978 Izu-Oshima-kinkai | Okawa | 1 | 1 | 2 | damage over 60 m long |
| 25 | 1978 Izu-Oshima-kinkai | Atagawa | 1 | 1 | 2 | damage over 400 m long |
| 26 | 1978 Izu-Oshima-kinkai | Shiroyama | 4 | 1 | 1 | a gigantic rock crashed and blocked the portal |
| 27 | 1978 Izu-Oshima-kinkai | Tomoro | 3 | 3 | 3 | cracking on the ground surface |
| 28 | 1978 Izu-Oshima-kinkai | Shirata | 4 - slide | 2 | 3 | steep slop cracking on the ground surface |
| 29 | 1978 Izu-Oshima-kinkai | Joto | 4 - slide | 1 | 4 | steep slope cracking on the ground surface |
| 30 | 1978 Izu-Oshima-kinkai | Kurone | 4 - slide | 2 | 1 | |

| ID | Earthquake | Name of Tunnel | Damage at Portals | Damge within 30 m of portals | Damage to Liner > 30 m from portal | Notes |
|---|---|---|---|---|---|---|
| 31 | 1978 Miyagiken-oki | Nakayama No.2 | 1 | 1 | 3 | |
| 32 | 1984 Naganoken-seibu | Otakigawa Dam | 1 | 1 | 2 | earthquake fault crossing suspected |
| 33 | 1993 Notohanto-oki | Kinoura | 2 | 4 | 3 | collapse extended by aftershocks |
| 34 | 1993 Hokkaido-nansei-oki | Shiraito No. 2 | 1 | 1 | 4 | falling rock hit the exposed tunnel lining |

*Table C-5b. Tunnels with Moderate to Heavy Damage (Japanese) – (2 of 2)*

EQNAME : Earthquake name
Mw: Moment Magnitude
TNAME : Tunnel name
OWNER OR REFERENCE:

| | |
|---|---|
| ATSF | = Santa Fe Railroad |
| CALTRAIN | = CALTRAIN (Bay Area commuter train) |
| CALTRANS | = California Department of Transportation |
| CDO | = City Development Office |
| COE | = Corps of Engineers |
| HHP | = Hanshin Highway Public Corp. |
| HOE | = Hokoshin Express |
| HRP | = Hyogo Road Public Corp. |
| HWC | = Hanshin Waterworks Company |
| HSB | = Honsyu Shikoku Bridge Authority |
| JHP | = Japan Highway Public Corp. |
| JRN | = JR Nishinippon |
| JTA | = Japan Tunneling Association |
| KBD | = Kobe Dentetsu |
| KEP | = Kansai Electric Plant |
| KER | = Kobe Electric Railway |
| KMS | = Kobe Municipal Subway |
| KPW | = Kobe Public Works Bureau |
| KTB | = Kobe Transportation Bureau |
| KWS | = Kobe Water Supply Bureau |
| LADWP | = Los Angeles Department of Water and Power |
| LAMT | = Los Angeles Metro |
| MRP | = Municipal Road Public Corp. |
| MWB | = Municipal Waterworks Bureau |
| MWD | = Metropolitan Water District of Southern California |
| Nat. RW | = National Railway |
| NCRR | = North Coast Railroad |
| NPC | = North Pacific Coast Railroad |
| NPS | = National Park Service |
| NTT | = Nippon Telephone and Telegraph |
| SC, BT, PR | = Santa Cruz-Big Trees-Pacific Railway |
| SCVWD | = Santa Clara Valley Water District |
| SFWD | = San Francisco Water Department |
| SPRE | = Southern Pacific Railroad |
| SU | = Stanford University |

FUN: Function of tunnel

| | |
|---|---|
| AC | = Particle accelerator |
| HW | = Highway |
| RE | = Railroad |
| UT | = Utility |
| WT | = Water |

Liner / support system
1 = Unlined 2 = Rock Bolt 3 = Timber 4 = Masonry/brick
5 = Unreinforced concrete 6 = Reinforced Concrete 7 = Steel pipe 9 = Unknown
Rock / Soil
R = Rock S = Soil
COVER: Depth of cover above tunnel (meters)
PGA : Peak Ground Acceleration in g
DM : Damage State (Table C-3)
1 = None 2 = slight 3 = moderate 4 = heavy
DM : Damage State (Table C-5)
1 = none
2 = slight (cracks, displacement, deformation)
3 = moderate (severe cracks, falling out, arch hanging down, swelling, invert cut)
4 = heavy (collapse)

*Table C-6. Legend for Tables C-2 and C-5*

Data was categorized in three damage states: no damage, minor damage and moderate damage. Each tunnel has a damage state and associated peak ground acceleration. Nine 'bins' (3 damage states x 3 PGA intervals) were used to sort the tunnels. The results are shown in Table C-7.

| Damage State/PGA | 0.0 to 0.2g | 0.2 to 0.5g | 0.5 to 0.7g | Total |
|---|---|---|---|---|
| No Damage | 30 | 9 | 0 | 39 |
| Minor Damage | 1 | 9 | 5 | 15 |
| Moderate Damage | 0 | 5 | 9 | 14 |
| **Total** | **31** | **23** | **14** | **68** |

*Table C-7. Number of Tunnels in Each Damage State Due to Ground Shaking*

The empirical data was then averaged to obtain the mean, median, standard deviation and beta for each damage state. The results are provided in Table C-8. Beta in Table C-8 includes uncertainty and randomness (same as $\beta_{total}$ in equation 5-2).

| Damage State/PGA | Mean (g) | Median (g) | Std. Dev (g) | Beta (total) |
|---|---|---|---|---|
| No Damage | 0.183 | 0.145 | 0.143 | 0.689 |
| Minor Damage | 0.387 | 0.353 | 0.174 | 0.428 |
| Moderate Damage | 0.513 | 0.500 | 0.116 | 0.224 |

*Table C-8. Statistics for Tunnel Damage States*

The data in Tables C-7 and C-8 include rock, alluvial and cut-and-cover tunnels, but no distinction is made between the three since the ground conditions were not reported in the literature for most of the tunnels.

Dowding [1978] reported that below 0.19g, there is no damage to either lined or unlined tunnels. Also, Owen [1981] concluded that rock tunnels perform better than alluvial or cut-and-cover tunnels. Specifically, little damage occurs to rock tunnels when accelerations at the ground surface is below 0.4g. Earthquake experience shows that most damage occurs to the tunnel liner, and such damage is well correlated with the quality of construction of the liner. For example, older-designed unreinforced concrete liners using wood sets and lagging for temporary support and without contact grouting are more susceptible to damage than are modern, cast-in-place concrete liners using steel sets and standard contact grouting.

For these reasons, fragility curves developed for HAZUS for ground shaking hazards distinguish between rock tunnels and other tunnels, and between poor and good quality construction. No distinction is made in the HAZUS fragility curves between tunnels with or without seismic design. Since the empirical database provided no indication of the original design basis, it is likely that seismic design was not included in many of the tunnels in the empirical database. The resulting HAZUS fragility curves are described in Tables C-9 through C-12.

**Alluvial Cut-and-cover Tunnels of poor-to-average construction.** The fragility curves are based on the data in Table C-8 with minor adjustments described below. Beta includes uncertainty and randomness.

| Item | Hazard | Damage State | Median PGA (g) | Beta | Median PGD (inch) | Beta |
|---|---|---|---|---|---|---|
| Liner | Ground Shaking | Minor cracking of tunnel liner; minor rock falls; spalling of shotcrete or other supporting material. | 0.35 | 0.4 | | |
| Liner | Ground Shaking | Moderate cracking of tunnel liner and rock falls. | 0.55 | 0.6 | | |
| Liner | Ground Failure | Moderate cracking of tunnel liner and rock falls | | | 12 | 0.5 |
| Liner | Ground Failure | Major localized cracking and possible collapse of tunnel liner and rock falls | | | 60 | 0.5 |
| Portal | Ground Failure | Debris from landslide closes portal | | | 60 | 0.5 |

*Table C-9. Tunnel – Alluvial or Cut-and-cover with Liner of Average to Poor Quality Construction*

Minor damage from ground shaking: median: 0.35g, beta 0.40. These values are close to the empirical data set values of Median .353g, Beta .428.

Moderate damage from ground shaking: median: 0.55g, beta 0.6. The median value of 0.55g is set 10% higher than the empirical value of 0.50g, based on judgment. The beta value of 0.6 is set much higher than the empirical value of 0.22. The empirical value is deemed too low due to the small data sample size. In fact, the moderate damage state is known with less certainty than the minor damage state, and the state of empirical data (circa 1978) was too incomplete to warrant a lower value.

Damage due to ground failure through the liner. The HAZUS fragility values are set at 12 inches of liner offset to mean moderate damage, and 60 inches of liner offset to mean major damage. This implies that the tunnel diameter is in the range of 8 to 12 feet (typical of water tunnels), and that the materials behind the liner are weak enough to cause some type of debris accumulation in the tunnel. For water tunnels, small amounts of debris will often be carried away by the water flow; large amounts of debris can result in clogging of the tunnel and damage to downstream water system components. If a large amount of debris occur, the tunnel may clog over a long period of time. No specific fragility curve is provided for fault offset through the liner, but it is understood that a fault offset of about 50% to 75% (or larger) of the inner diameter of the liner can be enough to immediately close off the tunnel. However, it has been noted that larger fault offsets (more than the diameter of the tunnel) can, in some cases, be accommodated by the tunnel without loss of flow capacity if the offset is distributed over a reasonable length of the tunnel, on the order of 20 to 50 feet. Current predictive models of fault offset are not so precise as to determine with high confidence whether the fault offset will be like a “knife edge”—which leads to tunnel closure if offset approaches or exceeds tunnel diameter—or distributed over a considerable shear zone, which may or may not lead to tunnel closure.

Damage due to ground failure of the portal area. Landslides at portal areas represent a credible hazard to all tunnels. Strong ground shaking can promote landslide movements, especially under saturated soil conditions. The HAZUS fragility model of 5 feet leading to closure of the portal is based on judgment, and assumes that the tunnel is about 8 to 12 feet in diameter.

**Alluvial and Cut-and-cover Tunnels of good construction.** The median values are increased from those of tunnels with average-to-poor construction by one lognormal standard deviation and then rounded. For example: for Minor Damage, 0.35g * exp (0.428) = 0.53g, set to 0.5g; for Major Damage, 0.55g * exp (0.224) = 0.688g, set to 0.7g (Table C-10). Beta includes uncertainty and randomness.

| Item | Hazard | Damage State | Median PGA (g) | Beta | Median PGD (inch) | Beta |
|---|---|---|---|---|---|---|
| Liner | Ground Shaking | Minor cracking of tunnel liner; minor rock falls; spalling of shotcrete or other supporting material. | 0.5 | 0.4 | | |
| Liner | Ground Shaking | Moderate cracking of tunnel liner and rock falls. | 0.7 | 0.6 | | |
| Liner | Ground Failure | Moderate cracking of tunnel liner and rock falls | | | 12 | 0.5 |
| Liner | Ground Failure | Major localized cracking and possible collapse of tunnel liner and rock falls | | | 60 | 0.5 |
| Portal | Ground Failure | Debris from landslide closes portal | | | 60 | 0.5 |

*Table C-10. Tunnel – Alluvial or Cut-and-cover with Liner of Good Quality Construction*

The HAZUS fragility curves for damage to liners due to ground shaking for tunnels of good quality construction were developed by increasing the median fragility levels from Table C-9 by about 30% to 40%, which represents an increase in the median acceleration levels of one standard deviation above those for tunnels of poor-to-average quality construction. This is based on judgment and the limited empirical data set. A similar approach was taken to establish fragility curves for rock tunnels (Tables C-11 and C-12).

**Rock Tunnels of poor to average construction**. The fragility curves are developed based on engineering judgment., with adjustments taken from rock tunnels of good quality construction. Beta includes uncertainty and randomness.

| Item | Hazard | Damage State | Median PGA (g) | Beta | Median PGD (inch) | Beta |
|---|---|---|---|---|---|---|
| Liner | Ground Shaking | Minor cracking of tunnel liner; minor rock falls; spalling of shotcrete or other supporting material. | 0.5 | 0.4 | | |
| Liner | Ground Shaking | Moderate cracking of tunnel liner and rock falls. | 0.7 | 0.6 | | |
| Liner | Ground Failure | Moderate cracking of tunnel liner and rock falls | | | 12 | 0.5 |
| Liner | Ground Failure | Major localized cracking and possible collapse of tunnel liner and rock falls | | | 60 | 0.5 |
| Portal | Ground Failure | Debris from landslide closes portal | | | 60 | 0.5 |

*Table C-11. Tunnel – Rock without Liner or with Liner of Average to Poor Quality Construction*

**Rock tunnels of good construction.** The median peak ground acceleration was derived recognizing that little damage occurs below 0.4g. It was assumed that the median PGA for minor damage to rock tunnels of good construction quality would occur one lognormal standard deviation above 0.4g. Beta includes uncertainty and randomness.

| Item | Hazard | Damage State | Median PGA (g) | Beta | Median PGD (inch) | Beta |
|---|---|---|---|---|---|---|
| Liner | Ground Shaking | Minor cracking of tunnel liner; minor rock falls; spalling of shotcrete or other supporting material. | 0.6 | 0.4 | | |
| Liner | Ground Shaking | Moderate cracking of tunnel liner and rock falls. | 0.8 | 0.6 | | |
| Liner | Ground Failure | Moderate cracking of tunnel liner and rock falls | | | 12 | 0.5 |
| Liner | Ground Failure | Major localized cracking and possible collapse of tunnel liner and rock falls | | | 60 | 0.5 |
| Portal | Ground Failure | Debris from landslide closes portal | | | 60 | 0.5 |

*Table C-12. Tunnel – Rock without Liner or with Liner of Good Quality Construction*

At the time when the tunnel fragility curves were prepared for the HAZUS program in the early 1990s, damage due to ground shaking that would result in tunnel closures was not considered likely; therefore, there is no effect to the functionality of the tunnels due to ground shaking in the damage algorithm. As will be described in subsequent sections, this “heavy” damage state has in fact been occasionally observed, suggesting that the HAZUS fragility curves might need to be modified.

For ground failures such as surface faulting through the interior of the tunnel, substantial permanent ground deformations need to occur before appreciable damage occurs. For moderate damage, a permanent ground deformation of one foot is used, and for major damage, a permanent ground deformation of five feet is used. These displacements are based on a typical water tunnel equivalent diameter of about 8 feet. For both moderate and major damage due to ground failure, tunnel closure is possible; tunnel closure could occur immediately or within a few days of the earthquake either due to aftershocks or continued erosion of the geology behind the failed liner.

If the tunnel portals are subjected to PGDs due to landslides, then the same PGDs are assumed to cause the tunnel major damage and closure. Rockfall-type avalanches are not specifically considered in the fragility curves.

### C.1.2 Comparison of HAZUS and ATC-13 Fragility Curves

Table C-13 compares the median peak ground accelerations for fragility curves developed in Tables C-10 and C-12 with the damage algorithms presented in ATC-13 [ATC, 1985]. Only median values are compared because the dispersions in the ATC-13 data do not reflect variability in the ground motion; the fragility curves developed here, do. The damage probability matrices given in the ATC-13 were converted to a cumulative probability distribution using the methodology described in ASCE [1985] and using the MMI-to-PGA conversion suggested by McCann et al [1980] (Table C-14).

| Tunnel Type/Damage State | HAZUS (PGA) | ATC-13 (PGA) |
|---|---|---|
| Rock | | |
| Moderate Damage | 0.8 g | 0.94 g |
| Minor Damage ** | 0.6 g | 0.45 g |
| Cut & Cover or Alluvial | | |
| Moderate Damage | 0.7 g | 0.74 – 0.84 g * |
| Minor Damage ** | 0.5 g | 0.40 – 0.44 g * |

* ATC-13 gives values for cut-and-cover and alluvial tunnels. Both PGAs are given above.
** For *Minor* Damage State shown above, the corresponding ATC-13 Damage State is *Light*.

*Table C-13. Comparison of Tunnel Fragility Curves*

| MMI | PGA Interval | PGA Used |
|---|---|---|
| VI | 0.09 – 0.15 | 0.12 |
| VII | 0.16 – 0.25 | 0.21 |
| VIII | 0.26 – 0.45 | 0.36 |
| IX | 0.46 – 0.60 | 0.53 |
| X | 0.61 – 0.80 | 0.71 |
| XI | 0.81 – 0.90 | 0.86 |
| XII | ≥ 0.91 | 1.15 |

*Table C-14. Modified Mercalli to PGA Conversion [after McCann et al, 1980]*

As can be seen in Table C-13, the median fragility values for the two damage states agree reasonably well.

## C.2 Databases of Owen and Scholl, Sharma and Judd

Owen and Scholl [1981] extended the database of Dowding and Rozen [1978] to a total of 127 cases. Additions to the database included observations from the 1906 San Francisco earthquake, 1971 San Fernando earthquake and a number of less well-documented earthquakes around the world. Based on their examination of the data, Owen and Scholl concluded the following:

- Little damage occurred in rock tunnels for peak ground accelerations below 0.4g.
- Severe damage and collapse of tunnels from shaking occurred only under extreme conditions, usually associated with marginal construction such as brick or plain concrete liners and lack of grout between wood lagging and the overbreak.
- Severe damage was inevitable when the underground structure was intersected by a fault that slipped during an earthquake. Cases of tunnel closure appeared to be associated with movement of an intersecting fault, landslide, or liquefied soil.
- Deep tunnels were less prone to damage than shallow tunnels.
- Damage to cut-and-cover structures appeared to be caused mainly by large increases in lateral forces from the surrounding soil backfill.
- Earthquake duration appeared to be an important factor contributing to the severity of damage.

Sharma and Judd [1991] further extended the database to 192 reported cases. In this study, the relationships between observed damage and parameters of the earthquake, tunnel support system and geologic conditions were examined. Parameters considered in their study included earthquake magnitude, epicentral distance, peak ground acceleration, form of tunnel internal support and lining, overburden depth and rock type. Sharma and Judd concluded that:

- Damage incidence decreased with increasing overburden depth.
- Damage incidence was higher for colluvium than for harder rocks.
- Internal tunnel support and lining system appeared not to affect damage incidence.
- Damage increased with increasing earthquake magnitude and decreasing epicentral distance.
- No damage or minor damage can be expected for peak accelerations at the ground surface less than about 0.15g.

## C.3 Database of Power et al

The tunnel studies described in Sections C.1 and C.2, while informative and indicative of generally good tunnel performance during earthquakes, contain some limitations:

- Many of the reported cases were observations from old and/or less well-documented earthquakes and the locations and/or magnitudes of a number of the earthquakes were poorly defined.

- The estimated ground shaking levels for the cases were calculated using empirical ground motion attenuation relationships developed in early 1970s. Peak ground accelerations were estimated using distances from earthquake epicenters to the tunnel sites. Ground motions calculated using epicentral distance could be misleading for sites located close to a long or extended fault rupture area. Recently developed ground motion attenuation relationships generally use some measure of the closest distance from the site to the fault rupture area. Furthermore, recently developed attenuation relationships are better constrained than the older relationships by having more data from many recent earthquakes.
- The damage cases reported and used in the previous studies included damage observations resulting from direct fault rupture through a tunnel and other major ground failure mechanisms such as landsliding and liquefaction. In examining the effects of ground shaking on tunnels, cases of damage due to these other failure mechanisms should not be included.

To consider these limitations, Power et al. [1998] critically examined the previously compiled databases summarized above and made the following revisions:

- Data was removed for poorly documented earthquakes such as earthquakes with unknown magnitudes or locations or uncertain tunnel performance.
- Data was removed for cases of damage due directly to fault displacement, landsliding, or liquefaction in order to examine trends for shaking-induced damage in the absence of ground failure.
- Data was not included for cut-and-cover tunnels or tubes, in order to develop trends and a correlation for bored tunnels only.
- Earthquake magnitudes were reported as moment magnitudes ($M_w$).
- Distances were evaluated as closest distances from the tunnel locations to the fault rupture surfaces of the earthquakes.
- Peak accelerations at the ground surface of actual or hypothetical rock outcroppings at the tunnel locations were estimated using recently-developed ground motion attenuation relationships.
- Data was added from recent, moderate-to-large magnitude and better-documented earthquakes: 1989 Loma Prieta, 1992 Petrolia, 1993 Hokkaido, 1994 Northridge and 1995 Kobe earthquakes. Some data were added from case histories from older earthquakes.

Table C-2 includes the complete database summarized in Table 6-1. Included in Table C-2 is information on the earthquake including name, date, and moment magnitude; tunnel name, owner, function, lining/support system, local geologic conditions and thickness of geologic cover; level of ground shaking; damage state; and references for data on the tunnels and tunnel performance observations.

In general, peak ground accelerations at the ground surface at tunnel locations were estimated as median ($50^{th}$ percentile) values using rock ground motion attenuation relationships developed by Sadigh et al. [1993, 1997] for earthquakes occurring on crustal faults. The rock relationship of Youngs et al [1993, 1997] for subduction zone earthquakes were used for the 1964 Alaska earthquake. The median peak accelerations for the 1994 Northridge earthquake were estimated using event-specific ground motion attenuation relationship developed for the Northridge earthquake [Woodward-Clyde Consultants, 1995]. Rock ground motion attenuation relationships were used because most of the reported cases in the database involve tunnels founded in rock and also due to the limited information available for the local geologic conditions. The actual ground motions experienced at the depth of the tunnels would tend to be less than the values estimated for the ground surface in Table C-2 due to well-known tendencies for ground motions to decrease with depth below the ground surface [e.g., Chang et al., 1986]. The highest median peak rock acceleration estimated for the entire database is about 0.7g, for the 1923 Kanto, 1971 San Fernando, and the 1994 Northridge earthquakes. Many estimated peak rock accelerations for the 1995 Kobe earthquakes are about 0.6g. The Kobe earthquake produced by far the most observations for moderate-to-high levels of shaking and include numerous estimated median peak rock accelerations at the ground surface above the tunnels in the range of about 0.4g to 0.6g.

Damage to the tunnels was categorized into four states: none; slight, for minor cracking and spalling of the tunnel lining; moderate, for major cracking and spalling; and heavy, for total or partial collapse of a tunnel.

Figure C-2 summarizes the observations of the effects of seismic ground shaking on tunnel performance for case histories 1 through 204 in Table C-2. As indicated previously, the data is for damage due only to shaking and excludes damage that was definitely or probably attributed to fault rupture, landsliding, or liquefaction. Also, the data is for bored tunnels only; data for cut-and-cover tunnels and tubes is not included. Figure C-2 shows the level of damage induced in tunnels with different types of linings subjected to the indicated levels of ground shaking.

The following trends can be inferred from Figure C-2:

- For peak ground accelerations (PGAs) equal to or less than about 0.2g, ground shaking caused very little damage in tunnels.
- For peak ground accelerations (PGAs) in the range of about 0.2g to 0.5g, some instances of damage occurred, ranging from slight to heavy.
- For peak ground accelerations (PGAs) exceeding about 0.5g, there were a number of instances of slight to heavy damage.
- Tunnels having stronger lining systems appeared to perform better, especially those with reinforced concrete and/or steel linings.

The three instances of heavy damage, indicated by solid diamonds in Figure C-2, are all from the 1923 Kanto, Japan earthquake. For the 1923 Kanto earthquake observation with PGA equal to 0.25g (see Table C-2 and Figure C-2), investigations indicated that the damage may have been due to landsliding. In the other two observed occurrences of heavy damage shown in Figure C-2, collapses occurred in the shallow portions of the tunnels.

The correlations observed in Figure C-2 show similar trends as those observed in the previous study by Dowding and Rozen in Figure C-1. For relatively low ground shaking levels, no damage or very little damage occurred for PGAs less than about 0.2g. Relatively few instances of moderate-to-heavy damage exist for accelerations at less than 0.5g, especially for stronger and well-constructed tunnels. This was evident during the 1995 Kobe earthquake, where only a few cases of moderate damage and no major damage were reported for bored tunnels at peak ground accelerations of about 0.6g.

Although the number of observations for the seismic performance of cut-and-cover tunnels are far fewer than those for bored tunnels, the available data, including observations from the 1995 Kobe earthquake, suggest that cut-and-cover box-like tunnels are more vulnerable to shaking than bored tunnels with more or less circular cross-sections. Cut-and-cover tunnels are vulnerable to racking-type deformations due to ground-imposed displacements of the top of the box structure relative to the base. The higher vulnerability of cut-and-cover tunnels as compared to bored tunnels is also probably due in part to the softer geologic materials surrounding cut-and-cover structures, which are constructed at shallower depths than are most bored tunnels.

## C.4 Additions to Empirical Database

Asakura and Sato [1998] expanded the compilation of tunnel performance data for the 1995 Kobe earthquake. Additional case histories obtained from their database during the present study are summarized in Table C-2 as entries 205 through 217.

As part of US/Japanese cooperative research and state-of-the-art studies of tunnel seismic design and performance by Prof. Thomas O'Rourke for MCEER, O'Rourke and Shiba [1997] summarized tunnel performance for 15 different earthquakes in Japan from 1923 to 1993. Table C-3 summarizes tunnel damage observed in these earthquakes. Table C-4 provides an explanation of the Japanese JMA intensity scale used in Table C-3. Figure C-3 shows a map of the locations of these earthquakes. The findings in Table C-3 are similar to those described in the Sections C.2 and C.3 and included the following observations:

- Generally, the most significant damage was to the portals, which was often attributed to landslides.
- Some of the most severe damage occurred because of fault movements.
- Generally, damage to tunnels due to shaking was associated with unreinforced masonry and unreinforced, cast-in-place concrete linings, and with tunnel locations where construction difficulties were experienced and poor geologic conditions were encountered.
- Significant damage to Japanese tunnels was observed predominately in locations where seismic intensities of V or higher on the JMA scale occurred, correlating approximately to MMI intensity VIII.

## C.5 Tunnels with Moderate to Heavy Damage from Ground Shaking

As previously discussed, the incidence of heavy damage or collapse of at least part of the liner system in tunnels from ground shaking has been relatively rare. The following sections summarize the specific tunnels that have collapsed possibly due to ground shaking.

### C.5.1 Kanto, Japan 1923 Earthquake

Table C-5 summarizes the earthquake damage observed in 34 tunnels after ten Japanese earthquakes. These tunnels were selected as those displaying the most severe damage for which there is sufficient description in the literature to convey a reasonably clear picture of the tunnel, earthquake, ground conditions and nature of the damage. The table summarizes information pertaining to tunnel location, use, length, cross-section, lining, geology, overburden and damage observed either at, within or beyond 30 m from the portals.

Collapse beyond 30 meters from the portals was observed in the absence of landslides and faulting at a few tunnels, mostly in the 1923 Kanto earthquake. In all instances, the length of tunnel that experienced collapse was relatively small, ranging from 1.5 to 60 m. The following describes specific tunnel failures:

- The Mineokayama Tunnel was under construction during the earthquake, and the collapse occurred in one of the drifts. The type and quantity of temporary support used in the drift were not reported.
- The Yose Railroad Tunnel was driven in soil for a length of 293 m at a distance from the epicenter of 48 km. The brick masonry lining was 46-69 cm thick, with soil cover ranging mostly from 4 to 21 m. The JMA intensity was V-VI. During construction in 1900, water inflow attributed to a heavy rainfall resulted in the collapse of a 20-m-long section. During the Kanto earthquake, a 60-m-long section collapsed, including the section that failed during construction. The collapsed section was about 55 m from the closest portal.
- The Toke Railroad Tunnel was driven in mudstone for a length of 353 m at a distance of 106 km from the epicenter, The brick masonry lining was 34-46 cm thick, with an overburden of 12 to 20 meters. The JMA intensity was IV. Significant inflows of water into the tunnel had persisted from the time of its construction in 1894-95. During the Kanto earthquake, a section of the brick arch, 2.7 m wide and 5.5 m long, failed, causing 90 $m^3$ of rock and soil to collapse into the tunnel.

### C.5.2 Noto Peninsular Offshore, Japan 1993 Earthquake

Tunnel collapses have been reported more recently for Japanese earthquakes. Kunita, et al. (1994) report on the collapse of the Kinoura Tunnel as a result of the 1993 Noto Peninsular Offshore earthquake. The earthquake magnitude was 6.8 and the tunnel was located 26 km from the epicenter with a JMA intensity of approximately V. This road tunnel was driven in 1965 through alternating strata of tuff and mudstone. The 76-meter-long horseshoe-shaped tunnel was 6 m wide and about 4 m high. Timber supports were used during construction, and the final lining was composed of 30-cm-thick concrete. It appears that the lining was unreinforced. After the main shock, a 4.5 x 4.5 m section of the arch lining collapsed at a distance of 21 m from the

nearest portal. An aftershock caused the fall zone to expand, and two days after the main shock, the tunnel was almost completely blocked with debris.

### C.5.3 Kobe, Japan 1994 Earthquake

During the 1994 Kobe earthquake, the cut-and-cover tunnel at the Daikai Subway Station collapsed catastrophically. It appears that this is the only instance of tunnel collapse resulting from the Kobe earthquake. The performance of the Daikai Station has been covered in the technical literature. Shear distortion from vertically propagating shear waves caused hinge formation where the central reinforced concrete columns were connected to the roof and invert. There was a lack of adequate confining steel in the central columns, which helped to promote column failure. See Figure C-4.

### C.5.4 Duzce, Turkey 1999 Earthquake

Twin tunnels, each 18 m in excavated diameter, were significantly and adversely affected by the 1999 Duzce, Turkey earthquake. They are located on Gurnosova-Gerede portion of the Northern Anatolian Motorway. The tunnels were being driven in a faulted and deformed sequence of rocks, including flysch, shale, sandstone, marble, granite and amphibolite. Tunneling was performed according to NATM principles, with shotcrete, rock bolts and light steel sets. The epicenter of the $M_w$ 7.2 earthquake was located about 20 km from the western portals of the tunnels. The surface rupture of the causative fault was within 3 km of these portals. Peak acceleration and velocity recorded at the nearest strong motion station at Bolu (6 km from the causative fault) were 0.81 g and 66 cm/s, respectively. Observations show that the tunnels performed remarkably well, especially in light of their close proximity to the seismic source. Some of the temporary shotcrete-supported sections, however, collapsed where the worst ground conditions were located, and these sections are discussed below.

- Adjacent twin sections collapsed in a fault zone with weak, intensely slickensided clay gouge and crushed metacrystalline rock with the consistency of silty clay. About 300-m-long sections were affected by full or partial collapse, each located approximated 240 m from the western portals. The tunnels in this location were supported with a 75-mm-thick shotcrete lining with rock bolts and light steel sets. Substantial deformation had been observed in these sections of the tunnel during construction, and it is likely that the initial lining had been subjected to considerable stress under static conditions.

- Partial collapse and severe initial lining deformation were observed near tunnel headings being driven from the eastern portals at the opposite end of the 3.3-km-long highway tunnel. Five-m-diameter tunnels were being driven as pilot bench tunnels along opposite sides of each 18-m-diameter highway tunnel. The intention was to drive the smaller tunnels initially through a fault zone and then partially fill them with concrete to act as reaction blocks for the shotcrete arch installed as the remaining parts of the heading were excavated. Each pilot bore tunnel was supported with a 30-cm-thick shotcrete lining, patterned rock bolts, and light steel sets. The pilot bores were driven in a fault zone with weak, intensely slickensided clay gouge. Thirty-m-long sections of the pilot bores were affected by significant invert heave, ruptured and partially collapsed shotcrete and buckled steel sets.

### C.5.5 Summary Observations

Full or partial collapse of tunnels resulting from earthquakes has occurred under highly localized conditions, involving weak, wet and highly fractured rock and soil. Collapse has been confined to relatively short sections of tunnel. In Japan, tunnel collapse has occurred in linings with unreinforced masonry or unreinforced concrete. Failure of the Daikai Subway Station (cut-and-cover tunnel) involved the failure of reinforced concrete columns with inadequate confining steel. The collapsed tunnel sections in Turkey are located in weak, highly fractured clay gouge where construction was in progress and only the initial support system had been installed.

Both the Daikai Subway Station and Bolu Highway Tunnel were affected by near-source ground motions involving high pulses of acceleration and velocity. Peak acceleration and velocity measured at the Kobe Marine Meteorological Observatory (KMMO), which was within several km of the Dakai Station, were 0.81 g and 84 cm/s, respectively. The strong motion recordings at Bolu, which were taken at distances comparable to those separating the Daikai Station and KMMO, show peak acceleration and velocity of 0.81 g and 66 cm/s. Tunnel damage in these instances is associated with high velocity that would have promoted high transient ground strains.

Accelerations inferred from JMA intensities are much less reliable than strong motion recordings. The accelerations estimated in this way from Table C-5 for the Yose, Toke and Kinoura Tunnels are 0.25-0.40 g, 0.025-0.08 g and 0.08-0.25 g, respectively.

In summary, two aspects of the strong motion deserve attention. First, the near-source ground motion affecting the Daikai Station and Bolu Tunnel was high. Although both structures were influenced either by remarkably poor ground (Bolu Tunnels) or weakness in structural support (Daikai Station), they were nonetheless subjected to significant peak velocities. Collapsed tunnels affected by the Kanto and Noto Peninsular Offshore earthquakes were apparently subjected to a wide range of accelerations, some of which were relatively small. The most prominent features of these tunnels affecting their seismic vulnerability appears to be poor ground conditions in combination with an unreinforced masonry or concrete lining. It seems reasonable, therefore, to conclude that poor ground and weak lining conditions are the most important factors affecting seismic performance. Strong motion in the near field can supply significant excitation that will promote local collapse in tunnel sections influenced by poor ground and lack of either sufficient or final structural support.

## C.6 Empirical Basis of the Tunnel Fragility Curves

Table C-2 presents the database of tunnels used in the development of fragility curves presented in Section 6-3 of the main report. Table C-15 summarizes this data set.

| PGA (g) | All Tunnels | DS = 1 | DS = 2 | DS = 3 | DS = 4 |
|---|---|---|---|---|---|
| 0.07 | 30 | 30 | 0 | 0 | 0 |
| 0.14 | 19 | 18 | 1 | 0 | 0 |
| 0.25 | 22 | 19 | 2 | 0 | 1 |
| 0.37 | 15 | 14 | 0 | 0 | 1 |
| 0.45 | 44 | 36 | 6 | 2 | 0 |
| 0.57 | 66 | 44 | 12 | 9 | 1 |
| 0.67 | 19 | 3 | 7 | 8 | 1 |
| 0.73 | 2 | 0 | 0 | 2 | 0 |
| **Total** | **217** | **164** | **28** | **21** | **4** |

*Table C-15. Complete Bored Tunnel Database (Summary of Table C-2)*

Tables C-16 through C-19 summarize the data sets based on bored tunnels with specific liner systems. Note that for a tunnel with multiple liner systems, the tunnel is classified according to the "best" liner type in the tunnel, according to the following ranking: unlined, timber/masonry/brick, unreinforced concrete, reinforced concrete/steel.

| PGA (g) | Unlined Tunnels | DS = 1 | DS = 2 | DS = 3 | DS = 4 |
|---|---|---|---|---|---|
| 0.05 | 5 | 5 | 0 | 0 | 0 |
| 0.13 | 4 | 4 | 0 | 0 | 0 |
| 0.25 | 10 | 9 | 1 | 0 | 0 |
| 0.35 | 2 | 1 | 0 | 0 | 1 |
| 0.42 | 2 | 0 | 2 | 0 | 0 |
| 0.55 | 2 | 0 | 1 | 1 | 0 |
| 0.66 | 2 | 0 | 1 | 1 | 0 |
| 0.73 | 1 | 0 | 0 | 1 | 0 |
| **Total** | **28** | **19** | **5** | **3** | **1** |

*Table C-16. Unlined Bored Tunnels*

| PGA (g) | Timber or Masonry Lined Tunnels | DS = 1 | DS = 2 | DS = 3 | DS = 4 |
|---|---|---|---|---|---|
| 0.26 | 2 | 1 | 0 | 0 | 1 |
| 0.40 | 1 | 1 | 0 | 0 | 1 |
| 0.42 | 4 | 3 | 1 | 0 | 0 |
| 0.60 | 2 | 0 | 0 | 2 | 0 |
| 0.67 | 5 | 0 | 1 | 4 | 0 |
| **Total** | **14** | **5** | **2** | **6** | **1** |

*Table C-17. Bored Timber and Masonry/Brick Lined Tunnels*

| PGA (g) | Unreinforced Concrete Lined Tunnels | DS = 1 | DS = 2 | DS = 3 | DS = 4 |
|---|---|---|---|---|---|
| 0.08 | 13 | 13 | 0 | 0 | 0 |
| 0.13 | 6 | 5 | 1 | 0 | 0 |
| 0.23 | 3 | 2 | 1 | 0 | 0 |
| 0.38 | 8 | 8 | 0 | 0 | 0 |
| 0.45 | 33 | 28 | 3 | 2 | 0 |
| 0.57 | 53 | 39 | 9 | 4 | 1 |
| 0.67 | 8 | 1 | 4 | 3 | 0 |
| 0.73 | 1 | 0 | 0 | 1 | 0 |
| **Total** | **125** | **96** | **18** | **10** | **1** |

*Table C-18. Bored Unreinforced Concrete Lined Tunnels*

| PGA (g) | Reinforced Concrete/ Steel Lined Tunnels | DS = 1 | DS = 2 | DS = 3 | DS = 4 |
|---|---|---|---|---|---|
| 0.07 | 9 | 9 | 0 | 0 | 0 |
| 0.15 | 5 | 5 | 0 | 0 | 0 |
| 0.27 | 6 | 6 | 0 | 0 | 0 |
| 0.35 | 4 | 4 | 0 | 0 | 0 |
| 0.45 | 4 | 4 | 0 | 0 | 0 |
| 0.57 | 6 | 3 | 2 | 1 | 0 |
| 0.66 | 4 | 2 | 1 | 0 | 1 |
| **Total** | **38** | **33** | **3** | **1** | **1** |

*Table C-19. Bored Reinforced Concrete or Steel Lined Tunnels*

## C.7 References

Asakura, T., and Sato, Y., "Mountain tunnels damage in the 1995 Hyogoken-Naubu earthquake," QR of RTRI, Vol. 39, No. 1, 1998.

Dowding, C.H. and Rozen, A., "Damage to Rock Tunnels from Earthquake Shaking," *Journal of the Geotechnical Engineering Division*, American Society of Civil Engineers, New York, NY, Feb. 1978.

ASCE, "Evaluation of Seismic Fragility and Validation of Probabilistic Models," The Fragility Evaluation/Validation Subgroup Joint Working Group on Seismic PRA of the ASCE Dynamic Analysis Committee, Draft Report, April 1985.

Chang, C.-Y., Power, M.S., Idriss, I.M., Somerville, P.G., Silva, W., and Chen, P.C., *Engineering characterization of ground motion – Task II: Observational data on spatial variations of earthquake ground motion*, Report prepared for US Nuclear Regulatory Commission, NUREG/CR-3805, Vol. 3, 1986.

Dowding, C.H. and Rozen, A., "Damage to Rock Tunnels from Earthquake Shaking," *Journal of the Geotechnical Engineering Division*, American Society of Civil Engineers, New York, NY, Feb. 1978.

HAZUS, *Earthquake Loss Estimation Methodology, Technical Manual, Volume II*, prepared by the National Institute of Building Sciences for Federal Emergency Management Agency, 1997.

Kunita, M., Takemata, R., and Lai, Y., "Restoration of a Tunnel Damaged by Earthquake," in *Tunneling and Underground Space Technology*, Vol. 9, No. 4, pp. 439-448, 1994.

Kunita, M., et al., "Rehabilitation of Tunnel Damage caused by Noto Peninsula Offshore Earthquake," *Tunnels and Underground*, Vol.24, No.11, pp. 7-13, 1993 (in Japanese).

McCann, M.W., Sauter, F., and Shah, H.C., "A Technical Note on PGA-Intensity Relationship with Applications to Damage Estimation," *BSSA*, Vol. 7, No. 2, pp 631-637, 1980.

O'Rourke, T.D. and Shiba, Y., *Seismic Performance and Design of Tunnels: Annual Report*, MCEER Highway Project, Sponsored by U.S. Department of Transportation, Federal Highway Administration, FHWA Contract DTFH61-92-C-00106, 1997.

Owen, G.N. and Scholl, R.E., *Earthquake Engineering of Large Underground Structures*, Federal Highway Administration and National Science Foundation, FHWA/RD-80/195, Jan. 1981.

Power, M.S., Rosidi, D., and Kaneshiro, J., Gilstrap, S.D., and Chiou, S.J., *Summary and Evaluation of Procedures for the Seismic Design of Tunnels*, Multidisciplinary Center for Earthquake Engineering Research, Technical Report MCEER-98-XXXX, Draft Report, Sept. 1998.

Sadigh, K., Chang, C.-Y., Abrahamson, N.A., Chiou, S.-J., and Power, M.S., "Specification of long-period ground motions: updated attenuation relationships for rock site conditions and adjustments factors for near-fault effects," *Proceedings of Applied Technology Council Seminar*

*on Seismic Isolation, Passive Energy Dissipation, and Active Control*, Publication No. ATC-17-1 San Francisco, California, p. 59-70, March 1993.

Sadigh, K., Chang, C.-Y., Egan, J.A. Makdisi, F.I., and Youngs, R.R., "Atteunuation Relationships for Shallow Crustal Earthquakes Based on California Strong Motion Data," *Seismological Research Letters*, Vol. 68, No. 1, p. 180-189, 1997.

Sharma, S., and Judd, W.R., "Underground Opening Damage From Earthquakes," *Engineering Geology*, Vol. 30, 1991.

Woodward-Clyde Consultants, Personal communication, 1995.

## C.8 Figures

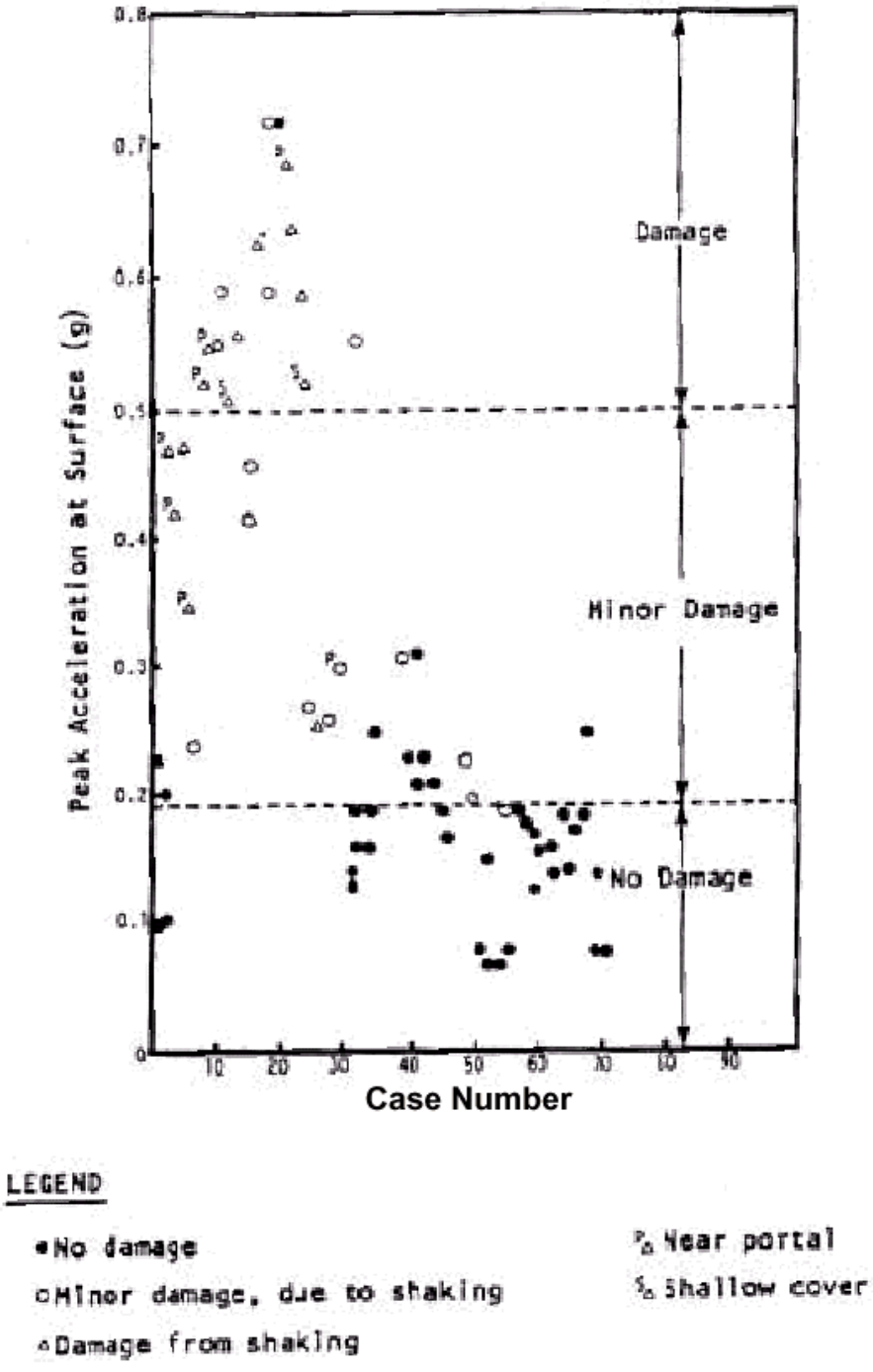


*Figure C-1. Peak Surface Acceleration and Associated Damage Observations for Earthquakes [after Dowding and Rozen, 1978]*

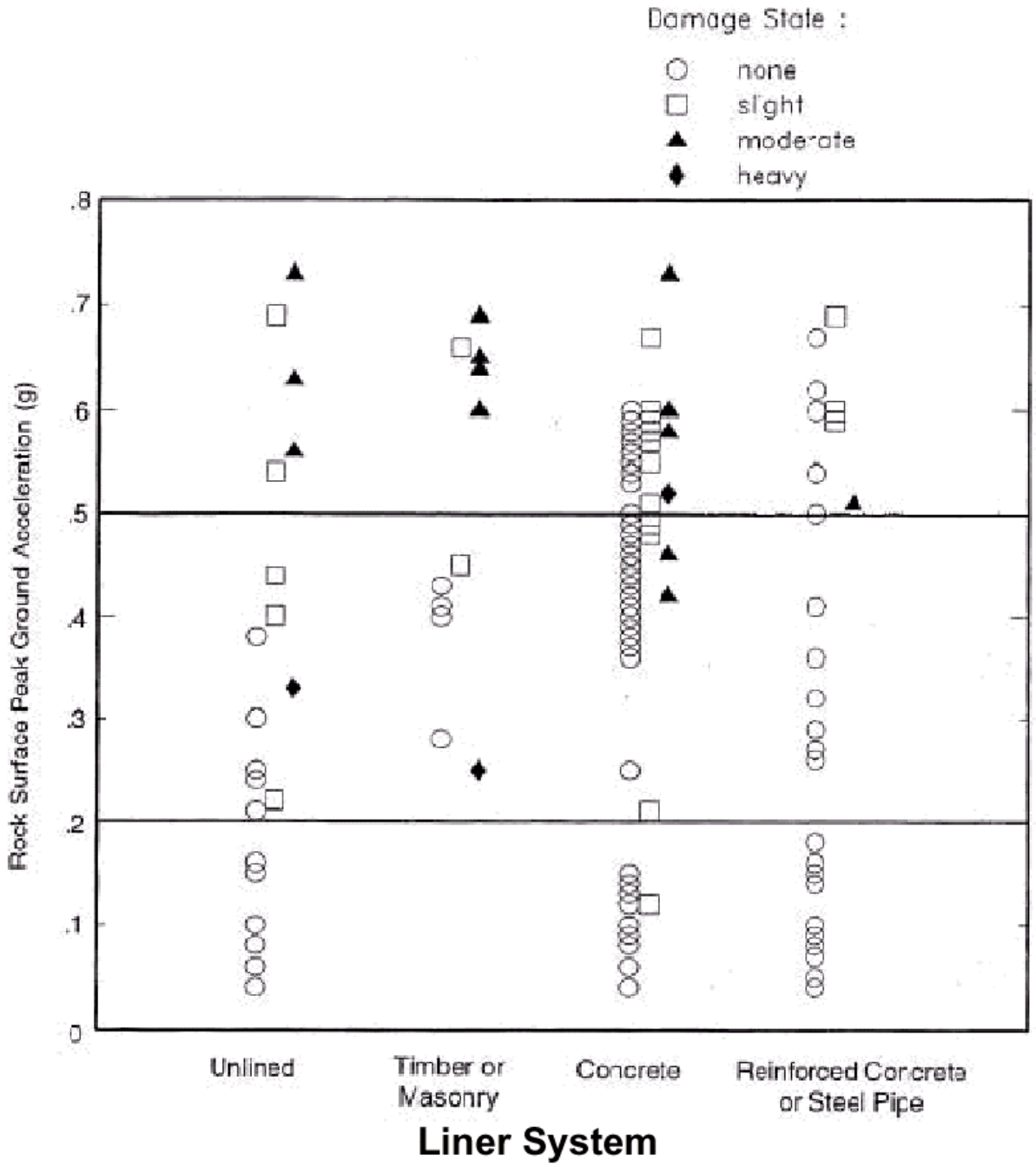


*Figure C-2. Summary of Empirical Observations of Seismic Ground Shaking-induced Damage for 204 Bored Tunnels [after Power et al, 1998]*

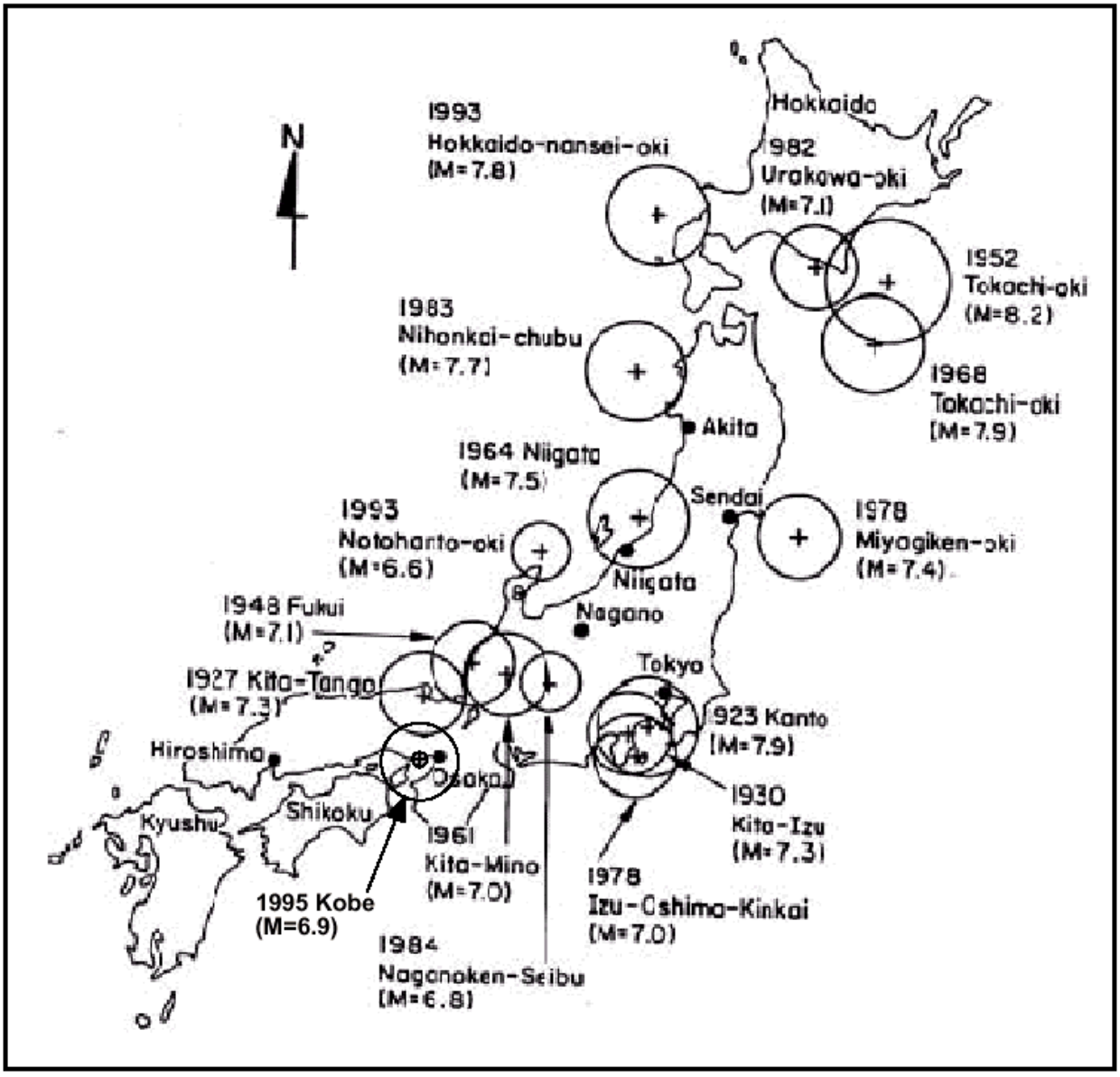


*Figure C-3. Map of Japan Showing Locations of 16 Earthquakes in Tunnel Database*

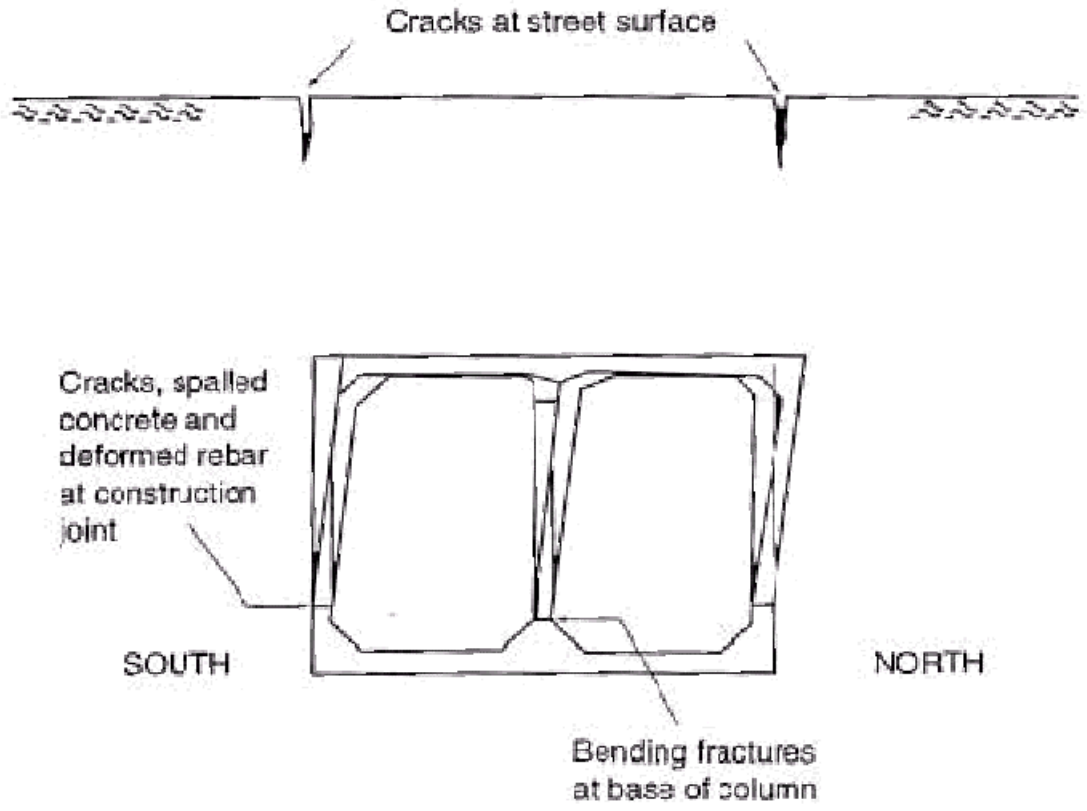


*Figure C-4. Deformations of Cut-and-cover Tunnel for Kobe Rapid Transit Railway [after O'Rourke and Shiba, 1997]*

# D. Commentary - Canals

## D.1 1979 Imperial Valley Earthquake

The 1979 Imperial Valley M 6.5 earthquake caused widespread damage to irrigation canals. The following descriptions are adapted from [Dobry et al].

The Imperial Valley is located near the US-Mexico border in Southern California. The area is flat and landslide movements are not significant in the area. Water for domestic, industrial and irrigation purposes originates at the Colorado River and is transported to a network of canals by the All-American Canal. The canals are either unlined or are lined with unreinforced concrete.

The most extensively damaged canal was the All-American Canal, constructed in the late 1930s. The total damage to the canal was estimated to be about $982,000 [Youd and Wieczorek]. Settlements, slumps, incipient slumps and incipient lateral spreads occurred along a 13-km-long section between Drop No. 5 near the Ash Canal and the East Highline Canal. The damage was concentrated on a 1.5-km-long section of the All American Canal, near the Alamo River. The repairs were made rapidly, preventing detailed mapping of the embankment deformations. Rotational earth slumps threatened to breach the canal, and incipient slumps, lateral spreads and many undifferentiated fissures caused extensive cracks on the embankment and also in the compacted fill around the structures. Along the All-American Canal, the damage was distributed as far as 10 km east and 3 km west of the causative Imperial fault. Youd and Wieczorek reported no evidence of large scale liquefaction around the canal, but localized liquefaction may have contributed to failure in some places.

Slumping and incipient slumping extended for about 500 m along the east side of the Highline Canal.

Both sides of the South Alamo Canal were badly cracked for a length of about 100 m; crack widths were about 15 mm and vertical crack offsets were 50 to 100 mm. At another location, the east bank showed fissures in a 500 m length. These fissures were caused by incipient slumping or lateral spreading towards the canal. The cracks at this site showed as much as 100 mm of opening and vertical offset.

The Barbara Worth Drain canal was also damaged in this earthquake.

In 1940, a M 7.1 earthquake occurred on much of the same fault as in the 1979 event. In the 1940 earthquake, damage to canals included Holtville Main Drain, All-American, Central Main, Alamo and Solfatara, for a total length of 119.7 km of damaged canal. The damage to these canals in the 1940 event was more severe than in the 1979 event. Although the 1940 damage was not clearly associated with the occurrence of liquefaction, the soil in the affected areas did contain sand layers; soils in the areas without canal damage did not.

Based on damage to the canal and irrigation ditch network in the 1979 earthquake, the authors analyzed the repair rate as a function of distance and recorded PGAs at representative distances from the nearest fault rupture. The results are shown in Figure D-1. In Figure D-1a, “conduit” represents either a canal or an irrigation ditch. The following trends are noted:

- The repair rate is highest for locations closest to the fault. For PGAs in the range of 0.5g to 0.8g, with corresponding PGVs of 22 in/sec to 35 in/sec, repair rates are about 0.15 to 0.25 repairs per kilometer. Repair rates drop to about one-tenth this rate when PGAs/PGVs have attenuated to about 0.2g/9 in/sec.
- Due to the lack of detailed design information for each canal or ditch in the area, we do not attempt to provide a fragility curve based on this information.

With regards to the operation of the All-American Canal in the 1979 earthquake, it was reported [EERI, 1980] that at the time of the earthquake, 3,700 cubic feet per second (cfs) of water was flowing in the canal. The bulk of this water was used for irrigation. Due to damage in the canal, flow was reduced to about 700 cfs, in order to prevent flooding over damaged levees of the canal. As repairs were made to the canal, flow was increased, reaching the required flow of 4,100 cfs by October 19, four days after the earthquake. During the four-day operation of the canal at low flows, there was sufficient raw water in an open cut reservoir for the city of El Centro's water treatment plant and, therefore, the damage to the canal did not directly affect treated water deliveries to customers in the city of El Centro—although damage to distribution pipelines did affect treated water deliveries.

## D.2 1980 Greenville Earthquake

The Contra Costa Canal is operated by the Contra Costa Water District. It transports raw water from the Delta to the City of Concord, California, and other nearby localities.

This canal underwent minor levels of ground shaking in the 1980 Greenville earthquake. PGAs were on the order of 0.02g to 0.10g. Minor damage was observed as a result of earth sloughing from adjacent earthen banks.

## D.3 1989 Loma Prieta Earthquake

The Contra Costa Canal underwent minor levels of ground shaking in the 1989 Loma Prieta earthquake. PGAs were on the order of 0.02g to 0.10g. No damage was observed.

The South Bay Aqueduct is operated by the State of California, Division of Water Resources. It transports water from the Delta to the cities of Livermore, Pleasanton and San Jose, California. This canal underwent moderate levels of ground shaking in the 1989 Loma Prieta earthquake. However, no canal lining damage was sustained. A bridge adjacent to the canal suffered moderate damage.

## D.4 References

Dobry, R., Baziar, M. H., O'Rourke, T. D., Roth, B. L., and Youd, T. L., "Liquefaction and Ground Failure in the Imperial Valley, Southern California During the 1979, 1981 and 1987 Earthquakes," in *Case Studies of Liquefaction and Lifeline Performance During Past Earthquakes, Volume 2, United States Case Studies*, Eds. T. D. O'Rourke and M. Hamada, NCEER Report 92-0002, Feb. 1992.

EERI, *Imperial County, California Earthquake Reconnaissance Report*, Earthquake Engineering Research Institute, G, Brandow Coordinator, D. Leeds, Editor, Feb. 1980.

Youd T.L. and Wieczorek G.F., "Liquefaction and Secondary Ground Failure in the Imperial Valley California Earthquake Oct 15, 1979," in *The Imperial Valley California Earthquake*, US Geological survey, Professional Paper 1254, pp. 223-246, 1982, Oct. 1979.

## D.5 Figures

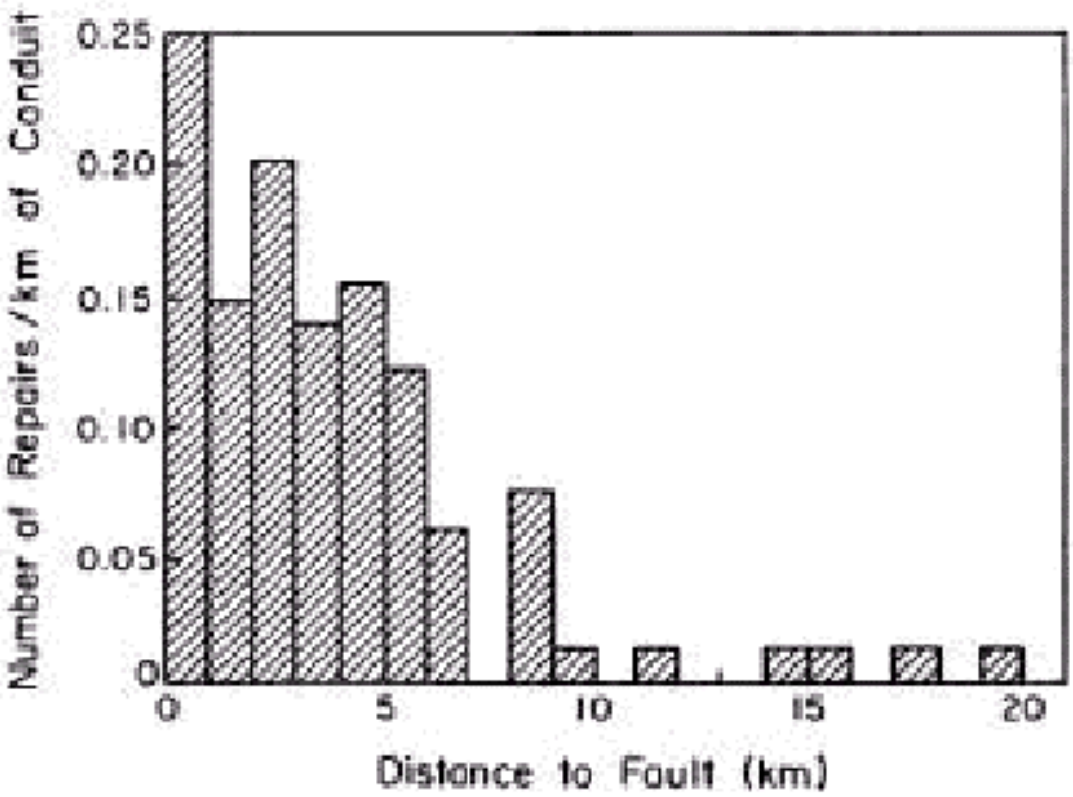


*D-1a. Repair Rate versus Distance to Nearest Fault*

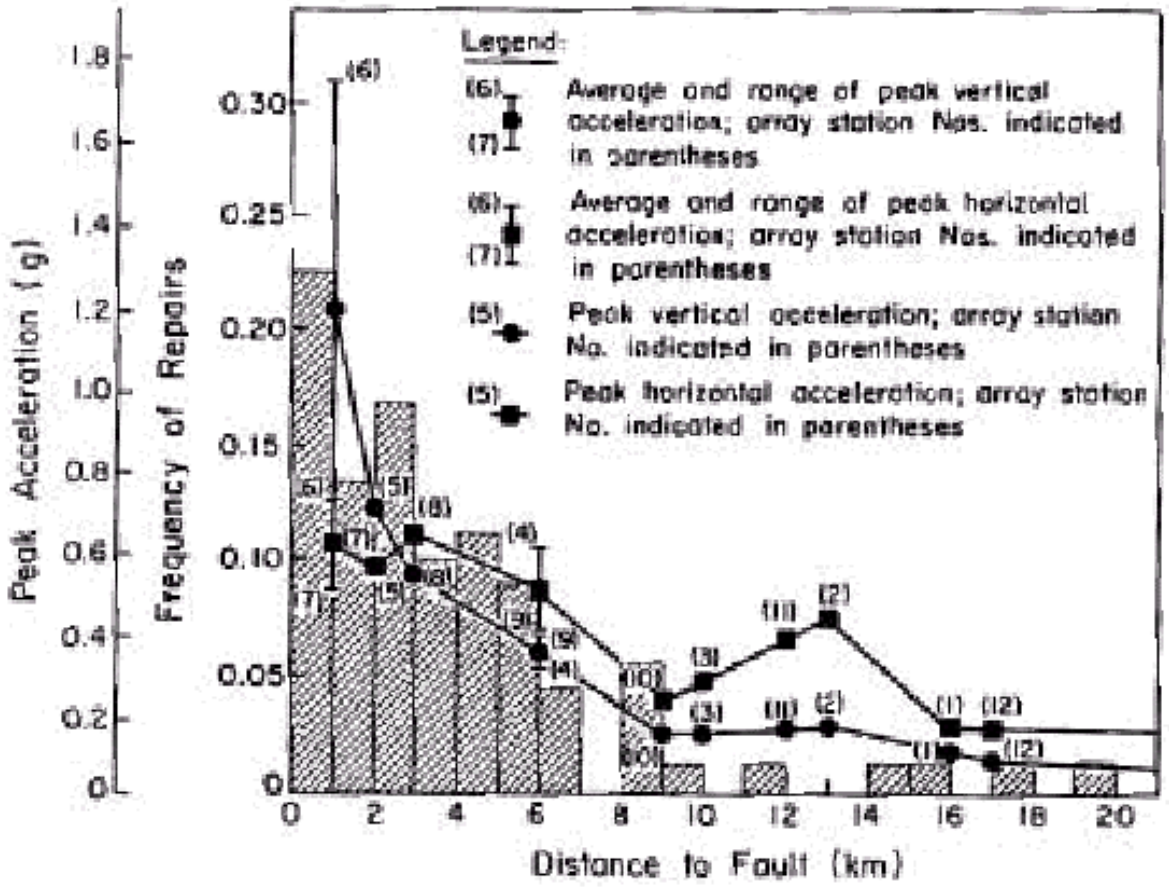


*D-1b. Repair Rate versus PGAs Recorded at Similar Distances to the Nearest Fault*

*Figure D-1. Canal and Ditch Repair Rates, 1979 Imperial Valley Earthquake [after Dobry et al]*

# E. Basic Statistical Models

Appendix E describes the general process used in establishing fragility curves.

## E.1 Options

Three general approaches can be used in developing fragility curves. These are:

- **The empirical approach.** This involves use of observed damage/non-damage from past earthquakes.
- **The analytical approach.** This involves the use of specific engineering characteristics of a component to assess its seismic capacity in a probabilistic way.
- **The engineering judgment approach.** This involves the review of available information by cognizant engineers and making an informed judgment as to the capacity of a component.

Part 1 uses all three approaches in developing fragility curves for the various components. Appendix E provides the mathematical models used in this process. Appendix G provides an alternate approach, called Bayesian Analysis, to standard regression analysis.

## E.2 Randomness and Random Variables

Randomness in a parameter means that more than one value is possible; the actual value is, to some degree, unpredictable. Mathematical representation of a random variable is a primary task in any probabilistic formulation.

In a loss estimation study, a prediction of the future is made using information from the past, including experience and judgment whenever possible. Thus, it is necessary to collect all relevant information from the past for this purpose. A typical flow chart of the steps involved is shown in Figure E-1. The information collected will constitute the sample space.

Appendices A-D provide empirical information for some of the water system components. The empirical information is likely to be incomplete, and further effort in reviewing the performance of water transmission system components would yield additional information that could be added to the sample space. It was not feasible in the current effort to consider every known piece of information. By expanding the data in the sample space, it is hoped that better fragility curves can be developed in the future.

The randomness characteristics of any sample space can be described graphically in the form of a histogram, or frequency diagram, as shown in Figure E-2. For a more general representation of the randomness, the frequency diagram can be fitted to some theoretical probability density function (PDF) $f_x(x)$. By integrating the probability density function thus obtained, a cumulative distribution function (CDF) $F_x(x)$ can be obtained.

To describe the PDF or CDF uniquely, some parameters of the distribution need to be estimated. The estimation of these parameters, called statistics, is a key step in the development of fragility curves.

### E.2.1 The Normal Distribution

A random variable usually can be described mathematically by a distribution. A random variable can be discrete or continuous. Most commonly used discrete random variable are described by the binomial distribution, Poisson, distribution, geometric distribution, etc. Continuous random variables are generally described by the normal distribution, lognormal distribution, exponential distribution, Gamma distribution, Beta distribution, Chi-Square distribution, etc. Refer to Benjamin and Cornell [1970] for a more complete description of various distributions.

Among the most important statistical parameters are the mean value, $\mu$, which denotes the average of expected value of the random variable, and the standard deviation, $\sigma$, which denotes the dispersion of a random variable with respect to the mean value. The coefficient of variation (COV) is the ratio of the standard deviation and the mean value.

For a discrete random variable, the mean and unbiased variance can be calculated as follows:

$$\mu_x = \frac{1}{n}\sum_{i=1}^{n} x_i$$

$$Var(x) = \frac{1}{n-1}\sum_{i=1}^{n}(x_i - \mu)^2$$

The standard deviation and COV are calculated from the following relationships once the mean and variance of a random variable are known.

$$\sigma_x = \sqrt{Var(x)}$$

$$COV = \sigma_x / \mu_x$$

### E.2.2 Which Distribution Model?

To develop a probabilistic model, the underlying distribution of a random variable and its statistics need to be known. The methods to empirically determine the distribution model are discussed in this section.

In practice, the choice of the probability distribution if often dictated by mathematical convenience. In many engineering evaluations of damage to water system components from past earthquakes, the functional form of the required probability distribution may not be easy to determine, as more than one distribution may fit the available data. The basis of the properties of the physical process may suggest the form of the required distribution.

The required probability distribution may be determined empirically, based entirely on the available observed data. A frequency diagram for the set of data can be constructed and a distribution model can be selected by visual comparison as shown in Figure E-2.

When the distribution model is obtained using this method, or when two or more distributions appear to be plausible probability distribution models, statistical tests (known as goodness-of-fit tests for distributions) can be carried out to verify the distribution model. Two such tests commonly used for this purpose are the Chi-Square $\chi^2$ and the Kolmogorov-Smirnov (K-S)

tests. For this report, the lognormal distribution is assumed in essentially all fragility formulations. This has been done as the lognormal distribution is mathematically convenient. See Section E.6 for further details. Other researchers may find that other dispersion models are better suited for specific applications.

### E.2.3 Lognormal Variables

In some special cases, suppose:

$$Y = X_1 \bullet X_2 \mathrm{L} \bullet X_n$$

where $X_i$ is a statistically independent lognormal variable with means $\mu_{X_i}$ and standard deviation $\sigma_{X_i}$; then Y is also a lognormal variable.

From an engineering point of view, for loss estimation of water system components, the form of the lognormal distribution has some advantages. The total response, Y, can be represented as the deterministic response value multiplied by a series of correction factors that are random and associated with various uncertainties. Irrespective of the proper distribution of these individual variables $X_i$, the product of the variable will be approximately lognormal. Another advantage of the lognormal function is that a variable cannot take negative values. For these reasons, it is commonly adopted to model a variable as a lognormal variable rather than a normal variable. Note that whether or not the real world is really "lognormal" is often ignored in the evaluation—but it is convenient that it should be.

Knowing the mean and variance for a random variable X, $\mu_X$ and $\sigma_X$ the two parameters of the lognormal distribution $\lambda_X$ (logarithmic mean) and $\varsigma_X$ (logarithmic standard deviation, beta, β) can be obtained as follows:

$$\lambda_X = \ln(\mu_X) - \frac{1}{2}\varsigma_X^2$$

and

$$\varsigma_X^2 = \ln\left(1 + \frac{\sigma_X^2}{\mu_X^2}\right)$$

Say that $x_m$ is the median ($x_{50}$) of the variable X. Then,

$$\lambda = \ln(x_m)$$

and the 84th percentile value of X (i.e., one standard deviation higher than the median) is

$$x_{84} = x_{50}e^{\beta} = x_m e^{\varsigma}$$

Since $X_i$s are lognormal, then ln($X_i$s) are normal and

$$\lambda_Y = Expected\_Value(\ln Y) = \sum_{i=1}^{n} \lambda_{X_i}$$

and

$$\varsigma_Y^2 = Var(\ln Y) = \sum_{i=1}^{n} \varsigma_{Xi}^2$$

### E.2.4 Regression Models

Some of the regression models used in this report for buried pipe are of the logarithmic regression form. In other words, if $Y_i$ is the repair rate per 1,000 feet and X*i* is the PGV in inches/sec, then:

$$Y_i = \alpha X_i^B z_i$$

where α and B are constants to be determined from a regression analysis, and $z_i$ is the error term. The solution for α and B using least squares methods can be found in many statistics textbooks. Appendix G provides an alternative approach, called Bayesian analysis.

This model can be simplified into the standard linear regression model by taking the log of the equation, thus:

$$\ln Y_i = \ln \alpha + B \ln X_i + e_i$$

## E.3 Simulation Methods

When performing loss estimates for water system components, the Monte Carlo simulation technique can be employed. This technique is readily adapted to computer techniques. One of its advantage is that many independent variables can be processed on an individual basis, and the distribution of the dependent variable can be examined by reviewing the results of many independent trials.

The number of simulations to be used will affect the accuracy of the final results. A larger number of simulations will reduce the effects of the tails of the derived distribution.

## E.4 Risk Evaluation

Using the procedures described in the previous sections, the uncertainties associated with the random resistance R and the random load S can be quantified. This is graphically shown in Figure E-3. The shaded region in Figure E-3 indicates the region where the loading function (S) is greater than the resistance function (R). The risk that the damage state R occurs is the area represented by the shaded region. Mathematically,

$$Risk = P(\text{damage state R occurs}) = P(R \le S)$$

$$= \int_0^{\infty} \left[ \int_0^{s} f_R(r)dr \right] f_S(s)ds$$

## E.5 Fragility Curve Fitting Procedure

For the fragility curves developed for tanks and tunnels, a best-fit regression analysis was performed. The approach was as follows:

The tanks and tunnels were "binned" into PGA bins. Each bin was for typically for a range of 0.1g, with the exception of PGAs over 0.7g. The higher g bins were wider as there were fewer tunnels in this PGA range. The PGA for each bin was set at the average of the PGA values for each tunnel in that bin. The percent of tunnels reaching or exceeding a particular damage state was calculated for each bin.

A lognormal fragility curve was calculated for each of the damage states. A fragility curve was calculated for all tanks or tunnels which reached damage state 2 (DS2) or above, DS3 or above, DS4 or above, and DS5, as applicable. The fragility curve uses the median acceleration to reach that damage state or above and a lognormal dispersion parameter, $\beta$. The best-fit fragility curve was selected by performing a least square regression for all possible fragility curves in the range of A=0.01g to 5.00g (in 0.01g steps) and $\beta$=0.01 to 0.80 (in 0.01 steps).

Since an unequal number of tanks or tunnels are in each bin, the analysis was performed using an unweighted regression analysis and also a weighted regression analysis. The weighted analysis is considered a better representation.

## E.6 Randomness and Uncertainty

In developing or updating fragility curves, this report often separately characterizes "randomness" from "uncertainty."

Randomness reflects variables in the real world that current technology and understanding cannot explain. In other words, no reasonable amount of additional study of the problem will reduce randomness. Randomness exists in the level of ground motion at two nearby sites, even if they have very similar soil profiles and distances from the fault rupture. Randomness is characterized using a logarithmic dispersion parameter:

$$\beta_R$$

$\beta_R$ can be determined by doing regressions for ground motion attenuation functions for the suitable parameter of PGA for tanks and tunnels and PGV and PGD for buried pipelines. There are many published references for these values, and it varies based on earthquake magnitude, type of faulting mechanism, type of soil, etc. Recent work by Geomatrix (Power, Wells and Coppersmith, et al) can be used to provide $\beta_R$ for permanent ground deformations (PGDs), fault offset, liquefaction and landslides.

Uncertainty reflects the uncertainty in the predictions, given the level of simplification taken in the analysis. For example, suppose a water utility wanted to do a quick earthquake loss estimate for buried transmission pipelines without having to do a detailed effort to ascertain exactly what type of buried pipelines are in use at which locations, how old they are, what their leak history is, which soils are most susceptible to corrosion, which soils are most susceptible to PGDs, what level of corrosion protection has been taken for a particular pipeline, and so on. In such a case, the fragility curve used should take into account that there is uncertainty in the pipeline inventory, as well as how that inventory would respond to a given level of ground motion. Uncertainty is characterized using a logarithmic dispersion parameter:

$$\beta_U$$

The total uncertainty is then expressed as:

$$\beta_T = \sqrt{\beta_R^2 + \beta_U^2}$$

### E.6.1 Total Randomness and Uncertainty

The method by which randomness and uncertainty are tabulated for this report considers the following:

- A possible update of the water pipeline/transmission system component fragilities in the HAZUS computer program. HAZUS makes many simplifying assumptions in order to get a computer program that is both easy to use and easy to program. Only one dispersion parameter is allowed in HAZUS, which is the equivalent of $\beta_T$.
- Depending on the source data sets used to establish the uncertainty parameters, the underlying uncertainty in the empirical data may or may not include $\beta_R$. A good quality data set using GIS techniques on a well document earthquake would primarily reflect $\beta_U$. In either case, the fragility curves in Part 1 must clearly indicated whether or not the dispersion parameter includes $\beta_R$. In so doing, the results in Part 1 can be suitably interpreted to allow for separation of uncertainty in ground motion and inventory response.
- To summarize, it would be ideal to present three measures of uncertainty: $\beta_T$ , if used in HAZUS or HAZUS-like programs; $\beta_R$ , so this could be varied by the type of earthquake and by future advances in geotechnical descriptions of ground motion; and $\beta_U$ , so that this can be used in programs that are more sophisticated than HAZUS, and for users who establish a high-quality inventory database.

## E.7 The Model to Estimate Fragility of a Structure or Piece of Equipment

The variability of how a structure or piece of equipment can respond can be described by a probability density function (PDF) as shown in Figure E-3 ($f_R(r.)$). Rarely does the engineer consider the shape of the PDF of the item being designed; instead, the item is designed to "code." For convenience, we call designing to code a "deterministic" design. Generally conservative parameters are used in deterministic design so that only a low probability exists that the actual seismic demand 'S' exceeds the actual seismic capacity. It is neither necessary nor desirable for the deterministic design to be so conservatively performed that the probability of failure is negligibly low.

In deterministic analysis, the deterministic factor of safety, $F_D$, is defined as the ratio of the deterministic code capacity, $C_D$, to the deterministic computed response, $R_D$, i.e.,

$$F_D = \frac{C_D}{R_D}$$

In probabilistic analysis, both the capacity C and the response R are random variables. Thus, the factor of safety is given by:

$$F = \frac{C}{R}$$

which is also a random variable. A capacity factor, $F_C$, can be defined as the ratio of the actual capacity, C, to the deterministic code capacity, $C_D$. Similarly, a response factor, $F_R$, is defined as the ratio of the deterministic computed response, $R_D$, to the actual response R, i.e.,

$$F_C = \frac{C}{C_D}; \qquad F_R = \frac{R_D}{R}$$

Thus, the probabilistic factor of safety, F, can be defined in terms of the deterministic factor of safety, $F_D$, by:

$$F = F_C \bullet F_R \bullet F_D$$

The probability of failure is the probability that the factor of safety, F, is less than 1. The reliability is the probability that the factor of safety, F, is 1 or greater.

Computation of the probability of failure is tractable mathematically when the capacity and the response factors, $F_D$ and $F_R$, are assumed to be lognormally distributed random variables. F is a lognormal random variable if $F_D$ and $F_R$ are lognormal random variables. The median value, $\hat{F}$, and the logarithmic standard deviation, $\beta_F$ of F are given by:

$$\hat{F} = \hat{F}_C \bullet \hat{F}_R \bullet F_D$$

$$\beta_F^2 = \beta_C^2 + \beta_R^2$$

where $\hat{F}_C$ and $\hat{F}_R$ are the median values and $\beta_C$ and $\beta_R$ and the logarithmic standard deviations for the capacity, $F_C$, and response , $F_R$ , factors. The probability of failure is then given by:

$$P_f = \Phi\left( \frac{\ln\left( 1 / \hat{F} \right)}{\beta_F} \right)$$

where $\Phi$ is the standard cumulative distribution function.

Section E.7 is concerned with estimating the capacity factor random variable, $F_C$, that, when combined with the response random variable, $F_R$, and a code-specified deterministic factor of safety, $F_D$, can be used to estimate a probabilistic factor of safety, F, and a probability of failure.

Section 3 of Part 1 of this report briefly describes how to compute $F_R$. It is beyond the scope of the current effort to determine ho to compute seismic response at a location.

Under dynamic loading, the capacity factor is assumed to be made up of two parts:

$$F_C = F_S \bullet F_\mu$$

where $F_S$ represents the strength factor for an equivalent static loading and $F_\mu$ represents the added capacity due to the ductility of the structure and the fact that the loading has limited energy content.

## E.8 References

Benjamin, J. R. and Cornell, C. A., *Probability, Statistics and Decision for Civil Engineers*, McGraw-Hill.

## E.9 Figures

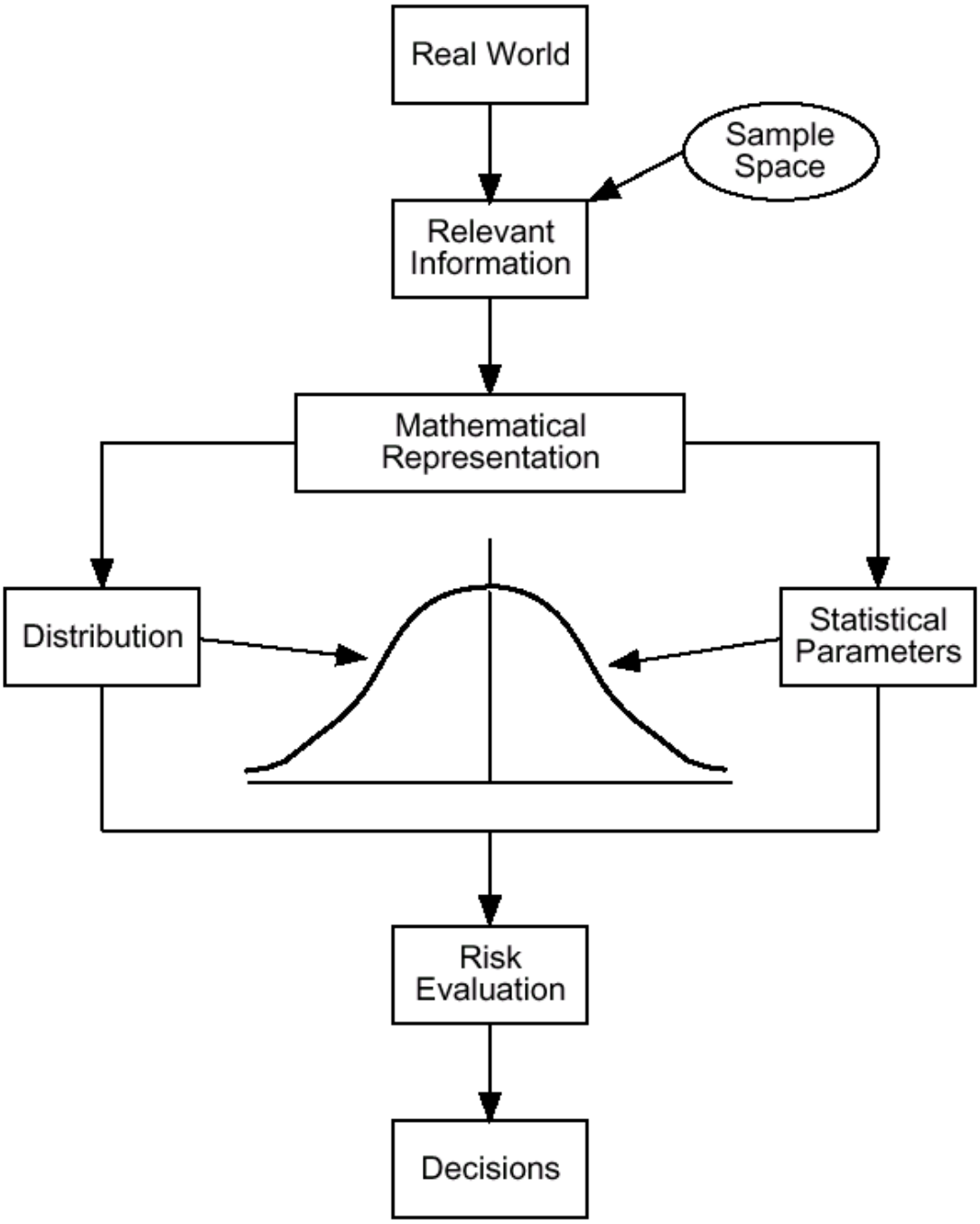


*Figure E-1. Steps in a Probabilistic Study*

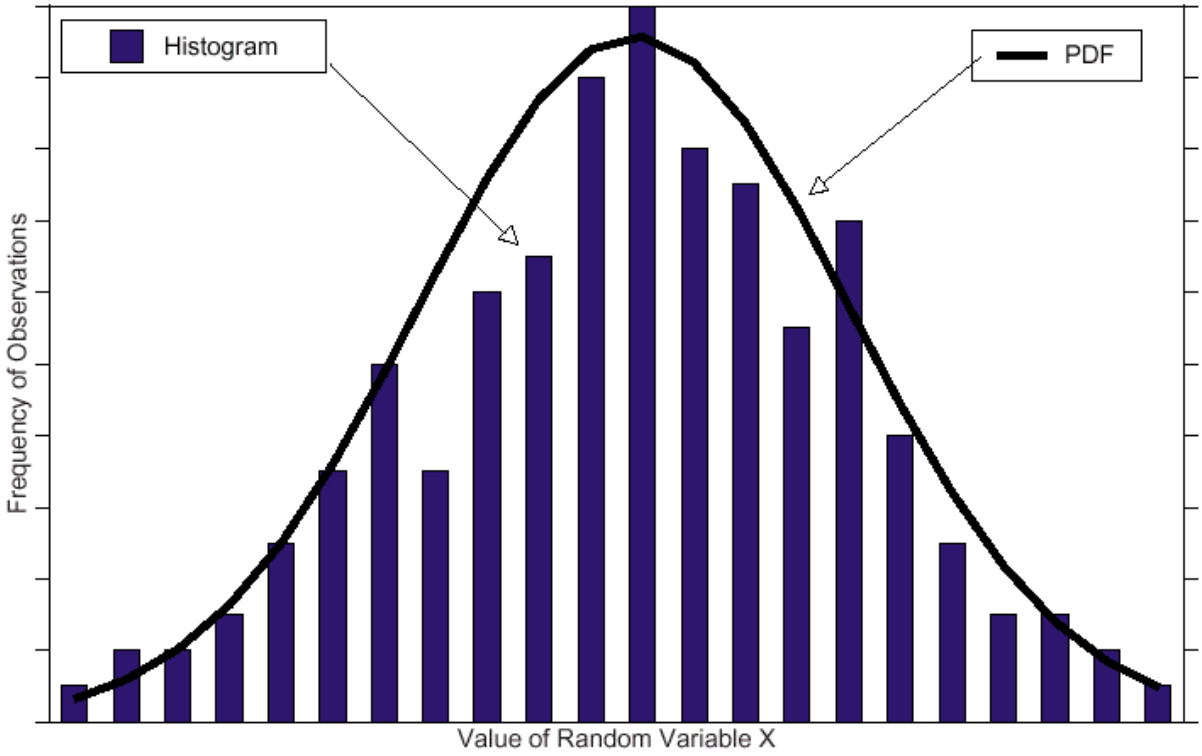


*Figure E-2. Typical Histogram or Frequency Diagram*

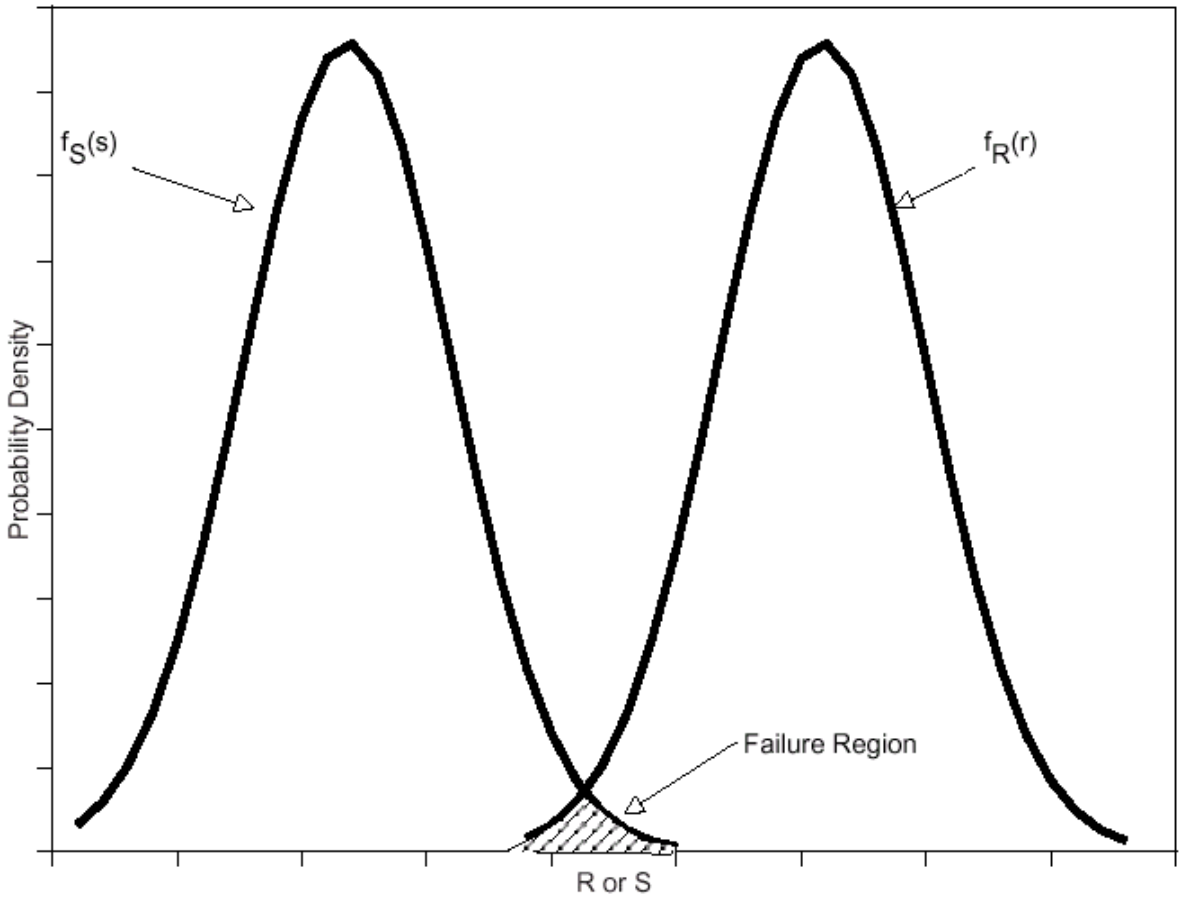


*Figure E-3. Risk Evaluation*

# F. Example

Data reflecting a portion of a California water transmission aqueduct built in the 1930s is examined in Appendix F. The aqueduct consists of 33,400 feet of 62-inch diameter concrete pipe with steel cylinder and 48,000 feet of 66-inch diameter welded steel pipe.

For the purpose of illustrating how to apply the guideline procedures, this portion of pipeline is further divided into the following four segments according to their surface geological conditions:

| Segment | Length | Material | Joint | Avg. Dist. from Fault Considered | Surface Geology |
|---|---|---|---|---|---|
| 1 | 7,200 ft | Conc. w/ steel cyl. | Welded | 2.3 mi. | Rock-like soils |
| 2 | 30,500 ft | Steel | Welded | 0.6 mi. | Firm soils |
| 3 | 17,500 ft | Steel | Welded | 1.5 mi. | Firm Soils |
| 4 | 26,200 ft | Conc. w/ steel cyl. | Welded | 3.7 mi. | Rock-like soils |

*Table F-1. Water Transmission Aqueduct Example*

Figure F-1 is a simplified map of the water transmission system of Table F-1. The issue at hand is to estimate the number of repairs that may be required for this portion of the pipeline during an earthquake with Richter moment magnitude of 7.1 ($M_w$7.1) generated by the fault near the pipeline.

Tables F-2a and F-2b give the summary results of the analysis.

| Segment | PGA | Number of Repairs | | | | |
|---|---|---|---|---|---|---|
| | | Ground Shaking | Liquefaction | | Landslide | Total |
| | | | Settlement only | With Lateral Spread | | |
| 1 [1] | 0.58g | 0.18 | | – | – | **0.18** |
| 2 [2] | 0.55g | 0.24 | 0.23 | – | – | **0.47** |
| 3 [3] | 0.40g | 0.0 | | 2.73 | – | **2.73** |
| 4 [4] | 0.40g | 0.60 | | – | 1.49 | **2.09** |
| **Total** | **–** | **1.02** | **0.23** | **2.73** | **1.49** | **5.47** |

Notes.
1. Detailed calculation provided in Section F.1.
2. Detailed calculation provided in Section F.2.
3. Detailed calculation provided in Section F.3.
4. Detailed calculation provided in Section F.4

*Table F-2a. Summary Results (Dry Conditions)*

| Segment | PGA | Number of Repairs | | | | |
|---|---|---|---|---|---|---|
| | | Ground Shaking | Liquefaction | | Landslide | Total |
| | | | Settlement only | With Lateral Spread | | |
| 1 [1] | 0.58g | 0.18 | | – | – | **0.18** |
| 2 [2] | 0.55g | 0.24 | 0.23 | – | – | **0.47** |
| 3 [3] | 0.40g | 0.0 | | 2.73 | – | **2.73** |
| 4 [4] | 0.40g | 0.50 | | – | 15.1 | **15.6** |
| **Total** | **–** | **0.92** | **0.23** | **2.73** | **15.1** | **19.0** |

Notes [1] to [4]. See Notes for Table F-2a.

*Table F-2b. Summary Results (Wet Conditions)*

## F.1 Calculations – Segment 1

This segment of welded steel pipeline is subject to strong ground shaking from the nearby fault. The pipe traverses an area best characterized as rock or rock-like material without potential for liquefaction or landslide.

### Ground Shaking

*Step 1. Obtain anticipated earthquake magnitude generated from an active fault. Calculate the site specific peak ground acceleration (PGA) from this earthquake.*

Assume $M_w$ = 7.1 and average PGA for this segment = 0.58g. The selection of the moment magnitude is beyond the scope of this report. Section 3.2 of Part 1 provides some guidance, differentiating between deterministic and probabilistic definitions of earthquakes. Lacking input from knowledgeable seismologists, a rational approach would be to evaluate the pipeline for a specific scenario earthquake. Select the moment magnitude $M_w$ for the scenario earthquake based on the length of the fault ($L_r$ in km), using an expression like:

$$\log_{10} L_r = -2.36 + 0.58 M_w$$

Once the magnitude of the scenario earthquake is selected, calculate the median horizontal ground acceleration (PGA) by using an equation like F.1—other equations might be more suitable, depending on location in the US, type of fault mechanism, etc. This assumes the pipeline is underlain by rock or rock-like soils.

$$\ln Z = -1.274 + 1.1M - 2.1\left[\ln\left(R + e^{-0.48451+0.524M}\right)\right] \qquad \text{(eqn. F.1)}$$

Assuming the average distance to the fault is 2.3 miles (= 3.7 km), gives ln Z = -0.543, or Z = 0.58g.

*Step 2: Calculate peak ground velocity (PGV) with a suitable attenuation relationship.*

For M=7.1 and rock-like soil conditions, assume PGV = 49.4 cm/sec = 19.4 inch/sec.

*Step 3: Calculate number of repairs per 1,000 feet based on PGV, pipe material, pipe joints, soil corrosiveness and pipe diameter.*

From Table 4-4, the repair rate for the "backbone" pipe fragility curve is RR = 0.00187 * PGV = 0.0363 repairs per 1,000 feet. From Table 4-5, apply K1 = 0.7 (large-diameter concrete cylinder pipe with lap welded joints), so the total repair rate is 0.0254 repairs per 1,000 feet.

*Step 4: Calculate total number of repairs in this segment due to ground shaking*

N = 0.0254 * 7200/1000 = 0.18.

## F.2 Calculations – Segment 2

This segment of welded steel pipeline is subject to strong ground shaking from the nearby fault. This segment also traverses reasonably competent soils that are subject to localized liquefaction.

**Ground Shaking**

*Step 1. Obtain anticipated earthquake magnitude generated from an active fault. Calculate the site-specific peak ground acceleration (PGA) from this earthquake.*

Calculate the median horizontal ground acceleration (PGA) using an attenuation model such as in Equation F.2. Again, other equations may be more suitable. This assumes the pipeline is underlain by firm soils.

$$\ln Z = -2.17 + 1.0M - 1.7\left[\ln\left(R + 0.3825e^{0.5882M}\right)\right] \qquad \text{(eqn. F.2)}$$

Assuming the average distance to the fault is 0.6 miles (= 1 km) gives Z = 0.55g.

*Step 2: Calculate peak ground velocity (PGV) with suitable attenuation relationship.*

For M=7.1 and firm soil conditions, PGV = 73.7 cm/sec = 29 inch/sec.

*Step 3: Calculate number of repairs per 1,000 feet based on PGV, pipe material, pipe joints, soil corrosiveness and pipe diameter.*

From Table 4-4, the repair rate for the "backbone" pipe fragility curve is RR = 0.00187 * PGV = 0.0543 repairs per 1,000 feet. From Table 4-5, apply K1 = 0.15 for large-diameter, single lap welded steel pipe, so the total repair rate is 0.00814 repairs per 1,000 feet.

*Step 4: Calculate total number of repairs in this segment due to ground shaking*

N = 0.00814 * 30500/1000 = 0.25. But note that the value N=0.25 assumes that the entire length of Segment 2 is not subject to liquefaction. As described below, about 4% of the length is subject to liquefaction. So the damage in the ground shaking zone is 96% of this value (=0.96 * 0.25).

## Liquefaction

*Step 1: For a scenario earthquake, calculate the level of shaking (PGA) at the particular location of the component being evaluated.*

M = 7.1, PGA = 0.55g (same as the value from the ground shaking calculations)

***Note that geotechnical investigation done by knowledgeable professionals is strongly recommended. Steps 2 through 5 below are to be used only when detailed geotechnical investigation is unavailable.***

*Step 2: Establish the geologic unit for the near surface environment at the component location.*

From a site-specific geotechnical report or USGS or CDMG publication, determine:

- Type of deposit: Alluvial.
- Age of deposit: Holocene

Chance of susceptibility to liquefaction is "Low."

*Step 3: Given the PGA, geologic unit and liquefaction susceptibility description, the estimated ground water depth and the magnitude of the earthquake, calculate the probability that liquefaction occurs at the location.*

For this PGA level, earthquake magnitude and ground water table, assume the probability of liquefaction is 80% for liquefiable deposits. Assume 5% of the deposits are liquefiable. Thus, the probability that a specific location liquefies is 4% (=0.8 * 0.05).

*Step 4: Given that the site liquefies, calculate the maximum permanent ground deformation or the probabilities for different settlement ranges.*

Assume the settlement ranges in Table F-3 are prepared using techniques outside the scope of this report.

| Settlement Range (in.) | Probability of settlement due to 4% probability of liquefaction |
|---|---|
| ≤ 1 | 4% * 35% = 1.4% |
| 1 – 3 | 4% * 60% = 2.4% |
| 3 – 6 | 4% * 4% = 0.16% |
| 6 -12 | 4% * 1% = 0.04% |

*Table F-3. Settlement Ranges – Segment 2*

*Step 5: If there is no lateral spread (e.g., the pipe is not adjacent to an open cut or a slope), calculate the repair rates per 1,000 feet using the vertical ground settlement.*

From Table 4-4 and 4-6, the repair rate for the "backbone" pipe fragility curve is RR = K2 * 1.06 * PGD repairs per 1,000 feet. From Table 4-6, apply K2 = 0.15 for large-diameter, single lap welded steel pipe. The vertical displacement will be the total estimated PGD parameter.

The average values of the settlement ranges in the first column of Table F-3 are used as the estimated PGDs.

| Assumed estimated PGD (in.) | Number of repairs per 1,000 ft. (Assume 100% probability for each estimated PGD) | Number of repairs per 1000 ft. |
|---|---|---|
| 1 | $n = 0.15 * 1.06 * (1)^{0.319} = 0.16$ | n = 0.16 * 1.4% = 0.00224 |
| 2 | $n = 0.15 * 1.06 * (2)^{0.319} = 0.20$ | n = 0.20 * 2.4% = 0.0048 |
| 4 | $n = 0.15 * 1.06 * (4)^{0.319} = 0.25$ | n = 0.25 * 0.16% = 0.00040 |
| 9 | $n = 0.15 * 1.06 * (9)^{0.319} = 0.32$ | n = 0.32 * 0.04% = 0.00013 |

*Table F-4. Pipe Repair Rates – Segment 2*

Repair rate per 1,000 feet = 0.00224 + 0.0048 + 0.00040 + 0.00013 = 0.0076.

*Step 6: Calculate total number of repairs in this segment due to liquefaction.*

N = .0076 * 30,500/1000 = 0.23

Note that the PGD algorithm already includes damage due to PGV.

*Step 7: Calculate total number of repairs (Ground Shaking and Liquefaction) for Segment 2.*

The total number of repairs for Segment 2:

Liquefaction zone: N = 0.23

Ground shaking zone without liquefaction:

N = 0.25 * 0.96 = 0.24

Total = 0.23 + 0.24 = 0.47.

## F.3 Calculations – Segment 3

Repair rates for liquefaction with and without lateral spread are calculated. Assume M=7.1 and average PGA for this segment=0.5g. The pipeline is assumed to be buried and to traverse liquefiable soils near a body of water. It is also assumed that the pipe has been installed using typical cut-and-cover trench techniques without special soil improvement to address liquefaction hazards. While the soil within the pipeline trench may be of various materials, the native soils underlying and adjacent to the pipe trench are assumed to control the overall potential for PGDs along the length of pipeline.

**Liquefaction**

*Step 1: For a scenario earthquake, calculate the level of shaking (PGA) at the particular location of the component being evaluated.*

M = 7.1, PGA = 0.40g. Note that for this segment, the pipe traverses modern young soils, and moderately high values of PGA (0.4g) may still have very high values of PGV (over 35 inches/sec).

***Note that geotechnical investigation done by knowledgeable professionals is strongly recommended. Steps 2 through 6 below are to be used only when no detailed geotechnical investigation is unavailable.***

*Step 2: Establish the geologic unit for the near surface environment at the component location.*

From a site-specific geotechnical report or USGS or CDMG publication, determine:

- Type of deposit: Delta
- Age of deposit: Modern

Chance of susceptibility to liquefaction is "Very High."

*Step 3: Given the PGA, geologic unit and liquefaction susceptibility description, the estimated ground water depth and the magnitude of the earthquake, calculate the probability that liquefaction occurs at the location.*

For this PGA level, earthquake magnitude and ground water table, assume the probability of liquefaction is 95% for liquefiable deposits. Assume 25% of the deposits are liquefiable. Thus, the probability that a specific location liquefies is 24% (=0.95 * 0.25).

*Step 4: Given that the site liquefies, calculate the maximum permanent ground deformation and the probabilities for different PGD ranges.*

*Step 4a. No Lateral Spread. Table F-5 gives a range of settlements for the specific soil deposits and earthquake conditions.*

| Settlement Range (in.) | Probability of settlement due to 24% probability of liquefaction |
|---|---|
| 1 – 3 | 24% * 5% = 1.2% |
| 3 – 6 | 24% * 25% = 6% |
| 6 - 12 | 24% * 50% = 12% |
| > 12 | 24% * 20% = 4.8% |

*Table F-5. Settlement Ranges – Segment 3*

*Step 4b. With Lateral Spread. Assume an analysis is performed that determines that a lateral spread with PGD = 82 inches is possible at locations so susceptible.*

*Step 5: For areas with no lateral spread, calculate the repair rates per 1,000 feet using the vertical ground settlement.*

From Table 4-4 and 4-6, the repair rate for the "backbone" pipe fragility curve is RR = K2 * 1.06 * PGD repairs per 1,000 feet. From Table 4-6, apply K2 = 0.15 for large-diameter, single lap welded steel pipe. The vertical displacement will be the total estimated PGD parameter.

The average values of the settlement ranges in the first column of Table F-6 are used as the estimated PGDs.

| Assumed estimated PGD (in.) | Number of repairs per 1000 ft. (Assume 100% probability for each estimated PGD) | Number of repairs per 1.000 ft. |
|---|---|---|
| 2 | $n = 0.15 * 1.06 * (2)^{0.319} = 0.20$ | n = 0.20 * 1.2 % = 0.0024 |
| 4 | $n = 0.15 * 1.06 * (4)^{0.319} = 0.25$ | n = 0.25 * 6.0 % = 0.015 |
| 9 | $n = 0.15 * 1.06 * (9)^{0.319} = 0.32$ | n = 0.32 * 12 % = 0.038 |
| 12 | $n = 0.15 * 1.06 * (12)^{0.319} = 0.35$ | n = 0.35 * 4.8 % = 0.017 |

*Table F-6. Pipe Repair Rates – Segment 3*

Repair rate per 1000 feet = 0.0024 + 0.015 + 0.038 + 0.017 = 0.072 (settlement only).

*Step 6: For area adjacent to an open cut where lateral spread is possible, calculate the repair rates per 1,000 feet using the vector sum of the ground settlement and the lateral displacement.*

The vector sum of the ground settlement and the lateral spread displacement should be used for PGD when lateral spread is possible. Assume the most probable settlement range is 6 to 12 inches. Conservatively, use the high value to calculate PGD.

$$\therefore PGD = \sqrt{(12)^2 + (82)^2} = 83 \text{ in.}$$

$K_2 = 0.15$ (steel pipe with welded joints), per Table 4-6.

Repair rate per 1,000 feet = $0.15 * 1.06 * (83)^{0.319} = 0.65$.

As the repair rate with lateral spread (0.65) is higher than the repair rate from settlement only (0.072), use the higher value in zones with liquefaction with potential for lateral spread.

*Step 7: Calculate the total number of repairs (Ground Shaking and Liquefaction) for Segment 3.*

The total number of repairs for Segment 3:

Liquefaction zone: N = 0.24 * 0.65 * 17,500/1,000 = 2.73.

Check damage rate if there was no liquefaction.

Assume PGV = 35 inches per second. RR = 0.15 * 0.00187 * 35 = 0.0098 per 1,000 ft.

N = 0.76 * .0098 * 17,500/1,000 = 0.13. since 0.13 << 2.73, liquefaction rate controls.

## F.4 Calculations – Segment 4

Repair rates for Segment 4 include the potential for landslide hazards along this length of pipeline. It is assumed that the entire Segment 4 length is located in sloped terrain.

**Landslide**

*Step 1: For a scenario earthquake, calculate the level of shaking (PGA) at the particular location of the component being evaluated.*

Assume an average PGA for this segment=0.4g, and that the typical soil profile is rock. While landslide zones may be characterized as having up to a few tens of feet of colluvial material, it is still reasonable to use a rock-type attenuation model to estimate ground motions at the pipe locations.

$\therefore A_{is} = 0.4g$

***Note that geotechnical investigation done by knowledgeable professionals is strongly recommended. Steps 2 thru 4 below are to be used only when detailed geotechnical investigation is unavailable.***

*Step 2: Determine slope angle and geologic group of the region or subregion being evaluated.*

Slope: 20° to 30°, based on site survey.

Geologic Group: Weakly cemented rock

*Step 3: Determine the susceptibility category, the critical acceleration, $a_c$, and the percentage of the landslide susceptibility area that is expected to be susceptible to landslide during dry and wet conditions.*

Dry condition : $\Rightarrow a_c = 0.30g$
Wet condition : $\Rightarrow a_c = 0.10g$

Assume the following percentage of the pipeline lengths that are within susceptible soils:

Dry condition: $\Rightarrow$ Percentage of Map Area with Landslide Susceptible Deposit = 8%
Wet condition: $\Rightarrow$ Percentage of Map Area with Landslide Susceptible Deposit = 25%

*Step 4: Estimate amount of PGD due to landslide based the critical acceleration ($a_c$), the induced acceleration ($a_{is}$), and the expected number of cycles.*

Dry condition: E[PGD] = 0.57 in.

Wet condition: E[PGD] = 23 in.

*Step 5: Calculate the repair rates for dry and wet conditions.*

Dry condition:

$N = 0.8 * 1.06 * (0.57)^{0.319} = 0.71$ per 1,000 ft. (covers 8% of pipe length).

N = 0.08 * 0.71 * 26,200/1,000 = 1.49 repairs.

Wet condition:

$N = 0.8 * 1.06 * (23)^{0.319} = 2.31$ per 1,000 ft. (covers 25% of pipe length).

N = 0.25 * 2.31 * 26,200/1,000 = 15.1 repairs.

*Step 6: Calculate the total number of repairs (Ground Shaking) for Segment 4.*

The total number of repairs for Segment 4:

Assume PGV = 0.4g * 85 cm/g = 13.4 inches per second.

RR = 1.0 * 0.00187 * 13.4 = 0.025 per 1,000 ft.

N = 0.92 * 0.025 * 26,200/1,000 = 0.60 (dry conditions).

N = 0.75 * 0.025 * 26,200/1,000 = 0.50 (wet conditions).

## F.5 Figures

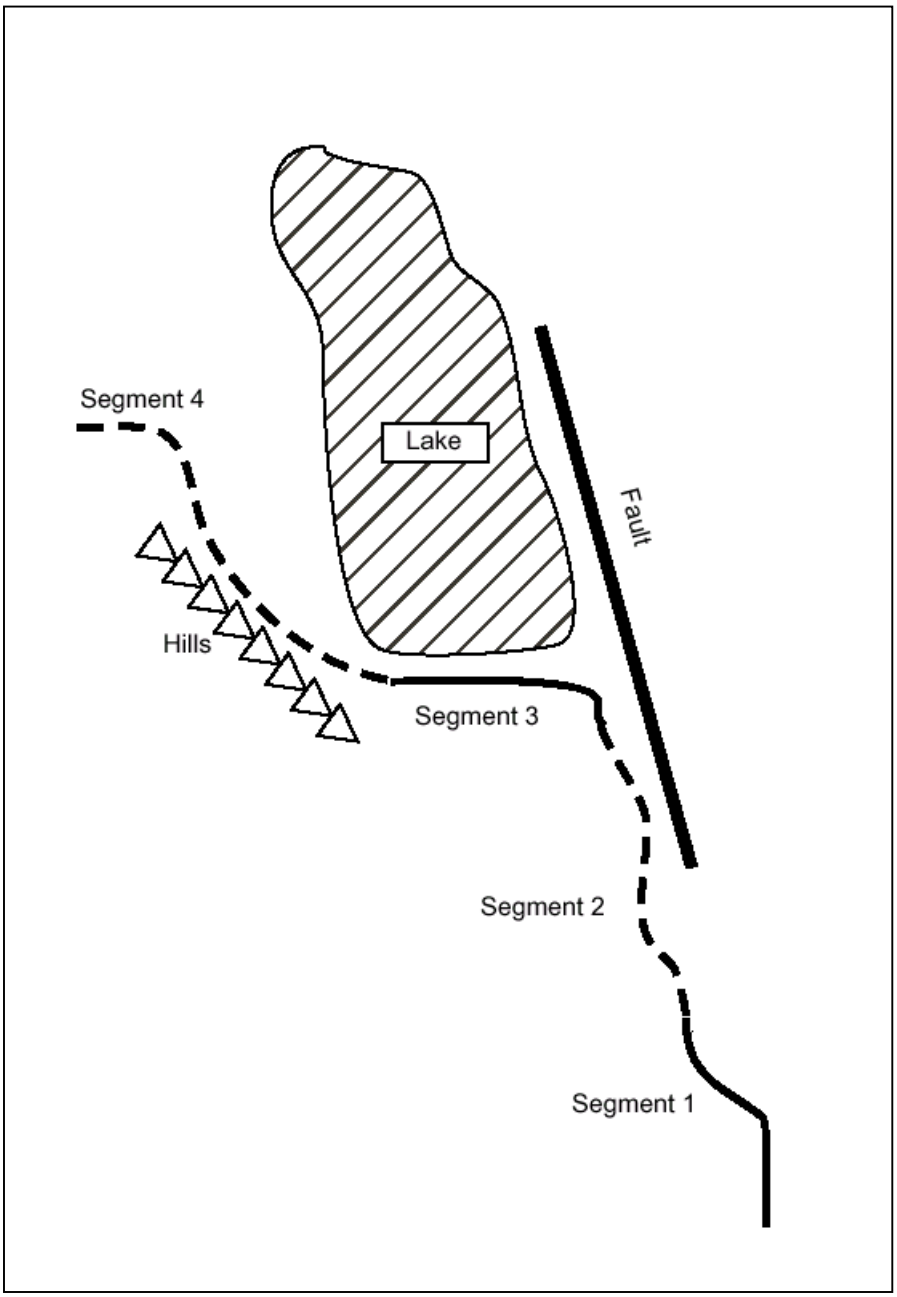


*Figure F-1. Example Water Transmission System*

# G. Bayesian Estimation of Pipe Damage

## G.1 Introduction

Appendix G provides an alternative approach for developing fragility curves to estimate damage potential for buried pipelines.

As described in Section 4.6.2 of Part 1, the complete empirical dataset exhibits a lot of scatter. It is the judgment of the authors that the form of the fragility function used to describe damage to buried pipelines due to wave passage effects is to use a straight line through the entire data set. Alternative approaches are investigated in Part 1, including a power model. The decision to use a straight line through the data set, fitted so that 50% of the empirical data points lied below and 50% lied above the curve, was selected for the following reasons:

- The scatter in the empirical dataset is large. Many different types of curves can be fitted through the dataset, but no one would be much better than the other, except for mathematical convenience.
- The theoretical basis for estimating strain in the ground from wave propagation is that it is linearly correlated with maximum ground velocity. For wave propagation, pipe strain is often assumed to be the same as the ground strain, which basically assumes that the pipe does not slide relative to the ground.
- The desired accuracy of the fragility model for ground shaking is perhaps not as important as that for permanent ground deformations. This is because the rate of pipeline damage in soils prone to PGDs is often an order of magnitude larger than the rate of pipeline damage in soils not prone to PGDs.
- Regression analyses that use weighted damage data (Figure A-15) show that the best-fit curve through the empirical data has an exponent of 0.99 ($RR = 0.001795 * PGV^{0.99}$), which is essentially linear.
- Bayesian analyses presented in Section G.10 for cast iron pipe with diameters 6" and 8", the most common type, show a linear trend (exponent of 0.9942).

Any method used to fit a fragility function through the pipeline empirical database must deal with the form of the empirical database. Specifically, the empirical database has the following issues that might influence how to fit a fragility function through it:

- The empirical data is expressed in terms of repairs per length of pipeline. Each empirical data point is ideally developed by calculating the actual PGV for each pipe of homogeneous attribute. A homogeneous attribute for a pipe mean that the pipe has the same material, same joinery, same diameter, same lay lengths, same installation method, same age, same corrosion protection system, same level of ground shaking and so on. The repair rate is calculated by adding up the entire length of pipe that experienced the same or nearly the same level of ground motion, adding up all the repairs made to that length of pipe, and taking the ratio = total repairs/total length of pipe with homogeneous attributes.

- For the empirical database presented in Section 4 of Part 1, only pipe repairs from the 1994 Northridge earthquake for the LADWP and the 1989 Loma Prieta earthquake for EBMUD have used rigorous GIS techniques to present the empirical data as homogeneous data points. Even so, the only attributes that the homogeneous data points that were evaluated were pipe barrel material, pipe diameter and level of ground shaking.
- When combining empirical data points using regression analysis, a limitation is that each data point is treated equally in the regression analysis. For example, a data point that represents 2 pipe repairs for 20 km of pipe at PGV = 15 inch/sec is 0.1 (=2/20). Another data point that represents 200 pipe repairs for 1,000 km of pipe at PGV = 15 inch/sec is 0.2 (=200/1,000). It is obvious that doing a regression analysis that incorporates these two data points should weight the 1,000 km inventory higher than the 20 km inventory; however, standard regression analysis equally weights the data points.

Recognizing these issues, Appendix G introduces an alternative way to fit fragility curves through the empirical data set. The method is called Bayesian Estimation.

Sections G.2 through G.9 use a portion of the entire empirical data set for purposes of sample application of the method. This introduces the following limitations on the results presented in these sections:

1. The empirical data sample is derived for only the Northridge earthquake for the LADWP water system and only for cast iron, ductile iron and asbestos cement type pipes.
2. The empirical data sample uses a different parameter for ground motion than that used in Part 1. Specifically, the data sample in Sections G.2 through G.9 uses the highest of the peak PGV of two horizontal directions, while Part 1 uses mean PGV of two horizontal directions. The differences in these two forms of PGV is about 21%.
3. The empirical data sample excludes known damage to pipelines for cases where the repair records had missing attributes. In other words, it is known that a pipe repair was made, but perhaps the pipe barrel material or the pipe diameter are unknown. This causes an undercount of pipe repairs by about 8%.
4. Section G.10 addresses these limitations by including additional empirical data from the Loma Prieta earthquake and making the necessary adjustments to allow combination of the Northridge and Loma Prieta datasets into one analysis.

## G.2 Background

Bayesian methods provide an alternative to statistical analysis of data that can be particularly effective for the assessment of seismic fragility based on field or laboratory observations. This approach has several features, including:

- The possibility of incorporating engineering expert opinion through a prior distribution.
- The ability to handle all types of information, including direct measurements, measurement of bounds, and indirect observations.

- The feasibility of properly and fully accounting for all types of aleatory (meaning random, in the sense of Section E.6) and epistemic (meaning uncertain, in the sense of Section E.6) uncertainties.
- The ease with which parameter estimates can be updated when new data becomes available.

Appendix G describes an application of the Bayesian approach to estimate the mean rate of damage along buried pipes caused by seismic ground shaking. The pipe damage data is the same as presented in Tables A.3-14, A.3-15 and A.3-16, but subdivided by pipe diameter; the data is given in Tables G-1, G-2 and G-3.

The Bayesian approach recognizes that uncertainties are always present in the estimation of parameters. Accordingly, the state of information about a set of parameters is expressed in terms of a probability distribution. The less dispersed this distribution, the more information it conveys about the parameters. As new information becomes available, the distribution is updated and could become more informative. As seen in Part 1, the collection of pipeline damage data across different earthquakes has not yet shown this trend, possibly because of non-homogenous sampling methods.

The Bayesian parameter estimation method is based on the following updating rule:

$$f(\theta) = kL(\theta)p(\theta) \qquad [G.1]$$

which has the following elements:

$\theta = [\theta_1, \theta_2, \mathrm{K}]^T$ is the vector of parameters to be estimated.

$p(\theta)$ is the prior distribution reflecting our state of knowledge about $\theta$ before new data is obtained. This distribution can be based on engineering expert opinion, which is subjective. A non-informative prior should be used if no prior information about the parameters is available.

$L(\theta)$ is the likelihood function and represents the objective information contained in the new data. This function is proportional to the conditional probability of observing the data, given the parameters $\theta$. Specific formulations of this function are given later in this appendix.

$k = \left[\int L(\theta)p(\theta)d\theta\right]^{-1}$ is a normalizing factor.

$f(\theta)$ is the posterior distribution representing our updated state of knowledge about $\theta$. This distribution combines the information contained in the prior, which can be subjective in nature, with the objective information contained in the likelihood.

Once the posterior distribution $f(\theta)$ is determined, the posterior mean vector of the parameters is obtained as:

$$M_\theta = \int \theta \; f(\theta) \; d\theta \qquad [G.2]$$

and the posterior mean-square matrix is obtained as:

$$E\left[\theta\theta^T\right] = \int \left(\theta\theta^T\right) f(\theta) d\theta \qquad [G.3]$$

where the superimposed T is the vector transpose. The posterior covariance matrix is computed as:

$$\Sigma_{\theta\theta} = E\left[\theta\theta^T\right] - M_\theta M_\theta^T \qquad [G.4]$$

The diagonal elements of $\Sigma_{\theta\theta}$ are the variances $\sigma_i^2$ of the parameters, where $\sigma_i$ denotes the standard deviation of $\theta_i$, and the off-diagonal elements are the covariances $\rho_{ij}\sigma_i\sigma_j$ from which the correlation coefficients $\rho_{ij}$ are obtained after division by the two standard deviations. The coefficient of variation (c.o.v.) of $\theta_i$ is defined as $\delta_i = \sigma_i / \mu_i$. The integrals in [G.2] and [G.3] are carried out over the applicable domain of $\theta$. A method for computing these integrals is described in Section G.9.

## G.3 Poisson Model for Pipe Damage

It can be conveniently assumed that damage along a length of buried pipe due to ground shaking can be modeled as a homogeneous Poisson process. According to this model, the probability that damage occurs at exactly *n* points along a pipe of length *L* is given by:

$$P(n,L) = \frac{(\lambda L)^n}{n!} \exp(-\lambda L), \quad n = 0,1,2,\text{K} \qquad [G.5]$$

This model has a single parameter $\lambda$ which is equal to the mean rate of events. Thus, the mean number of damage points along a pipe of length *L* is given by $\lambda L$. The objective of the Bayesian analysis is to estimate parameter $\lambda$.

## G.4 Pipe Damage Data

Tables G-1, G-2 and G-3 present pipeline damage data for cast iron (CI), ductile iron (DI) and asbestos cement (AC) pipe from LADWP for the 1994 Northridge earthquake. Section G-1 presents some limitations to this data that would be required to combine it with data from the other sources presented in this report.

Each data point is for a homogeneous length of pipeline *L* with diameter D that experienced a range (bin) of peak ground velocity centered on PGV (cm/s) and that experienced *n* known pipe repairs. Blank entries in the tables indicate that there were no pipes of the specified diameter that were located in an area that experienced ground motion PGV in the specified bin.

The mean rate of damage along a buried pipe may depend on such variables as the intensity of the ground motion, the material of the pipe, the pipe diameter and wall thickness, the depth of soil cover, the lay length of the pipe, the corrosiveness of the soil, the corrosion protection system for the pipe, the number and type of laterals, etc. Determining the mean rate of damage as a function of all these variables would require a large matrix of observed pipe damage data for each set of these variables, which is not available at this time. As a result, the data has to be

"binned" together to make estimates of the mean rate as a function of only a subset of these variables.

The data in Tables G-1 to G-3 is used in the following sections to estimate λ as a function of the PGV for each pipe type. In the case of CI pipes with diameters in the range of 4 to 12 inches, the data is sufficiently rich to allow inferring a dependence of λ on the pipe diameter as well. Note that Figure A-11 using another dataset does not show the same dependence on diameter. For larger diameter CI pipes or for DI and AC pipes, the data is not sufficiently rich to allow inferring the dependence of λ on the pipe diameter.

As is the case with any statistical estimate, the results and conclusions derived in the following analyses are conditioned on the database. If the data is changed or modified, the results and conclusions may also vary.

## G.5 Estimation of λ for Cast Iron Pipes

Examination of the data for CI pipes in Table G-1 reveals there is fairly uniform data available for pipe sizes 4 to 12 inches in diameter, except for pipes of 10-inch diameter. Specifically, for these pipe sizes, observations for relatively long pipe segments of tens or hundreds of kilometers have been made. In contrast, the data for pipe sizes 16 to 24 inches in diameter is relatively sparse. If data for all pipe sizes were combined, obviously the smaller pipes with larger data would dominate the result. For this reason, separate analyses for these two ranges of pipe diameters are performed.

### G.5.1 Cast Iron Pipes with 4 to 12" Diameter

In order to estimate λ as a function of the PGV and the pipe diameter, an interpolation model is needed. We select the relation:

$$\lambda = a * V^{b} * D^{-c} \qquad [G.6]$$

where V is PGV is in cm/sec and D is the pipe diameter in inches and a, b and c are the parameters to be estimated. Note that by selecting the form of equation [G.6], the Bayesian model assumes that pipe damage increases with increasing PGV and decreases with increasing D; that is, if parameters b and c are positive. The issue as to whether pipe damage increases with PGV seems to be well-accepted. The issue as to whether pipe damage rate should decrease with increasing D seems to be indicated in some data sets, but not in others. For purposes of Sections G.2 through G.9, the [G.6] model is presented as illustrative of the technique using the particular data sets of Tables G-1, G-2 and G-3, recognizing that the smoothness inferred from this model is not well-represented in the more complete empirical database currently available. Section G.10 examines this issue in more detail.

Using this relation in [G.5], the probability that a pipe of length, *L*, having diameter, *D*, will experience *n* damage points due to a ground motion with PGV equal to *V*, is given by:

$$P(n, L) = \frac{(aV^{b}D^{-c}L)^{n}}{n!} \exp(-aV^{b}D^{-c}L) \qquad [G.7]$$

| PGV | Pipe Diameter, Inches | | | | | | | | | | | | | | | | | |
|---|---|---|---|---|---|---|---|---|---|---|---|---|---|---|---|---|---|---|
| cm / sec | 4 | | 6 | | 8 | | 10 | | 12 | | 16 | | 18 | | 20 | | 24 | |
| | L | n | L | n | L | n | L | n | L | n | L | n | L | n | L | n | L | n |
| 5 | 33.8 | 0 | 126.5 | 0 | 47.5 | 0 | 3.7 | 0 | 23.3 | 0 | 7.8 | 0 | 0.2 | 0 | 8 | 0 | | |
| 15 | 263.8 | 7 | 768.7 | 24 | 379.5 | 5 | 16.5 | 0 | 193 | 6 | 32.4 | 2 | 2.3 | 0 | 32 | 0 | 0.8 | 0 |
| 25 | 387.2 | 64 | 878.8 | 66 | 574.1 | 25 | 30.6 | 3 | 263 | 7 | 43.8 | 0 | 4.4 | 1 | 11 | 0 | 0.5 | 0 |
| 35 | 129.5 | 29 | 536.9 | 58 | 298.5 | 14 | 3 | 0 | 125 | 8 | 19.7 | 1 | 0.2 | 0 | 5.3 | 1 | 1.9 | 0 |
| 45 | 52.3 | 24 | 427.7 | 22 | 230.5 | 9 | | | 84.7 | 4 | 9.2 | 0 | | | 0.6 | 0 | | |
| 55 | 23.3 | 18 | 276 | 23 | 140 | 10 | | | 56 | 5 | 6.9 | 0 | | | | | | |
| 65 | 22.4 | 15 | 195.5 | 45 | 90.9 | 18 | | | 34.9 | 7 | 11.9 | 2 | | | 0.7 | 0 | | |
| 75 | 9.4 | 6 | 84.7 | 21 | 62 | 11 | | | 19.7 | 1 | 2.3 | 0 | | | 0.6 | 0 | | |
| 85 | 10.4 | 2 | 72.4 | 10 | 42.1 | 11 | | | 8.4 | 1 | 3.9 | 0 | | | 2.9 | 1 | | |
| 95 | 8 | 0 | 48.2 | 1 | 21 | 1 | | | 10.7 | 0 | 3 | 0 | | | 1.2 | 0 | | |
| 105 | 9.9 | 0 | 53.1 | 1 | 23.1 | 1 | | | 7.9 | 0 | 1.8 | 0 | | | 0.2 | 0 | | |
| 115 | 9.2 | 0 | 47.9 | 3 | 22.8 | 2 | | | 4 | 0 | 2.4 | 0 | | | 0.4 | 0 | | |
| 125 | 7.5 | 0 | 40.4 | 4 | 17 | 1 | | | 6.4 | 1 | 4.3 | 0 | | | 0.6 | 0 | | |
| 135 | 4.8 | 0 | 28.5 | 0 | 24.4 | 2 | | | 7.5 | 0 | 5 | 0 | | | 1.2 | 0 | | |
| 145 | 3.3 | 3 | 33.9 | 2 | 19.8 | 3 | | | 4.6 | 1 | 2.7 | 0 | | | | | | |
| 155 | 3.6 | 0 | 30.9 | 9 | 15.6 | 5 | | | 6.8 | 2 | 2.1 | 0 | | | 0.9 | 0 | | |
| 165 | 4.1 | 5 | 32 | 19 | 24.8 | 20 | | | 5.4 | 0 | | | | | | | | |
| Total | 982.5 | 173 | 3682 | 308 | 2034 | 138 | 53.8 | 3 | 861.3 | 43 | 159.2 | 5 | 7.1 | 1 | 65.6 | 2 | 3.2 | 0 |

Notes

L = length of pipeline in km, within the specified PGV bin

n = number of repairs

See Section G.1 for further description of the data

*Table G-1. Cast Iron Pipe Damage, 1994 Northridge Earthquake, LADWP*

| PGV | Pipeline Diameter, Inches | | | | | | | | | | | |
|---|---|---|---|---|---|---|---|---|---|---|---|---|
| cm / sec | 4 | | 6 | | 8 | | 12 | | 16 | | 20 | |
| | L | n | L | n | L | n | L | n | L | n | L | n |
| 5 | 0.9 | 0 | 19.9 | 0 | 11.6 | 0 | 5.3 | 0 | 3.4 | 0 | 1.1 | 0 |
| 15 | 2.2 | 0 | 53.2 | 1 | 32.4 | 0 | 21.4 | 0 | 4.6 | 0 | 2.9 | 0 |
| 25 | 2.5 | 1 | 47.5 | 5 | 33 | 0 | 8 | 0 | 1.7 | 0 | | |
| 35 | 1.3 | 1 | 16 | 0 | 12.8 | 1 | 6.5 | 0 | 2.3 | 0 | 1.4 | 0 |
| 45 | 1.7 | 1 | 10.8 | 1 | 10.6 | 1 | 8.4 | 0 | 0.7 | 0 | | |
| 55 | 2.1 | 0 | 6.2 | 1 | 8.5 | 0 | 1.3 | 0 | 0 | 0 | | |
| 65 | 2.1 | 0 | 5.6 | 3 | 3.4 | 1 | 1.4 | 0 | 0.2 | 0 | 0.2 | 0 |
| 75 | 1.3 | 1 | 1.7 | 0 | 2.3 | 1 | 2.3 | 0 | | | | |
| 85 | 0.3 | 0 | 2 | 1 | 0.4 | 0 | 2.6 | 0 | | | | |
| 95 | 2.6 | 0 | 6.2 | 0 | 4.5 | 0 | 2.7 | 0 | 0.1 | 1 | | |
| 105 | 0.6 | 0 | 2.8 | 0 | 2.1 | 0 | 0.2 | 0 | 1.7 | 0 | | |
| 115 | 1.5 | 0 | 3.9 | 0 | 6.5 | 0 | 2.2 | 1 | 1.4 | 0 | 0.2 | 0 |
| 125 | 0.8 | 0 | 2.5 | 0 | 1.3 | 0 | 0.7 | 0 | | | 0.6 | 0 |
| 135 | 0.5 | 0 | 2.7 | 0 | 0.4 | 0 | 0.7 | 0 | 0.8 | 0 | 0.3 | 0 |
| 145 | 0.3 | 0 | 3.2 | 0 | 1.4 | 0 | | | 0.7 | 0 | 0.1 | 0 |
| 155 | | | 4.3 | 0 | 0.1 | 1 | 0.7 | 0 | 0.3 | 0 | | |
| 165 | | | 2.6 | 1 | | | 0.7 | 0 | | | | |
| Total | 20.7 | 4 | 191.1 | 13 | 131.3 | 5 | 65.1 | 1 | 17.9 | 1 | 6.8 | 0 |

Notes

L = length of pipeline in km, within the specified PGV bin

n = number of repairs

See Section G.1 for further description of the data

*Table G-2. Ductile Iron Pipe Damage, 1994 Northridge Earthquake, LADWP*

| PGV cm / sec | Pipeline Diameter, Inches | | | | | | | | | |
|---|---|---|---|---|---|---|---|---|---|---|
| | 4 | | 6 | | 8 | | 10 | | 12 | |
| | L | n | L | n | L | n | L | n | L | n |
| 5 | 9.5 | 0 | 79.3 | 0 | 53.4 | 0 | | | 15.1 | 0 |
| 15 | 14.1 | 0 | 180.5 | 2 | 88.1 | 0 | 1.9 | 0 | 23.2 | 0 |
| 25 | 12.5 | 6 | 129.7 | 7 | 82.1 | 2 | | | 11.2 | 0 |
| 35 | 8 | 0 | 73.2 | 1 | 32.2 | 1 | | | 4.3 | 0 |
| 45 | 1.1 | 0 | 22.6 | 0 | 13.1 | 0 | | | 1 | 0 |
| 55 | 2.8 | 0 | 25.1 | 0 | 5.4 | 0 | | | 0.7 | 0 |
| 65 | 2.6 | 7 | 17.6 | 0 | 3.9 | 0 | | | 0.2 | 0 |
| 75 | 2.4 | 0 | 7 | 0 | 1.5 | 0 | | | | |
| 85 | 0.7 | 0 | 2.1 | 0 | 0.1 | 0 | | | | |
| 95 | 0.3 | 0 | 0.9 | 0 | | | | | | |
| 105 | 0.5 | 0 | 3.2 | 0 | 1.2 | 0 | | | | |
| 115 | 0.2 | 0 | 1 | 0 | 0.4 | 0 | | | | |
| 125 | 0.3 | 0 | 3.4 | 0 | 0.1 | 0 | | | | |
| 135 | 0.6 | 0 | 5.5 | 0 | 1.1 | 0 | | | | |
| 145 | 0.2 | 0 | 3 | 0 | 1.8 | 0 | | | | |
| 155 | 0.5 | 0 | 3.4 | 0 | 1.9 | 0 | | | | |
| 165 | 0.1 | 0 | 2.6 | 0 | 0.9 | 0 | | | | |
| Total | 56.4 | 13 | 560.1 | 10 | 287.2 | 3 | 1.9 | 0 | 55.7 | 0 |

Notes

L = length of pipeline in km, within the specified PGV bin

n = number of repairs

See Section G.1 for further description of the data

*Table G-3. Asbestos Cement Pipe Damage, 1994 Northridge Earthquake, LADWP*

As mentioned earlier, the likelihood function is proportional to the conditional probability of the data, given the set of parameters. The data in this case consists of observations $V_i$, $D_i$, $L_i$ and $n_i$, $i = 1, \mathrm{K}, N$, as listed in Table G-1 for the considered pipe sizes. Assuming statistical independence between the observations and using [G.7], the likelihood function takes the form:

$$L(a,b,c) = \prod_{i=1}^{N} \left[ \frac{(aV_i^b D_i^{-c} L_i)^{n_i}}{n_i!} \exp(-aV_i^b D_i^{-c} L_i) \right] \qquad [G.8]$$

For Bayesian updating analysis, a prior distribution needs to be selected. If prior information on the parameters were available, it would be included through this distribution. For purposes of Appendix G, we use a non-informative prior, which for the case of positive-valued parameters, is proportional to their reciprocals [see Box and Tiao 1992], i.e.,:

$$p(a,b,c) \propto 1/abc \qquad [G.9]$$

With the likelihood function and the prior distribution formulated, the Bayesian analysis is carried out by use of the updating rule in [G.1]. Once the posterior density is determined, the posterior means, standard deviations and correlation coefficients are computed using [G.2]-[G.4]. Sections G.9 and G.11 describes the computational method used for this purpose.

Table G-4 lists the posterior means, standard deviations and correlation coefficients of the model parameters obtained for this case. These are computed with an accuracy of 5% c.o.v. in the estimated means (see Section G.9). It is important to note that these parameter estimates are for the units indicated in parenthesis in the title of the table.

| Parameter | $\mu_i$ | $\sigma_i$ | $\rho_{ij}$ | | |
|---|---|---|---|---|---|
| | | | *a* | *b* | *c* |
| *a* | 0.0631 | 0.0205 | 1.000 | –0.640 | 0.720 |
| *b* | 0.8424 | 0.0547 | –0.640 | 1.000 | 0.021 |
| *c* | 1.4568 | 0.1378 | 0.720 | 0.021 | 1.000 |

*Table G-4. Posterior statistics of parameters a, b and c for CI pipes of diameter 4 to 12 inches (for V in cm/s, D in inches, and λ per km$^{-1}$).*

With the posterior statistics of the parameters available, we can now estimate the mean and coefficient of variation of λ. Using first-order approximations [Ang and Tang 1975], the mean of λ is given by:

$$\mu_\lambda \cong \mu_a V^{\mu_b} D^{-\mu_c} \qquad [G.10]$$

and its c.o.v., $\delta_\lambda$, is given by:

$$\delta_\lambda^2 \cong \frac{1}{\mu_\lambda^2}\sum_i\sum_i \frac{\partial\lambda}{\partial\theta_i}\frac{\partial\lambda}{\partial\theta_j}\rho_{ij}\sigma_i\sigma_j$$
$$= \delta_a^2 + (\ln V)^2\sigma_b^2 + (\ln D)^2\sigma_c^2 \qquad [G.11]$$
$$+ 2(\ln V)\delta_a\sigma_b\rho_{ab} - 2(\ln D)\delta_a\sigma_c\rho_{ac} - 2(\ln V)(\ln D)\sigma_b\sigma_c\rho_{bc}$$

These values are plotted in Figures G-1 and G-2 (solid curves) as functions of the PGV (in in/sec) for different diameter pipes. The estimates for the mean are multiplied by 0.3048 to find the mean rate of damage per 1,000 ft of pipe.

It is noted in Figure G-1 that for these pipes the mean rate of damage is strongly influenced by the pipe diameter. The mean rate of damage shows a steady increase with the PGV for all pipe sizes. The c.o.v. of λ, which is a measure of the epistemic uncertainty in measuring the mean rate of damage, is of the order of 10-15%. Note that the percent difference between the estimated mean rates for different pipe sizes is much greater than the estimated c.o.v., which would appear to justify the use of the pipe diameter as a variable for estimating λ, at least for this data set, even though other datasets do not seem to support this hypothesis; for an example, see Figure A-11.

### G.5.2 Cast Iron Pipes with 16 to 24" Diameter

For this group of pipes, the data in Table G-1 is rather sparse. Analysis with the three-parameter formula in [G.6] leads to results that cannot be justified. Specifically, the percent difference between estimates of the mean rate of damage for different pipe sizes is smaller than the estimated c.o.v. of λ. This implies that, based on the present data, the differentiation of the pipe sizes is not justified. Therefore, for these pipes the two-parameter formula is used:

$$\lambda = aV^b \qquad [G.12]$$

where $a$, $b$ are the parameters to be estimated. The likelihood function in this case takes the form:

$$L(a,b) = \prod_{i=1}^{N}\left[\frac{(aV_i^b L_i)^{n_i}}{n_i!}\exp(-aV_i^b L_i)\right] \qquad [G.13]$$

And select the non-informative prior:

$$p(a,b) \propto \frac{1}{ab} \qquad [G.14]$$

Table G-5 lists the posterior means, standard deviations and correlation coefficients of the model parameters for this case. These are estimated with an accuracy of 5% or less c.o.v. of the estimated means. Note again that these parameter estimates are valid for the units indicated in parenthesis in the title of the table.

| Parameter | $\mu_i$ | $\sigma_i$ | $\rho_{ij}$ | |
|---|---|---|---|---|
| | | | *a* | *b* |
| *a* | 0.0230 | 0.0139 | 1.000 | –0.686 |
| *b* | 0.1658 | 0.2270 | –0.686 | 1.00 |

*Table G-5. Posterior statistics of parameters a and b for CI pipes of diameter 16 to 24 inches (for V in cm/s and λ per km$^{-1}$).*

The mean and c.o.v. of λ are computed, based on first-order approximations, from:

$$\mu_\lambda \cong \mu_a V^{\mu_b} \qquad [G.15]$$

$$\delta_\lambda^2 \cong \delta_a^2 + (\ln V)^2 \sigma_b^2 + 2(\ln V)\delta_a \sigma_b \rho_{ab} \qquad [G.16]$$

The results are shown in Figures G-1 and G-2, respectively, as dashed lines. The c.o.v. of λ is around 50% to 90%, indicating a high level of epistemic uncertainty in the estimation. This could be due to the sparseness of the data for this range of pipe sizes or other unknown factors. It is noted that the mean of λ only mildly increases with the PGV for this type of pipe.

## G.6 Estimation of λ for Ductile Iron Pipes

The data for DI pipes in Table G-2 is rather sparse for all pipe sizes and use of the three-parameter formula [G.6] cannot be justified. Instead, the two-parameter formula in [G.12] is used with $\theta = (a,b)$ as the set of parameters. Table G-6 lists the posterior statistics of the parameters.

| Parameter | $\mu_i$ | $\sigma_i$ | $\rho_{ij}$ | |
|---|---|---|---|---|
| | | | *a* | *b* |
| *a* | 0.0073 | 0.0071 | 1.000 | –0.840 |
| *b* | 0.6770 | 0.2510 | –0.840 | 1.00 |

*Table G-6. Posterior statistics of parameters a and b for DI pipes (for V in cm/s and λ per km$^{-1}$)*

The mean and c.o.v. of λ are computed by use of [G.15] and [G.16]. These are plotted in Figures G-3 and G-4, respectively, as functions of the PGV (in in/sec). The estimates for the mean are multiplied by 0.3048 to find the mean rate of damage per 1,000 ft of pipe. The c.o.v. of λ is around 50% to 70%, signifying a large epistemic uncertainty in the estimation. This could be due to the sparseness of the data for the DI pipes or other factors. A rapid increase in the mean of λ with the PGV is observed in Figure G-3.

## G.7 Estimation of λ for Asbestos Cement Pipes

The data for AC pipes in Table G-3 is rather sparse for all pipe sizes use of the three-parameter formula [G.6] cannot be justified. Instead, the two-parameter formula in [G.12] is used with $\theta = (a,b)$ as the set of parameters. Table G-7 lists the posterior statistics of the parameters.

| Parameter | $\mu_i$ | $\sigma_i$ | $\rho_{ij}$ | |
|---|---|---|---|---|
| | | | *A* | *b* |
| *a* | 0.0044 | 0.0038 | 1.000 | –0.860 |
| *b* | 0.6625 | 0.2477 | –0.860 | 1.00 |

*Table G-7. Posterior statistics of parameters a and b for AC pipes (for V in cm/s and λ per km$^{-1}$)*

The mean and c.o.v. of λ are computed by use of [G.15] and [G.16]. These are plotted in Figures G-5 and G-6, respectively, as functions of the PGV (in in/sec). The estimates for the mean are multiplied by 0.3048 to find the mean rate of damage per 1,000 feet of pipe. The c.o.v. of λ is around 45% to 65%, signifying a large epistemic uncertainty in the estimation. This might be due to the sparseness of the data for the AC pipes or other factors. The mean of λ shows a rapid increase with the PGV in Figure G-5.

## G.8 Comparison of Results for Different Pipe Materials

Figures G-7 and G-8 compare the mean and c.o.v. estimates of λ for all the pipes, respectively. Solid lines are for CI pipes of different diameter, as indicated, dotted lines are for the DI pipes with 4 to 20" diameter, and dashed lines are for AC pipes with 4 to 12" diameter. It is clear from Figure G-8 that the estimation is most accurate for the CI pipes with 4 to 12" diameter, for which a large amount of data is available. The estimates for the CI pipes with 16 to 24" diameter and for the DI and AC pipes are much more uncertain.

The mean estimates in Figure G-1 indicate that large-diameter CI pipes and AC pipes have the lowest mean damage rates. However, this conclusion should be used with caution, particularly for AC pipes, because of the large epistemic uncertainty present in the estimation. Further data collection can help reduce this uncertainty.

If and when new data becomes available, the posterior statistics obtained in Appendix E can be used to formulate a prior distribution for the parameters. The updating procedure can then be used to derive posterior statistics of the parameters that incorporate the information gained from the new data.

## G.9 Integration by Importance Sampling

Determination of the normalizing factor in the Bayesian updating rule [G.1] and the posterior statistics in [G.2] and [G.3] require multi-dimensional integral calculations. Conventional numerical integration methods may not be effective for more than two parameters. Section G.9 presents a method for evaluation of these integrals by importance sampling that is effective for any number of parameters. Section G.11 provides computation routines to apply this method.

The integrals to be computed can all be written in the unified form:

$$I = \int K(\theta) L(\theta)\, p(\theta)\, d\theta \qquad [G.17]$$

For $K(\theta) = 1$, the integral yields the reciprocal of the normalizing factor *k*; for $K(\theta) = k\,\theta$, the integral yields the posterior mean vector $\mathbf{M}_\theta$; and for $K(\theta) = k\,\theta\theta^{\mathrm{T}}$, the integral yields the posterior mean-square matrix $\mathrm{E}[\theta\theta^{\mathrm{T}}]$, from which the posterior covariance matrix is computed as in [G.4]. In the following, the computation of a typical integral is described as in [G.17].

Let $h(\theta)$ denote a suitable sampling probability density function that has a non-zero value within the domain of $\theta$. We can rewrite [G.17] as:

$$I = \int \frac{K(\theta)L(\theta)\,p(\theta)}{h(\theta)}\,h(\theta)\,d\theta = \mathrm{E}\left[\frac{K(\theta)L(\theta)\,p(\theta)}{h(\theta)}\right] \qquad \text{[G.18]}$$

where E[•] denotes expectation. It is clear that the integral of interest is equal to the mean of $K(\theta)L(\theta)\,p(\theta)/h(\theta)$ with respect to the sampling density $h(\theta)$. Therefore, a simple method for computing the integral *I* is:

1. Generate a sample of parameter values $\theta_i$, $i = 1,2,\mathrm{K},N$, according to the probability density function $h(\theta)$.
2. Compute the corresponding values $I_i = K(\theta_i)L(\theta_i)\,p(\theta_i)/h(\theta_i)$.
3. Compute the sample mean $\bar{I} = \sum_{i=1}^{N} I_i/N$.
4. As *N* becomes large, $\bar{I}$ asymptotically approaches the integral $I$. A measure of accuracy of the computation is given by the c.o.v. of $\bar{I}$. This is computed as $\delta I/\sqrt{N}$, where $\delta I$ is the c.o.v. of the sampled values $I_i$, $i = 1,2,\mathrm{K},N$.

Matlab routines for computing the posterior statistics of the three-parameter model [G.6] are presented in Section G.11. For the sampling density function $h(\theta)$, owing to the non-negativeness of the parameters, a joint lognormal distribution is used. For faster convergence, it is important that the sampling density have a mean vector and a covariance matrix that are close to the posterior mean vector and covariance matrix of the parameters. Since these values are not known in advance, an adaptive approach is used. That is, start with an assumed mean vector and covariance matrix for the sampling density $h(\theta)$ and make a first estimate of the posterior statistics of the parameters. The mean vector and covariance matrix of the sampling density are then replaced by the estimated posterior mean and covariance matrix and the calculation is repeated. This process is continued until sufficiently small c.o.v. values of the estimated posterior mean values are obtained. For numerical stability, it is also important that the normalizing factor $k$ be neither too small nor too large. A scale parameter for the likelihood function is provided in the Matlab code that can be adjusted to control the magnitude of the normalizing factor.

## G.10 Updated Bayesian Analyses

The analytical results presented in Sections G.1 through G.8 are based on application of the Bayesian model using data only from the 1994 Northridge earthquake in Tables G-1, G-2 and G-3. To further examine the Bayesian model, the analyses were repeated, this time also using the data from the 1989 Loma Prieta earthquake in Tables A.3-7, A.3-8 and A.3-9.

As described elsewhere in this report, the available empirical datasets from these two earthquakes do not use precisely the same definitions of PGV. The differences are that the Northridge data set uses peak of two horizontal directions versus the Loma Prieta data set, which uses median of two horizontal directions. The Northridge data set excludes 7.9% of main damage (see Section A.3.12).

Table G-8 provides a summary of the computed mean *a*, *b* and *c* values from the updated Bayesian analyses. For small-diameter cast iron pipe, the parameters are for the model in equation G.6. for other entries, the parameters are for the model in equation G.12.

| Pipe Material | Diameter | a | b | c |
|---|---|---|---|---|
| Cast Iron | 4-12" | 0.0324 | 0.9942 | 1.3188 |
| Cast Iron | 16-24" | 0.0187 | 0.2454 | |
| Asbestos Cement | 4-12" | 0.0016 | 0.8804 | |
| Ductile Iron | 4-20" | 0.0073 | 0.677 | |
| Welded Steel | 4-30" | 0.000213 | 1.8678 | |

*Table G-8. Summary of Updated Bayesian Analysis Parameters a, b, c*
*Units are: (for V in cm/s, D in inches, and $\lambda$ repairs per $km^{-1}$)*

Table G-9 compares the updated Bayesian analysis results with those presented elsewhere in this report. The most common pipe material in the empirical dataset is 6- and 8-inch diameter cast iron pipe. The Bayesian analysis assumes an explicit diameter value ($D^{-c}$) in equation G.6. To make comparisons, this factor is evaluated and the Bayesian 'a' value is adjusted accordingly. The results are in Table G-9. The Bayesian analysis predicts parameter 'b' to be 0.9942, which is essentially unity. By averaging the most common empirical data, the Bayesian analysis would suggest a model of:

$RR = 0.0197\ (PGV)^{0.9942}$, with RR = repairs per 1,000 feet and PGV in inches per second.

This model is very similar to that derived using a slightly wider data set using weighted regression, and also very similar to the small diameter cast iron fragility model provided in the main report (Table 4-4, with K1 = 1.0 from Table 4-5).

| Pipe Material | Diameter | Adjusted Parameter a | Parameter b | Notes |
|---|---|---|---|---|
| Cast Iron | 6" | 0.00234 | 0.9942 | Bayesian, LP+NR |
| Cast Iron | 8" | 0.00160 | 0.9942 | Bayesian, LP+NR |
| Cast iron | Avg 6", 8" | 0.00197 | 0.9942 | Bayesian Average, LP+NR |
| Cast Iron | All diameters | 0.00180 | 0.99 | Weighted Regression, Fig A-15, LP+NR |
| Cast Iron | Up to 12" | 0.00187 | 1.00 | Tables 4-4, 4-5 |

*Table G-9. Comparison of Fragility Models for Small-Diameter Cast Iron Pipe*

## G.11 Matlab Routines

Section G.11 provides the Matlab source code and data input files used to compute the statistics presented in Appendix G.

Posterior2.m: computes the posterior statistics of the parameters for the two-parameter model (CI pipes 16-24" diameter, DI pipes, AC pipes). It calls Loglhood2.m.

Posterior3.m: computes the posterior statistics of the parameters for the three-parameter model (CI pipes 4-12" diameter). It calls Loglhood3.m.

Loglhood2.m: computes the natural logarithm of the likelihood function for the two-parameter model. It calls Data2.m.

Loglhood3.m: computes the natural logarithm of the likelihood function for the three-parameter model. It calls Data3.m.

Data2.m: contains the pipe damage data for the two-parameter model (listed data is for DI pipes).

Data3.m: contains the pipe data for the three-parameter model (listed data is for CI pipes 4-12" diameter).

Note that in Data2.m, the lengths of pipe segments and the number of damage points at each PGV level are combined.

Data_CI_16_24.m: contains the combined data for CI pipes 16-24" diameter.

Data_AC.m: contains the combined data for AC pipes.

To run the Matlab routine for the two-parameter model, do the following:

1. Put all *.m files in a single directory on the path of Matlab.
2. Copy the data file of interest into Data2.m. Right now, Data2.m has the data for DI pipes.
3. Adjust the input parameters in Posterior2.m. Read the heading for guidelines. The parameters are now set for the DI pipes.
4. Issue the command Posterior2 in the Matlab environment.
5. The computation will take quite some time. To do a quick check without high accuracy, change parameter ‘nmax’ to something small like nmax=1000. The posterior results will

appear on the screen. They will also be stored in the file Results2.mat. Read the guidelines regarding the accuracy of estimation.

To run the program for the 3-parameter model (CI pipes of 4 to 12" diameter), do as above but replace 2 with 3. The Data3.m file now contains the data for the CI pipes with diameter 4 to 12".

## *Posterior2.m*

```
%%%%%%%%%%%%%%%%%%%%%%%%%%%%%%%%%%%%%%%%%%%%%%%%%%%%%%%%%%%%%%%%%%%%%%%%%%%%
%
% This program computes the posterior means, standard deviations and
% correlation matrix of the parameters of a 2-parameter model describing
% the mean rate of damage points along a pipe. It uses importance sampling
% to carry out the necessary integrations over the Bayesian kernel. The
% joint lognormal distribution with specified means, standard deviations
% and correlation matrix is used for the sampling distribution. Convergence
% will be faster if these statistics of the sampling distribution are close
% to the corresponding statistics of the posterior distribution that are
% to be computed. The program may be run several times to adjust the
% statistics of the sampling distribution.
%
%  For numerical stability, it is important that the normalizing factor
%  k in the Bayesian updating formula be neither too small nor too large.
%  This factor can be adjusted by scaling the likelihood function. In this
%  program this is done by adjusting the "scale" parameter.
%
%  Run the program with trial estimates of the means, standard deviation
%  and correlation matrix of the sampling density, and of the scale
%  parameter.  This will give a first estimate of the reciprocal of the
%  normalizing factor k and the posterior statistics of the parameters.
%  Make sure that the sampling density has sufficiently large standard
%  deviations (no smaller than the posterior standard deviations estimated).
%  Use the first posterior estimates as the new means, standard deviations
%  and correlation matrix of the sampling distribution and adjust the
%  scale parameter (decrease it if k is too large, increase it if k is too
%  small). Run the program again to obtain a second set of posterior estimates.
%  Repeat this process until sufficient accuracy in the posterior estimates
%  is achieved.
%
%  The accuracy is measured in terms of the coefficients of variation of
%  the posterior mean estimates (denoted cov_p_mean in this program).
%  A value less than 5% for each element of cov_p_mean is a good level
%  of accuracy.
%
%  The results of the computation are stored in the file "Results2.mat"
%  as follows:
%
%          nmin   minimum number of simulations
%          nmax   maximum number of simulations
%          npar   number of parameters
%             k   normalizing factor in the updating formula
%        p_mean   posterior mean vector
%    cov_p_mean   c.o.v. of the posterior mean estimates
%      p_st_dev   vector of posterior standard deviations
%         p_cov   vector of posterior c.o.v.'s
%         p_cor   posterior correlation matrix
%
%%%%%%%%%%%%%%%%%%%%%%%%%%%%%%%%%%%%%%%%%%%%%%%%%%%%%%%%%%%%%%%%%%%%%%%%%%%%

clear

%----- Specify the means, standard deviations and correlation matrix
%----- of the sampling density
```

```
M     = [0.0081;          % mean vector of sampling density
         0.657];

D = [0.01 0.00;           % diagonal matrix of standard deviations of
     0.00 0.30];          % the sampling density

R = [  1.00 -0.80;  % correlation matrix of the sampling density
      -0.80  1.00];

%----- Specify the scale parameter

scale = 20;

%----- Set minimum and maximum number of simulations:

nmin = 50000;
nmax = 200000;

%----- Begin calculations

d = diag(D);              % vector of standard deviations
cov = d ./ M;             % c.o.v.'s
z = sqrt(log(1+(cov).^2)); % zeta parameters of lognormal distribution
LAM = log(M) - 0.5 * (z).^2;     % lambda parameters of lognormal dist.
Z = diag(z);              % diagonal matrix of zeta's
S = Z*R*Z;                % covariance matrix of transformed normals
L= chol(S)';              % lower choleski decomposition of S
iS = inv(S);              % inverse of S


%----- Initialize integral values:
I1 = 0;
I2 = 0;
I3 = 0;
I4 = 0;

npar = length(M);         % number of parameters
i_counter = 0;
flag = 1;
constant = 1/( (6.28318531)^(npar/2) * sqrt(det(S)) );

%----- Begin importance sampling:

for i = 1:nmax

       %-- simulate standard normal random variables;
       u = random('Normal',0,1,npar,1);
       theta = exp( LAM + L*u);   % simulated lognormal theta's

       %-- define three kernels
       K1 = 1;      % this is for computing the normalizing constant k
       K2 =  theta;        % this is for computing the mean
       K3 =  theta*theta';     % this is for computing the mean squares

       %-- compute the scaled likelihhod function
         lhood = exp(Loglhood2(theta)+scale);

       %--- compute the prior distribution (non-informative):
```

```
        p = 1/(theta(1)*theta(2));

       %--- compute the sampling probability density
       h = constant * exp(-0.5*(log(theta)-LAM)'*iS*(log(theta)-LAM));
       h = h/(theta(1)*theta(2));

       %--- compute (kernel*likelihood*prior)/sampling-density:
       I1 = I1 + K1*lhood*p/h;
       I2 = I2 + K2*lhood*p/h;
       I3 = I3 + K3*lhood*p/h;

        I4 = I4 + (K2*lhood*p/h).^2;  % this is for computing cov_p_mean

       %--- reciprocal of the normalizing constant
       k = I1/i;

       %--- posterior mean and its c.o.v.
       p_mean = I2/I1;
       cov_p_mean = sqrt(( 1/i*(I4/(k^2*i)-(I2/(k*i)).^2) ))./abs(p_mean);

       %--- posterior covariance matrix
       p_cov = I3/I1 - p_mean*p_mean';

        % check if c.o.v is <= 0.05 for all the posterior means, but
       % make sure that at least nmin simulations are performed.
        % flag = 0 means that convergence has been achieved.
        i_counter = i_counter+1;
        if max(cov_p_mean) <= 0.05 &  i_counter>nmin
                flag = 0;
                break
        end
end

%----- display results:
%
disp('--- Number of simulations')
disp(i_counter);

disp('--- Number of parameters')
disp(npar)

disp('========== Bayesian Posterior Estimates ==========')

disp('--- Reciprocal of normalizing factor k')
disp(k);

disp('--- Posterior means')
disp(p_mean');

disp('--- c.o.v.s for the posterior means')
disp(cov_p_mean')

for i=1:npar
       p_st_dev(i) = sqrt(p_cov(i,i));
       p_c_o_v(i) = p_st_dev(i)/abs(p_mean(i));
end
disp('--- Posterior standard deviations')
disp(p_st_dev)
```

```
disp('--- Posterior c.o.v.s')
disp(p_c_o_v)
for i=1:npar
        for j=1:npar
                p_cor(i,j)=p_cov(i,j)/(p_st_dev(i)*p_st_dev(j));
        end
end
disp('--- Posterior correlation matrix')
disp(p_cor);

%--- save results
save Results2 i_counter npar k p_mean cov_p_mean p_st_dev p_c_o_v p_cor
```

## *Posterior3.m*

```
%%%%%%%%%%%%%%%%%%%%%%%%%%%%%%%%%%%%%%%%%%%%%%%%%%%%%%%%%%%%%%%%%%%%%%%%%%%%
%
%  This program computes the posterior means, standard deviations  and
%  correlation matrix of the parameters of a 3-parameter model describing
%  the mean rate of damage points along a pipe. It uses importance sampling
%  to carry out the necessary integrations over the Bayesian kernel. The
%  joint lognormal distribution with specified means, standard deviations
%  and correlation matrix is used for the sampling distribution.
%  Convergence will be faster if these statistics of the sampling
%  distribution are close to the corresponding statistics of the
%  posterior distribution that are to be computed. The program may be
%  run several times to adjust the statistics of the sampling distribution.
%
%  For numerical stability, it is important that the normalizing factor
%  k in the Bayesian updating formula be neither too small nor too large.
%  This factor can be adjusted by scaling the likelihood function. In this
%  program this is done by adjusting the "scale" parameter.
%
%  Run the program with trial estimates of the means, standard deviation
%  and correlation matrix of the sampling density, and of the scale
%  parameter.  This will give a first estimate of the reciprocal of the
%  normalizing factor k and the posterior statistics of the parameters.
%  Make sure that the sampling density has sufficiently large standard
%  deviations (no smaller than the posterior standard deviations estimated).
%  Use the first posterior estimates as the new means, standard deviations
%  and correlation matrix of the sampling distribution and adjust the
%  scale parameter (decrease it if k is too large, increase it if k is too
%  small). Run the program again to obtain a second set of posterior estimates.
%  Repeat this process until sufficient accuracy in the posterior estimates
%  is achieved.
%
%  The accuracy is measured in terms of the coefficients of variation of
%  the posterior mean estimates (denoted cov_p_mean in this program).
%  A value less than 5% for each element of cov_p_mean is a good level
%  of accuracy.
%
%  The results of the computation are stored in the file "Results3.mat"
%  as follows:
%
%          nmin   minimum number of simulations
%          nmax   maximum number of simulations
%          npar   number of parameters
%             k   normalizing factor in the updating formula
```

```
%        p_mean   posterior mean vector
%    cov_p_mean   c.o.v. of the posterior mean estimates
%      p_st_dev   vector of posterior standard deviations
%         p_cov   vector of posterior c.o.v.'s
%         p_cor   posterior correlation matrix
%
%%%%%%%%%%%%%%%%%%%%%%%%%%%%%%%%%%%%%%%%%%%%%%%%%%%%%%%%%%%%%%%%%%%%%%%%%%%%%%%

clear

%----- Specify the means, standard deviations and correlation matrix
%----- of the sampling density

M     = [0.06;            % mean vector of sampling density
         0.8;
         1.5];

D = [0.03 0.00 0.00;       % diagonal matrix of standard deviations of
     0.00 0.06 0.00;    % the sampling density
     0.00 0.00 0.14];

R = [ 1.00 -0.60  0.70;    % correlation matrix of the sampling density
     -0.60  1.00  0.00;
      0.70  0.00  1.00];

%----- Specify the scale parameter

scale = 310;

%----- Set minimum and maximum number of simulations:

nmin = 50000;
nmax = 200000;

%----- Begin calculations

d = diag(D);               % vector of standard deviations
cov = d ./ M;              % c.o.v.'s
z = sqrt(log(1+(cov).^2)); % zeta parameters of lognormal distribution
LAM = log(M) - 0.5 * (z).^2;     % lambda parameters of lognormal dist.
Z = diag(z);               % diagonal matrix of zeta's
S = Z*R*Z;                 % covariance matrix of transformed normals
L= chol(S)';               % lower choleski decomposition of S
iS = inv(S);               % inverse of S


%----- Initialize integral values:
I1 = 0;
I2 = 0;
I3 = 0;
I4 = 0;

npar = length(M);          % number of parameters
i_counter = 0;
flag = 1;
constant = 1/( (6.28318531)^(npar/2) * sqrt(det(S)) );

%----- Begin importance sampling:
```

```
for i = 1:nmax

       %-- simulate standard normal random variables;
       u = random('Normal',0,1,npar,1);
       theta = exp( LAM + L*u);   % simulated lognormal theta's

       %-- define three kernels
       K1 = 1;      % this is for computing the normalizing constant k
       K2 =  theta;        % this is for computing the mean
       K3 =  theta*theta';     % this is for computing the mean squares

       %-- compute the scaled likelihhod function
        lhood = exp(Loglhood3(theta)+scale);

       %--- compute the prior distribution (non-informative):
        p = 1/(theta(1)*theta(2)*theta(3));

       %--- compute the sampling probability density
       h = constant * exp(-0.5*(log(theta)-LAM)'*iS*(log(theta)-LAM));
       h = h/(theta(1)*theta(2)*theta(3));

       %--- compute (kernel*likelihood*prior)/sampling-density:
       I1 = I1 + K1*lhood*p/h;
       I2 = I2 + K2*lhood*p/h;
       I3 = I3 + K3*lhood*p/h;

        I4 = I4 + (K2*lhood*p/h).^2;  % this is for computing cov_p_mean

       %--- reciprocal of normalizing constant
       k = I1/i;

       %--- posterior mean and its c.o.v.
       p_mean = I2/I1;
       cov_p_mean = sqrt(( 1/i*(I4/(k^2*i)-(I2/(k*i)).^2) ))./abs(p_mean);

       %--- posterior covariance matrix
       p_cov = I3/I1 - p_mean*p_mean';

        % check if c.o.v is <= 0.05 for all the posterior means, but
       % make sure that at least nmin simulations are performed.
        % flag = 0 means that convergence has been achieved.
        i_counter = i_counter+1;
        if max(cov_p_mean) <= 0.05 &  i_counter>nmin
                flag = 0;
                break
        end
end

%----- display results:
%
disp('--- Number of simulations')
disp(i_counter);

disp('--- Number of parameters')
disp(npar)

disp('========== Bayesian Posterior Estimates ==========')
```

```
disp('--- Reciprocal of normalizing factor k')
disp(k);

disp('--- Posterior means')
disp(p_mean');

disp('--- c.o.v.s for the posterior means')
disp(cov_p_mean')

for i=1:npar
       p_st_dev(i) = sqrt(p_cov(i,i));
       p_c_o_v(i) = p_st_dev(i)/abs(p_mean(i));
end
disp('--- Posterior standard deviations')
disp(p_st_dev)
disp('--- Posterior c.o.v.s')
disp(p_c_o_v)
for i=1:npar
        for j=1:npar
                p_cor(i,j)=p_cov(i,j)/(p_st_dev(i)*p_st_dev(j));
        end
end
disp('--- Posterior correlation matrix')
disp(p_cor);

%--- save results
save Results3 i_counter npar k p_mean cov_p_mean p_st_dev p_c_o_v p_cor
```

*Loglhood2.m*

```
%  FUNCTION STATEMENT
%  Loglhood2 is a string containing the name of a function that computes
%  the logarithm of the likelihood function for the 2-parameter model
%  of the mean rate of pipe damage. This function reads the necessary
%  data stored in array "x" from the file named "Data2.m".

%  ** VARIABLE DESCRIPTION **
%  theta = model parameters;
%  Loglhood2 = logarithm of the likelihood function.

function[Loglhood2] = Loglhood2(theta)

% load data stored in array x:

Data2

[nobsrv] = size(x);
a = theta(1);
b = theta(2);

% Log-likelihood calculation
Loglhood2 = 0;

for i = 1 : nobsrv

       Vi = x(i,1);    %  PGV in cm/s
       Li = x(i,2);    %  Pipe length in km
```

```
       Ni = x(i,4);    %  Number of damage points

       lambdaL = a * (Vi^b) * Li;
       if Ni==0
       LogP = -lambdaL;
       elseif Ni>0
       LogP = Ni*log(lambdaL) - log(factorial(Ni)) - lambdaL;
       end

        Loglhood2 = Loglhood2 + LogP;

end
```

*Loglhood3.m*

```
%  FUNCTION STATEMENT
%  Loglhood3 is a string containing the name of a function that computes
%  the logarithm of the likelihood function for the 3-parameter model
%  of the mean rate of pipe damage. This function reads the necessary
%  data stored in array "x" from the file named "Data3.m".

%  ** VARIABLE DESCRIPTION **
%  theta = model parameters;
%  Loglhood3 = logarithm of the likelihood function.

function[Loglhood3] = Loglhood3(theta)

% load data stored in array x:

Data3

[nobsrv] = size(x);
a = theta(1);
b = theta(2);
c = theta(3);

% Log-likelihood calculation
Loglhood3 = 0;

for i = 1 : nobsrv

       Vi = x(i,1);    %  PGV in cm/s
       Li = x(i,2);    %  Pipe length in km
       Di = x(i,3);    %  Pipe diameter in inches
       Ni = x(i,4);    %  Number of damage points

       lambdaL = a * (Vi^b) * (Di^(-c)) * Li;
       if Ni==0
       LogP = -lambdaL;
       elseif Ni>0
       LogP = Ni*log(lambdaL) - log(factorial(Ni)) - lambdaL;
       end

        Loglhood3 = Loglhood3 + LogP;

end
```

## *Data2.m*

```
%  This file contains failure data on pipes damaged in past earthquakes.
%   This data is for Ductile Iron pipes and was collected by O'Rourke
%   and Jeon after the Northridge 1994 earthquake.
%
%   V = Peak Ground Velocity, cm/s
%   L = Pipe segment length, km
%   D = Range of pipe diameters (not used in the calculation)
%   N = Number of damage points in the pipe segment.

%     V    L      D   N
x = [ 5   42.2   420  0;
      15  116.7  420  1;
      25  92.7   420  6;
      35  40.3   420  2;
      45  32.2   420  3;
      55  18.1   420  1;
      65  12.8   420  4;
      75  7.5    420  2;
      85  5.3    420  1;
      95  16.1   420  1;
      105 7.4    420  0;
      115 15.6   420  1;
      125 5.8    420  0;
      135 5.4    420  0;
      145 5.7    420  0;
      155 5.4    420  1;
      165 3.3    420  1];
```

*Data3.m*

```
%  This file contains failure data on pipes damaged in past earthquakes.
%  and Jeon after the Northridge 1994 earthquake.
%  This data is for Cast Iron pipes with diameters  4-12 inches.
%
%   V = Peak Ground Velocity, cm/s
%   L = Pipe segment length, km
%   D = Pipe diameter, in
%   N = Number of damage points in the pipe segment.
%
%     V    L     D  N

x = [ 5   33.8   4  0;
      15  263.8  4  7;
      25  387.2  4  64;
      35  129.5  4  29;
      45  52.3   4  24;
      55  23.3   4  18;
      65  22.4   4  15;
      75  9.4    4  6;
      85  10.4   4  2;
      95  8.0    4  0;
      105 9.9    4  0;
      115 9.2    4  0;
      125 7.5    4  0;
      135 4.8    4  0;
      145 3.3    4  4;
      155 3.6    4  0;
      165 4.1    4  5;
      5   126.5  6  0;
      15  768.7  6  24;
      25  878.8  6  66;
      35  536.9  6  58;
      45  427.7  6  22;
      55  276.0  6  23;
      65  195.5  6  45;
      75  84.7   6  21;
      85  72.4   6  10;
      95  48.2   6  1;
      105 53.1   6  1;
      115 47.7   6  3;
      125 40.4   6  4;
      135 28.5   6  0;
      145 33.9   6  2;
      155 30.9   6  9;
      165 32.0   6  19;
      5   47.5   8  0;
      15  379.5  8  5;
      25  574.1  8  25;
      35  298.5  8  14;
      45  230.5  8  9;
      55  140.0  8  10;
      65  90.9   8  18;
      75  62.0   8  11;
      85  42.1   8  11;
      95  21.0   8  1;
      105 23.1   8  1;
```

```
      115 22.8   8  2;
      125 17.0   8  1;
      135 24.4   8  2;
      145 19.8   8  3;
      155 15.6   8  5;
      165 24.8   8  20;
      5   3.7    10  0;
      15  16.5   10  0;
      25  30.6   10  3;
      35  3.0    10  0;
      5   23.3   12  0;
      15  193.0  12  6;
      25  263.0  12  7;
      35  125.0  12  8;
      45  84.7   12  4;
      55  56.0   12  5;
      65  34.9   12  7;
      75  19.7   12  1;
      85  8.4    12  1;
      95  10.7   12  0;
      105 7.9    12  0;
      115 4.0    12  0;
      125 6.4    12  1;
      135 7.5    12  0;
      145 4.6    12  1;
      155 6.8    12  2;
      165 5.4    12  0];
```

*Data_AC.m*

```
%  This file contains failure data on pipes damaged in past earthquakes.
%   This data is for Asbestos Cement pipes and was collected by O'Rourke
%   and Jeon after the Northridge 1994 earthquake.
%
%   V = Peak Ground Velocity, cm/s
%   L = Pipe segment length, km
%   D = Range of pipe diameters, in (not used in the analysis)
%   N = Number of damage points in the pipe segment.
%
%     V    L     D   N

x = [ 5   157.3  412  0;
      15  307.9  412  2;
      25  235.5  412  15;
      35  117.7  412  2;
      45  37.8   412  0;
      55  34.1   412  0;
      65  24.4   412  7;
      75  10.9   412  0;
      85  3.0    412  0;
      95  1.2    412  0;
      105 4.8    412  0;
      115 1.6    412  0;
      125 3.9    412  0;
      135 7.2    412  0;
      145 5.0    412  0;
      155 5.8    412  0;
      165 3.5    412  0];
```

*Data_CI_16_24.m*

```
%  This file contains failure data on pipes damaged in past earthquakes.
%   This data is for Cast Iron pipes and was collected by O'Rourke
%   and Jeon after the Northridge 1994 earthquake.
%
%   V = Peak Ground Velocity, cm/s
%   L = Pipe segment length, km
%   D = Range of pipe diameters, in (not used in the analysis)
%   N = Number of damage points in the pipe segment.
%
%     V    L      D    N

x = [ 5   15.9   1624  0;
      15  67.6   1624  2;
      25  59.8   1624  1;
      35  27.2   1624  2;
      45  9.8    1624  0;
      55  6.9    1624  0;
      65  12.6   1624  2;
      75  2.8    1624  0;
      85  6.8    1624  1;
      95  4.3    1624  0;
      105 2.0    1624  0;
      115 2.9    1624  0;
      125 4.9    1624  0;
      135 6.2    1624  0;
      145 2.7    1624  0;
      155 2.9    1624  0;
      165 0.0
```

## G.12 References

Ang, A. H-S., and W-H. Tang. *Probability concepts in engineering planning and design, Vol. I - Basic Principles*. John Wiley & Sons, New York, N.Y, 1975.

Box, G.E.P., and Tiao, G.C. *Bayesian Inference in Statistical Analysis,* Addison-Wesley, Reading, Mass, 1992.

## G.13 Figures

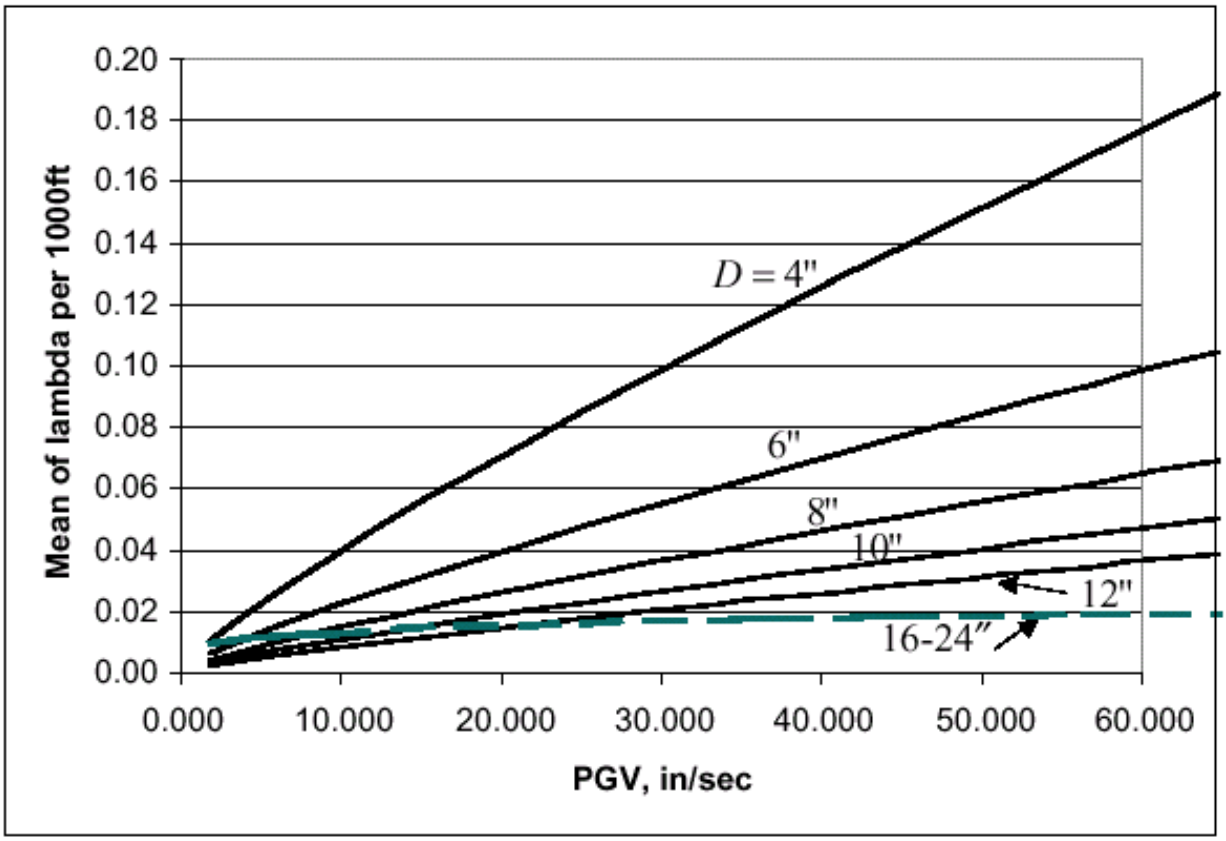


*Figure G-1. Mean of λ for CI Pipes*

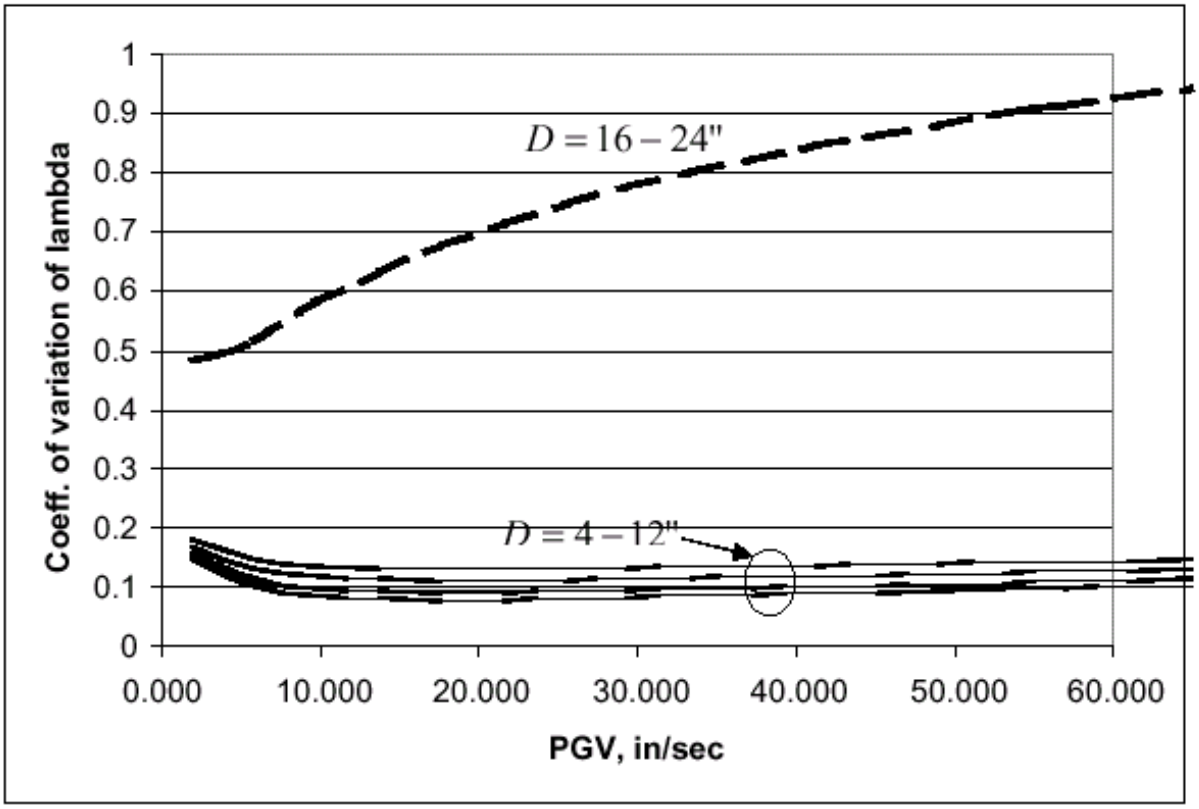


*Figure G-2. Coefficient of Variation of λ for CI Pipes*

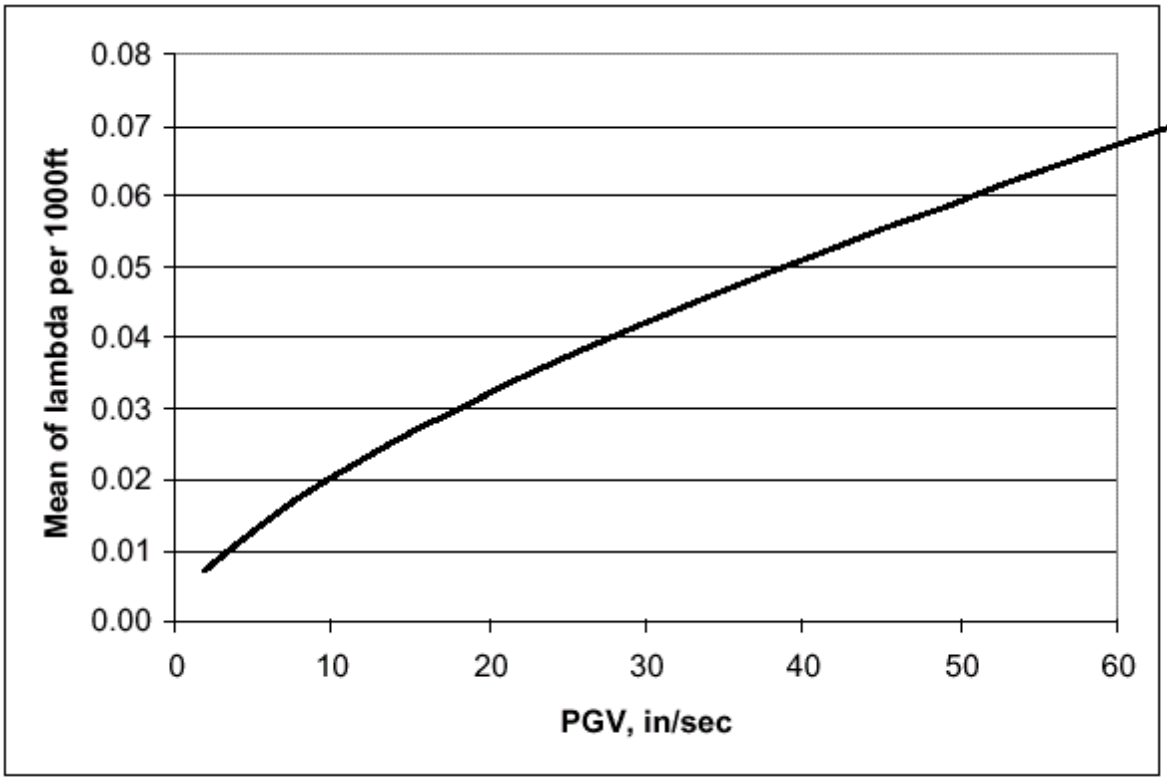


*Figure G-3. Mean of λ for DI Pipes*

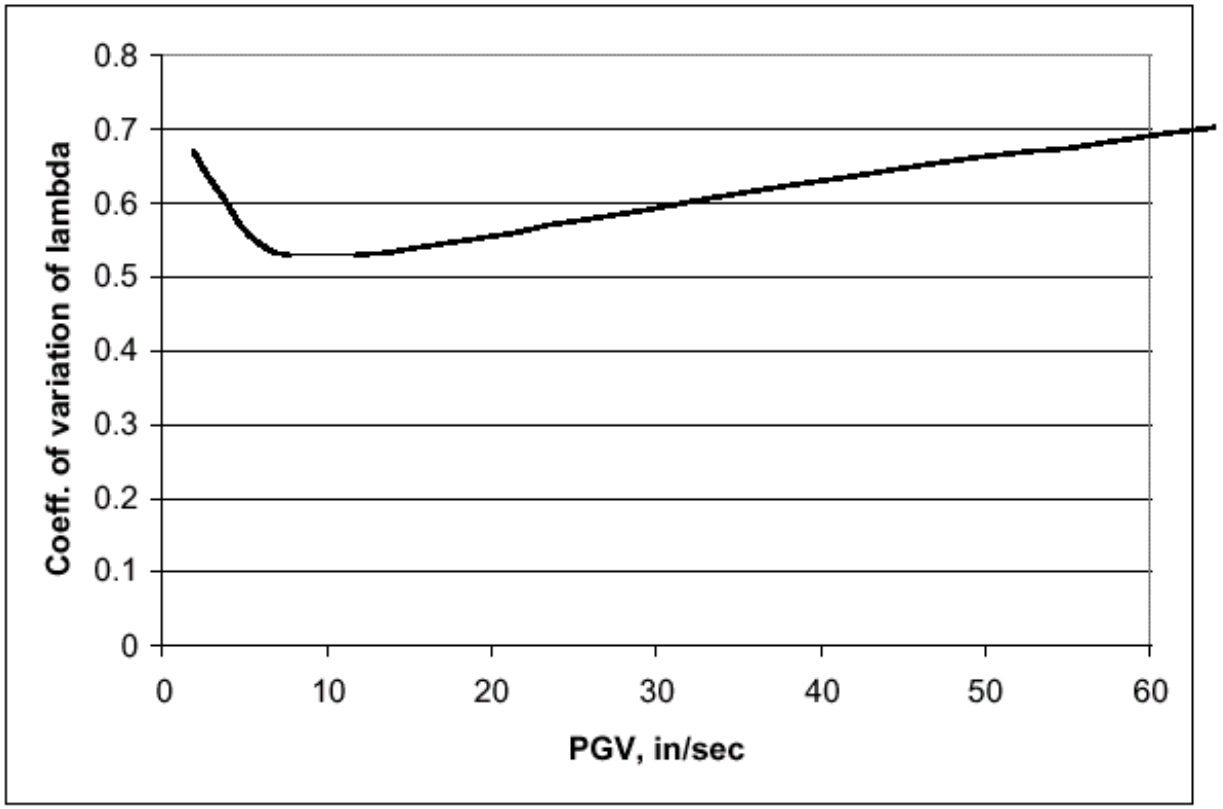


*Figure G-4. Coefficient of Variation of λ for DI Pipes*

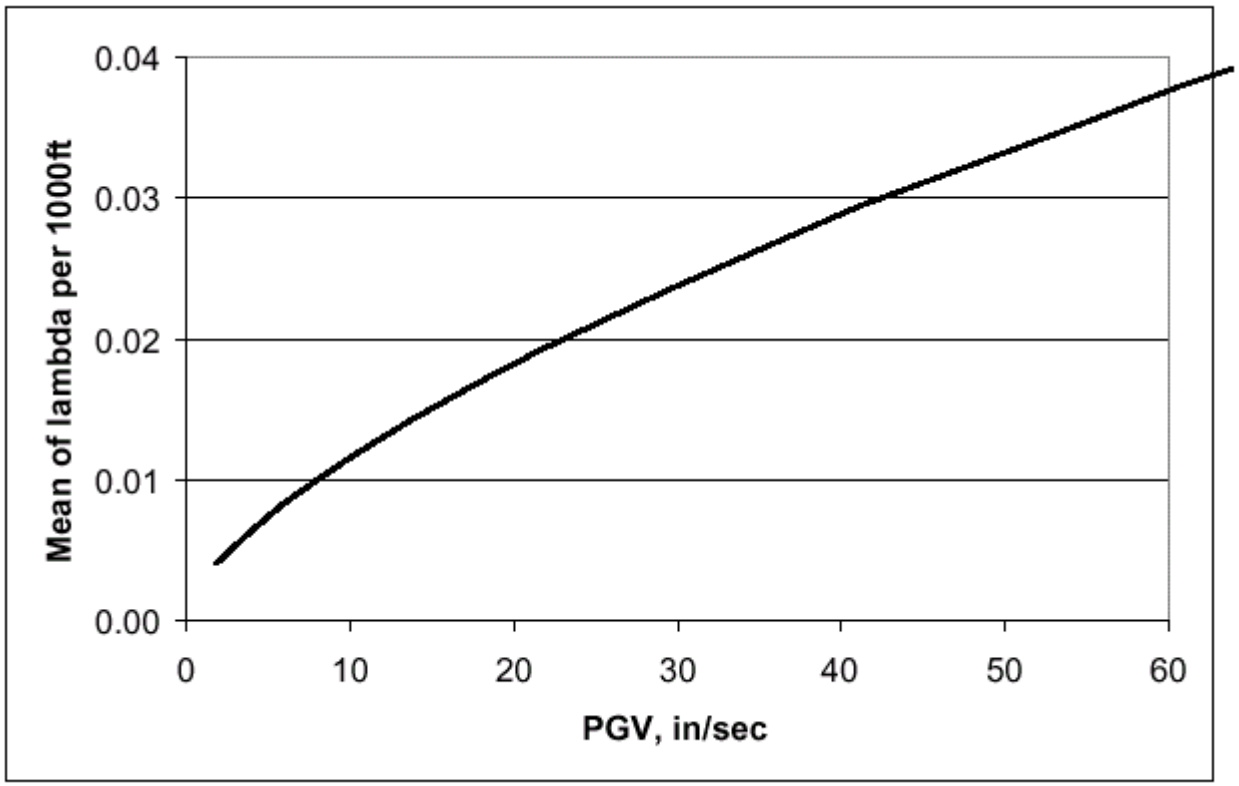


*Figure G-5. Mean of λ for AC Pipes*

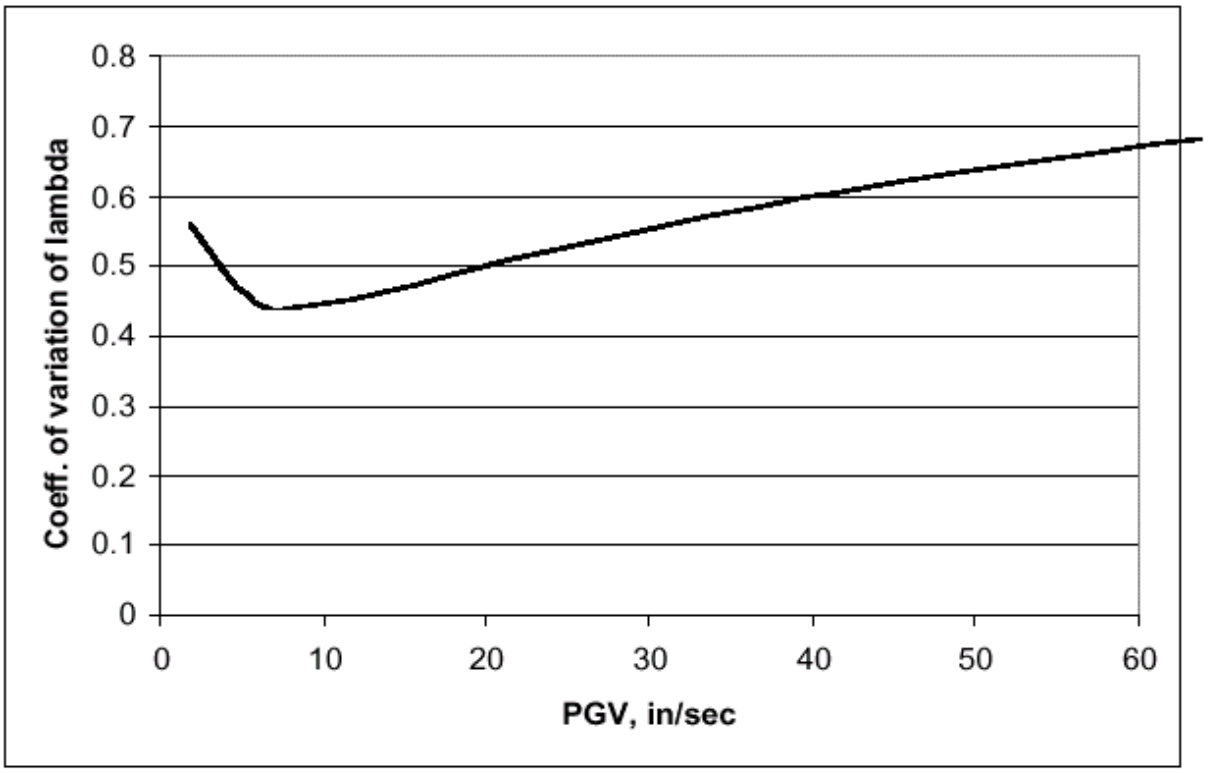


*Figure G-6. Coefficient of Variation of λ forAC Pipes*

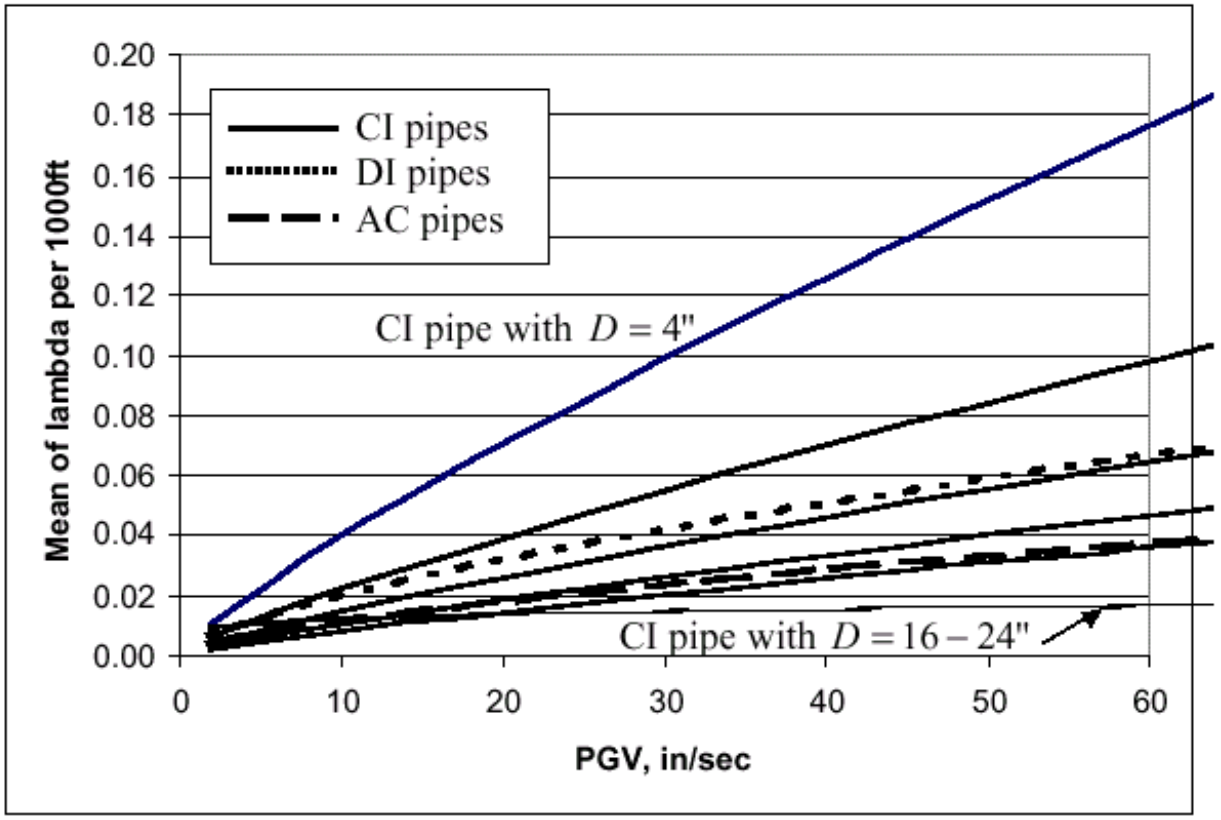


*Figure G-7. Comparison of Mean of λ for Pipes of Different Materials and Diameter*

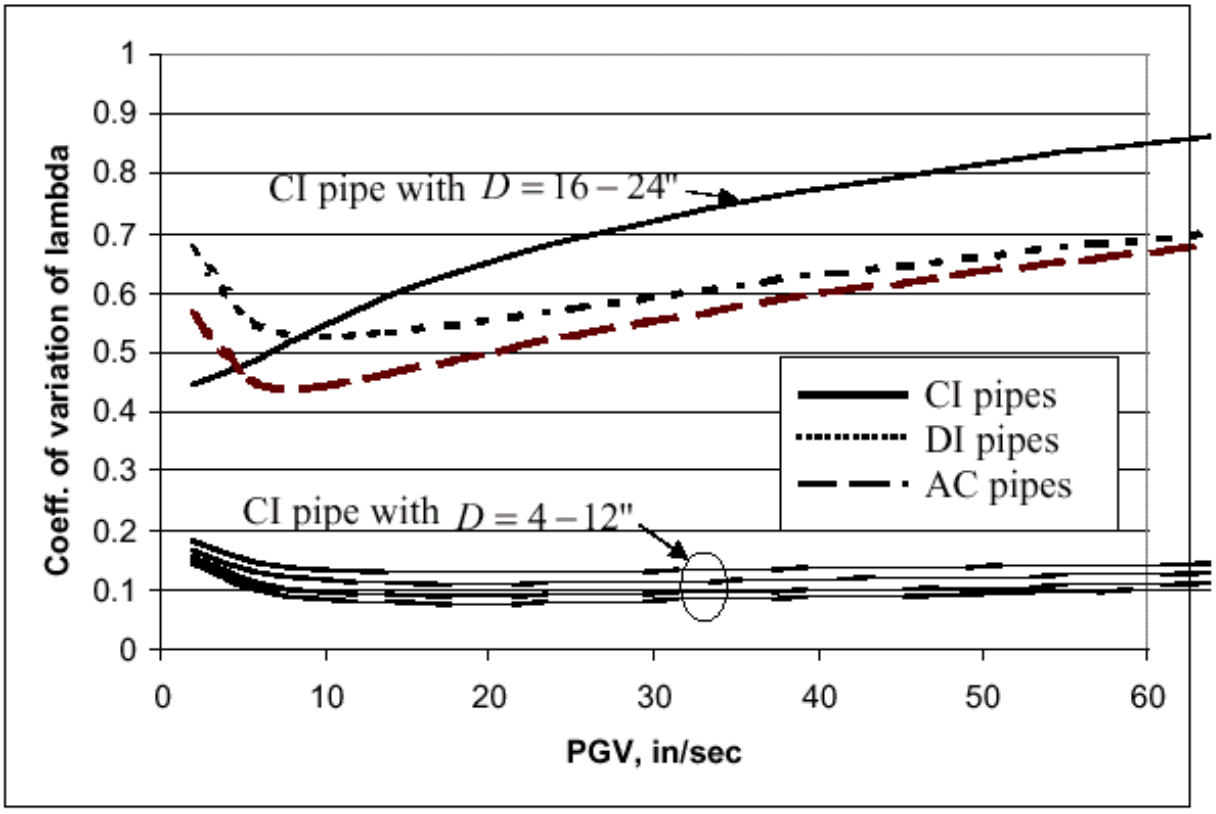


*Figure G-8. Comparison of C.O.V. of λ for Pipes of Different Materials and Diameter*